NTNU

Norwegian University of
Science and Technology

Cytotoxic and inflammatory responses of human lung cells exposed to multi-walled carbon nanotubes

Lone Nilsen

Biotechnology
Submission date: May 2011
Supervisor: Aage Haugen, IBT
Co-supervisor: Shanbeh Zienolddiny, STAMI

Norwegian University of Science and Technology
Department of Biotechnology

Acknowledgements

This study was carried out at the national Institute of Occupational Health (NIOH) and the MSc degree in Biotechnology was obtained at Norwegian University of Science and Technology (NTNU). Supervisors were Professor Dr.philos Aage Haugen and Dr.philos Shan Zienolddiny.

First of all, I would like to thank my supervisor Shan for always encouraging me to do my best and for his great optimism. This year has been an experience, with new knowledge to further bring along. Further I would like to express my gratefulness to have had the chance to get to know and be assisted by Nina Elisabeth Landvik. Thank you for your enthusiasm, guidance and for always being there. Kristine Haugen, thank you for your kindness and encouragement when needed the most, and for your great smile. I would also like to thank Yke Arnoldussen for your great guidance and support through the work. In addition, I would like to give a special thanks to Tove Andreassen for your endless patience, kindness and good support, likewise I will thank Vidar Skaug for his support in the work and good advice. Asbjørn Skogstad, thank for your practical assistance in this report. Finally, I would like to give my thanks to the rest of the Tox group at NIOH for making me feel welcome.

To my fellow students Torunn Rønningen and Audun Bersaas, thank you for your cooperation. I would not have survived without our good talks. To the rest of you on the 5th floor, thank you for all your support.

To all my friends; thank you for your kindness and enduring my ups and downs.

A special great thanks to my family for believing in me and supporting me through the whole period. Thank you for being there.

Oslo, May 2011

Lone Nilsen

Abstract

With the emergence of the nanotechnology industry, there has been a rapid expansion of different types and numbers of nanomaterials to be used in various applications. However, little is known of their potential to cause harmful effects on human health. Among other nanomaterials, carbon nanotubes, are found to harbor attractive characteristics that can be used in many applications. However, the same properties may cause harmful effects on human health that has raised serious concerns. The main route of exposure to carbon nanotubes is through the respiratory system with subsequent deposition in the lungs. Carbon nanotubes in contrast to other nanomaterials have fiber-like structures similar to the asbestos fibers. Exposure to asbestos has been associated with serious lung diseases such as fibrosis and cancer.

A common type of carbon nanotubes called multiwalled carbon nanotubes has many valuable properties and several potential applications in different nanoproducts, manufactured commercially. It seems that the toxicological effects differ from product to product. Through this study potential harmful effects of two multiwalled carbon nanotubes designated as MWCNT-NO (produced in Norway) and MWCNT-JP (produced in Japan) have been investigated *in vitro* in normal human lung cells. The well known crocidolite asbestos was included to compare the effects with nanotubes. Hydrogen peroxide, a well known oxidative agent was also included since it has been hypothesized that carbon nanotubes may exert their effects through oxidative stress mechanisms. Cellular responses such as cytotoxicity, apoptosis and changes in expression of some inflammatory and apoptotic genes were studied.

The results of the cytotoxicity assays (WST-8 assay) indicated a reduction of cell viability for carbon nanotubes and crocidolite asbestos, depending on the dose and time of exposure. However, MWCNTs, especially MWCNT-JP, were more toxic than crocidolite asbestos. For the hydrogen peroxide, the reduction in cell viability tended to depend only on the dose. Little differences between the two cell-lines were observed. Hoechst/PI staining revealed that cell death occurred essentially by necrosis and not apoptosis following exposure.

Exposure to MWCNT-NO resulted in an increased expression of the *IL1B*, *IL8* and *IL6* inflammatory genes (qRT-PCR). This differed from the MWCNT-JP type where little changes in the expression were observed. Some differences between the two cell lines were also observed. The overall potential of the tested carbon nanotubes to cause harmful effects in normal human lung cells needs further verifications with improved particle characterization.

Abbrevations

8-OHdG	8-hydroxydeoxyguanosine
AD	Arc discharge
AP-1	Activator protein-1
B(a)P	Benzo(a)pyrene
Bcl-2	B-cell lymphoma 2
Caspases	Cystein-aspartat proteases
cdk	Cyclin dependent kinase
cDNA	Complementary DNA
CNT	Carbonnanotube
COPD	Chronic obstructive pulmonary disease
COX-2/*PTGS2*	Cyclooxygenase-2/ Prostaglandin-endoperoxide synthase 2
Cq	Threshold cycle
CVD	Chemical vapor deposition
DM	Dispersion medium
DNA	Deoxyribonucleic acid
DPPC	Diapalmitoylphosphatidylcholine
EGFR	Epidermal growth factor receptors
ELISA	Enzymed linked immunosorbent assay
ERK	Etracellular signal regulated kinases
H_2O_2	Hydrogene peroxide
HBECs	Human bronchial epithelial cells
hTERT	human telomerase reverse transcriptase
IC	Inhibitory concentration
IL1-Ra	Interleukin -1 receptor anagonist
IL-1β	Interleukin-1beta
IL-6	Interleukin-6
IL-8	Interleukin-8
iNOS	inducible nitric oxide
IKB	Inhibitor of kappaB
JAK/STAT	Janus kinase/ signal transducer and activator of transcription
LA	Laser abaltion
LAF	Laminar air flow
LC	Lethal concentration
LPO	Lipid peroxidation
M	Molar
MAPK	Mitogen-activated protein kinases
MPO	Myelloperoxidase
MWCNT-JP	Multi walled carbonnanotubes-Japan
MWCNT-NO	Multi walled carbonnanotubes-Norway
NF-κB	Nucleor factor-kappaB
NM	Nanomaterial
NO	nitric oxide
OD	Optical density
P	Probability
PAH	Polyaromatric hydrocarbons
PBS	Phosphate buffered saline
PCR	Plomerase chain reaction
PI	Propidium iodide
qRT-PCR	Quantitative real time PCR
RNA	Ribonucleic acid
RNS	Reactive nitrogen species
ROS	Reactive oxygen species
SD	Standard deviation
SE	Standard error
SEM	Scanning electron microsscopy
SEM	Scanning electron microscopy
SNP	Single nucleotide polymorphism
SOD	Superoxide dismutase
SOM	Oncostatin M
SWCNT	Single walled carbon nanotubes
TEM	transmission electron microscopy
TG	Thapsigargin
TNF-α	Tumor necrosis factor α
TP53	Tumor protein 53

Contents

1. Introduction

1.1. Nanomaterials

Nanotechnology is a growing industry where materials at nanoscale, ranging from 1-100 nm in size, are used. [1]. Nanomaterials (NMs) are representing major component of all "nano" products, and nanoparticles (NPs) are their building blocks [2].

Changes in particles at nanoscale may improve its physical and chemical properties, which is appellant and of great interest for industrial and biomedical purposes [3].With a constant exploration of new applications the potential for NPs is infinite [4]. More than 1300 "nano" consumer products currently exist on the market and are used in electronics, cosmetics, automotive and medical products [5]. The big challenge now, is to integrate health, environment and safety together with this fast growing technology.

The existing diversity of NPs that possibly can be synthesized is almost endless. This makes the classification of the particles difficult. The major NPs include fullerenes, carbon nanotubes (CNTs), inorganic NPs (e.g. TiO2), organic NPs, nanocapsules, nanospheres, nanoshells, dendrimers and quantum dots (QD) [6]. The different NPs have been ranked in regard to their possible adverse effects on health (table 1.1), where CNTs were given the highest concern (Berube et al (2010)).

Table1.1: Classification of potentially or actually problematic nanoparticles. From Berube et al.[7]

Nanopatricles (NPs)
1. Carbon nanotubes (CNTs) – Fibrous NM
2. Quantum dots (QDs)
3. Metal oxides e.g. TiO2 NPs, ZnO NPs, silica NPs, FeO NPs
4. Metals e.g. Au NPs, Ag NPs, Co-Cr NPs
5. Fullerenes
6. Polymers

1.2. Nanomaterials - nanoparticles

1.2.1. Carbon nanotubes

CNTs contain a unique physical structure and many distinctive physical and chemical properties that are valuable in nanotechnology [8]. They are made of graphene sheets with specific strength and surface properties and exists in more than one form (allotropes) [9]. CNTs differ in relation to number of walls or layers, being single walled carbon nanotubes (SWCNTs) or multi walled carbon nanotubes (MWCNTs).

1.2.2. Production and exposure

A large amount of engineered NMs are produced annually, and each material has its own distinctive features. NPs are either generated from degradation of bulk materials or designed from the molecular level [4]. Together with multiple sources of NPs, there are also several means of exposure, where inhalation is the major route [10]. Different types of exposure to

NPs can cause diverse effects of NP toxicity [10]. Major interest has been directed toward CNTs for industrial use, such as their good material strength, conductivity and utility value for biomedical applications [11]. Their features are versatile and are used in various industries such as; cosmetic, food, textile, electronic and medical industry. [10]. Possible exposure from consumer products would result from wear and tear of these products. Direct human exposure through medical applications, wear and tear of consumer products and surrounding air pollution is of concern.

Manufacture of CNTs occurs through three various processes; chemical vapor deposition (CVD), arc discharge (AD), and laser ablation (LA) [12]. The resemblance of the three methods is adding energy to a carbon source and creating layers or groups of single carbon atoms. The various energy sources are heat from furnace for CVD, electricity from an arc discharge and high intensity light from laser for laser ablation [13]. Laser ablation and AD processes produce CNTs that are less contaminated with metals and with few structural defects, improving their physical attributes. It is possible to produce MWCNTs without metals, even though existence of metal catalyst helps aligning the nanotubes [12].

NPs are produced with the purpose to create new materials with improved features. Mass production of NPs started a few years ago, with no occupational exposure limit so far, and possible health effects has not been fully elucidated. General safety considerations are recommended to be used when working with dried carbon NMs. Less consideration has been dedicated to workplace exposure and safety of carbon NMs in liquid suspensions. Exposure may not only affect the primary production industry, but also in downstream producers that use CNT materials [14]. Composites of CNTs can cause exposure when the material is machined or drilled, during wear and tear, and also during removal. In the future the use of CNTs for drug delivery and imaging may be a new route of exposure for both manufacturer and people using them [15]. The route of exposure by NP aerosol with NPs in a dispersed or aggregated form is most likely to affect workers by inhalation. Other possible routes of exposure are mostly through skin (dermal) and a smaller amount by ingestion. Exposure by ingestion can occur if an inhaled material is swallowed, or a consequence of hand-to-mouth contact. The risk associated with occupational manufacturing, processing and handling of NMs such as CNTs is poorly understood and the ability of CNTs to form different levels of agglomeration and/or aggregation states, makes the exposure assessment difficult [14-16].

1.2.3. Parameters and adverse effects

Physico-chemical properties play a central role in NPs toxicity. In regard to CNTs, the main concern has been raised towards their morphological properties, although the particles chemical composition, purity and solubility of the particles (how loose (agglomerated) or fast (aggregated) particles are connected together) also are important as to toxicological considerations. The respiratory system is the main target for CNTs exposure, where the particles may affect the lung tissue directly, or other organs through systemic interactions.

It is the small size of NPs that gives them their industrial advantages, and contrary their toxic potential [17]. Upon exposure to NPs, their small size allows the particles to reach several target organs. At the cellular level they may penetrate the cell membrane and enter compartments within the cell. Previous studies indicated NPs to have increased ability to accumulate in cells and organs compared to larger materials [18]. The surface reactivity of NPs could cause hazardous effects that may not be present in the larger materials with similar composition. For CNTs, diameter and length are important properties. These features vary among CNTs and depend on the manufacturing process. Purified CNTs tend to be shorter in length due to the processes used when purified. Wall number or number of layers affect the diameter of MWCNTs, varying from a few to a few tens of nm, and their length can attain many micrometers [9]. Multilayer carbon nanotubes (MWCNTs) contain several layers of carbon cylinders piled one inside of the other [19]. CNTs with their nanometric diameter are known to have a great surface area. The accessible surface area depends on length, diameter, and the number of walls. The surface area of CNTs will decrease as the number of walls increases. This indicates that huge MWCNTs and nanofibers, will contain a small surface area as long as they do not turn porous. In theory, MWCNTs tend to have surface areas of a few hundred m^2/g [20] .

The shape of NPs is important and relevant concerning genotoxic endpoints. Genotoxicity can be divided into primary and secondary effects. The primary effect rely on intrinsic activity of the particles e.g. the ability to produce reactive oxygen species (ROS). The secondary effect is connected with inflammatory actions, produced by particles in e.g. the lung [21]. Muller et al. showed that MWCNTs had the potential to cause mutations in lung epithelial cells [21]. Furthermore, Yamashita et al. reported that the MWCNTs ability to cause DNA damage and inflammation depended on their size and shape. Longer and thicker MWCNTs were more harmful than the shorter and thinner MWCNTs. Also MWCNTs were more potent in inducing DNA damage, compared to SWCNTs [22].

To get a full understanding of NPs and their interaction with biological systems, a thorough understanding of surface composition is necessary [2], since the surfaces of NPs come in touch with cells. Surface charge and chemical composition are related to surface reactivity and affects the toxicity of particles. A chemical change on the particle surface can be important when considering health effects [1]. The specific surface chemistry of NPs, mediates the ability of protein adsorption and the cellular binding of NPs [10]. Dispersion of NPs in solutions depends on their hydrophobicity. NPs with high adsorption capacity may turn out to be coated with specific proteins when they come into contact with biological liquids. NPs have been demonstrated (*in vitro)* to alter the conformation of proteins in biological systems [18]. Factors such as particle surface, size, aggregation state and particle concentration determine the composition of the resulting NP-protein complex [23].

Surface contamination could also have a role in the reactions of NMs within the cell. The large surface area of NPs increases their surface energy increasing the catalytic activity. [18] The high surface energy, creates agglomeration among particles and also adsorption to the

surrounding environment [18]. High adsorptive particles could bind contaminating compounds during, for instance, the manufacturing process. Surface contamination may come from transition metals (e.g., Fe, Cu, Mn & Ni), organic compounds such as polyaromatic hydrocarbons (PAH, combustion particles) and biological materials (e.g., endotoxins and allergens) [2]. Limited knowledge exists on how the attributes size, shape and surface properties can affect bio-distribution, cellular internalization and intracellular trafficking of NMs [24].

One typical attribute for NPs is their propensity to aggregate and agglomerate. Airborne particles are often invisible alone as a single particle, but are frequently found in large aggregates and agglomerates. Aggregates are primary particles held together by strong chemical bonds. Agglomerates are a collection of NPs bundled together by van der Waals forces and electrostatic forces. The state of agglomeration is important to consider when evaluating factors influencing toxicity [2] though agglomeration of NPs may affect toxicological responses [25]. A high concentration of particles can increase agglomeration, decrease total surface area resulting in a decreased toxic response. Agglomeration of particles can occur quickly at high concentrations and influence both particle size and structure [18]. An increase of the particle size can create particles outside the nanoscale range, with a subsequent change in the particle behavior. The electrostatic nature of CNTs, involves a tendency to create large agglomerates of CNTs often far outside the range of e.g., respirable particles. Agglomeration of CNTs can occur when the bundling sheets of graphite bind together [11]. An interesting factor to consider when examining NPs, is whether the agglomerated particles cause toxic responses or manage to de-agglomerate again. Surface-coatings can be used for studies to change surface properties and thereby prevent aggregation or agglomeration with various particles [1]. Surface coatings with purpose to increase dispersion of NPs or reduce aggregation, may enhance NP translocation and delivery trough the body. The state of agglomeration can be modified once inside a biological system, through contacts with biological fluids and proteins. [18]. Previous studies have proved that presence of proteins and surfactants can help in the dispersion of NPs [25]. Certain proteins can stabilize the NPs while protein surfactants may flake off small collections of nanotubes and thereby decrease their agglomeration. Pulmonary surfactants cover the bronchioles and alveoli within the lung. Inhaled particles can come in contact with surfactants in the bronchioles and alveoli resulting in particle coating and variation of the surface chemistry [26].

1.2.4. CNTs and asbestos-like effects

The inhalation of asbestos fibers is associated with fibrosis of the lung, lung cancer and mesothelioma [8]. Long and thin fibers have the potential to reach the gas-exchange region of the lung, and persistence may occur when clearance mechanisms fail. The needle-like and fiber-shape of CNTs have been compared to the asbestos fibers, and the deposition is therefore suggested to be related to the aerosolized form of CNTs. Length of the fiber is crucial concerning clearance and deposition. Fibers longer than the macrophages diameters (10-20 µm) are representing a potential problem since the macrophages will have difficulties

in clearing them. Frustrated phagocytosis may therefore occur. A scheme showing the fate of particle once entered the lung is shown in Figure 1.1.

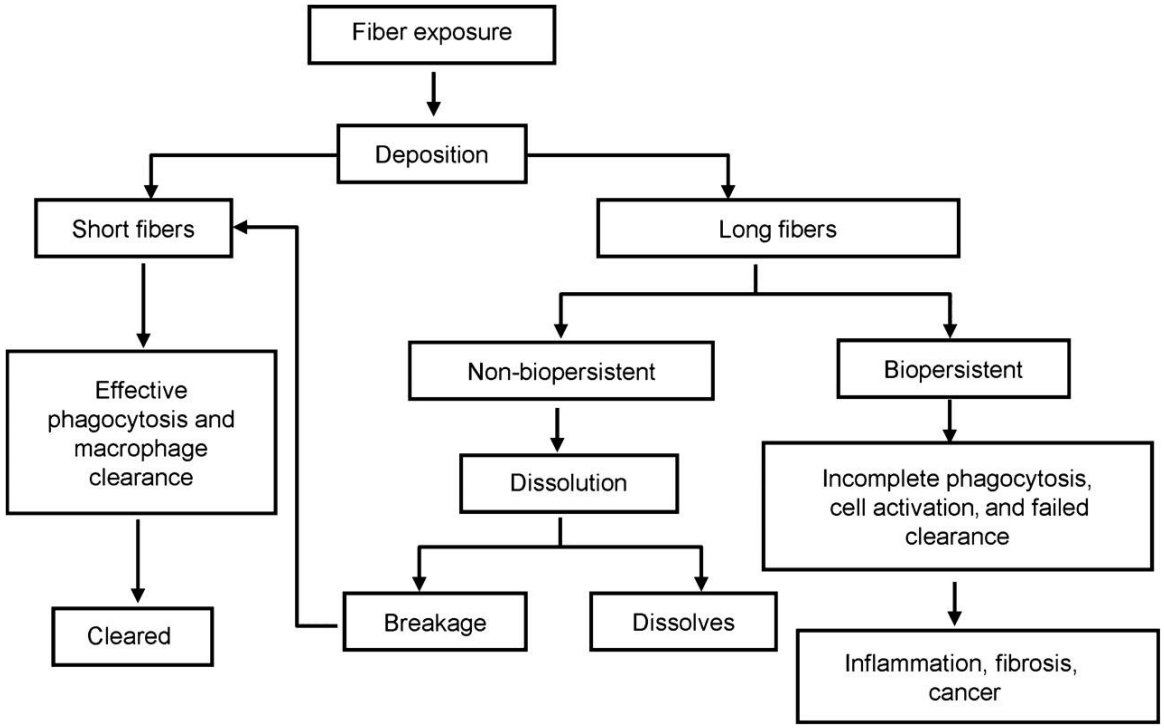

Figure 1.1: A model of both the fate and pathogenic effects of fibers entering the body. From Donaldson et al. [8].

A pilot study by Poland et al compared among others, MWCNTs used in this study (supplied by Mitsui and Co) with asbestos [27]. The tested MWCNTs indicated to contain high amounts of long and straight fibers (longer than 20 µm). The long and isolated MWCNTs demonstrated further to produce an inflammatory response and an asbestos-like, length-dependent, pathogenic behavior. Poland and his colleagues suggest that long CNTs may lead to mesothelioma *in vivo*, a cancer type also caused by asbestos [27]. Mechanisms of asbestos toxicity, may also apply to a number of other particles e.g. CNTs. Asbestos has demonstrated to initiate damage through ROS/reactive nitrogen species (RNS), and thereby affect intracellular signaling and activate transcription factors directly or indirectly (via ROS/RNS). This results in changes in gene expression affecting many cellular responses [28]. Toxicity is often determined by the biopersistence (durability and physiological clearance) of an inhaled NP. Figure 1.2 illustrates the important factors regarding persistence of inhaled particles which may result in undesirable pulmonary effects [29]. Muller and his colleagues observed in rats that the administered MWCNTs (0.5, 2 or 5 mg/rat) persisted in the lungs for a long time, and that the length and dispersion affected clearance kinetics. High amounts of MWCNTs were still present in the lungs after 60 days (80 % of the highest doses and 40 % of the lowest dose) and adverse pulmonary effects were observed 2 months post exposure [11]. Another study performed by Takagi et al. observed how intraperitonally administered MWCNT (3 mg/ml) to p53 heterozygous mice induced asbestos-like effects. Induction of mesothelioma was observed in both MWCNTs and Crocidolite treated mice (87.5 % versus

77.8 %) [30]. The authors suggested the MWCNT effects to resemble asbestos with regard to size, shape and biopersistency [30]. However, Dr. Ken Donaldson raised skepticism to the study of Takagi et al, due to the high inappropriate exposure methods, the extremely high dose level used and the sensitiveness of p53 deficient mouse model for mesothelioma detection [30]. Dr. Ken Donaldson mentions that the used dose is beyond the maximum tolerated dose that a person would take, and that the type of mouse study represents false-positive effects [31].

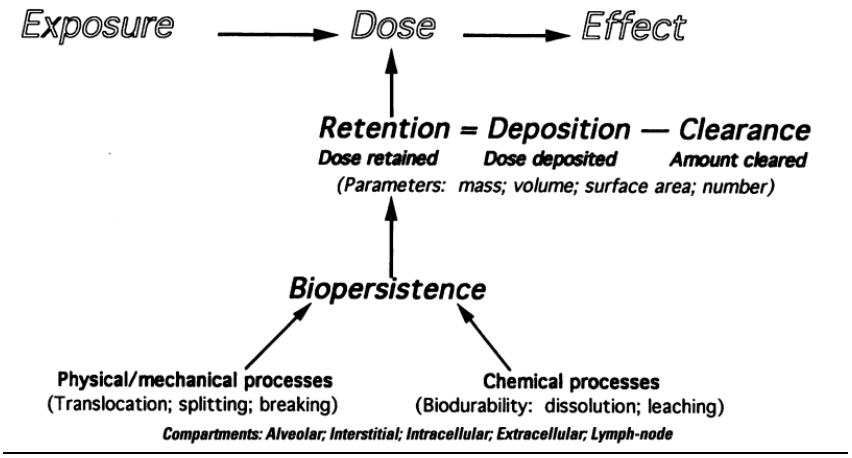

Figure 1.2: Important factors for persistence of inhaled non-fibrous and fibrous particles are; deposition, clearance, retention, and translocation and dissolution that further may cause harmful pulmonary effects. From Oberdorster et al. [29].

The ability of fibers to dissolve in the lung tissue is important when decreasing the effect of biopersistence. Fibers that do not dissolve, weaken or disappear and may create a risk to persist in the lungs. Even though asbestos is known as a fiber resisting to dissolution, fibers differ and some types will undergo an entire dissolution. The biopersistence of fibers is important in the fiber's pathogenicity.

1.2.5. Nanoparticles- uptake and translocation

The different NPs existing on the market, may give different health effects compared to particles with comparable physico-chemical properties [1]. The differences determine their manners of aerosolization, biodistribution, translocation, cellular interactions and the outcomes [3]. Many of the outcomes at the respiratory tract (organ of entry) can be analogous but different effects are observed at secondary organs. Particles not deposited in the upper airways, are deposited in the alveolar region to an increased extent. Deposited particles can thereafter be eliminated through three distinct pathways [32]:

a) Eliminated through the tracheobronchial tree by the mucocilliary clearance system, followed by ingestion into the gastrointestinal tract before excreted in the feces.
b) Transmitted to the pulmonary lymph nodes.
c) Translocated into the blood circulation.

Three different hypotheses also exist as to the mechanisms of translocations at the air-blood barrier [32]:

1. Phagocytosis by macrophages (the uptake of large particles) or endocytosis by alveolar epithelial cells and endothelial cells (active transport, where extracellular particles are engulfed)
2. Diffusion (passive transport, where particles penetrate across the cellular membrane)
3. Transfer through pores in the cytoplasm of endothelial cells or gaps among epithelial cells (active and passive transport).

Previous studies demonstrate how inhaled NPs can evade phagocytosis, cross cell membranes and enter the circulation [10, 32]. The uptake and internalization of NMs by living cells have indicated to be affected by the symmetry or the aspect-ratio of particles. Particles containing a high - aspect-ratio i.e., less symmetry, results in increased rate of uptake compared to low-aspect-ratio particles. CNTs contain a tremendous aspect-ratio, presuming toxic attributes as observed with other fibrous particles e.g., asbestos fibers [11]. Several studies have indicated how the form of a NPs influences the rate of uptake e.g., rod-shaped NPs have indicated lower rate of uptake compared to spherical shaped NPs [33]. Needle-shaped CNTs have, for instance, shown geometric effects when they impale entire cells. This might carry along adverse or altered effects [18]. Figure 1:3 illustrates possible mechanisms for CNT uptake.

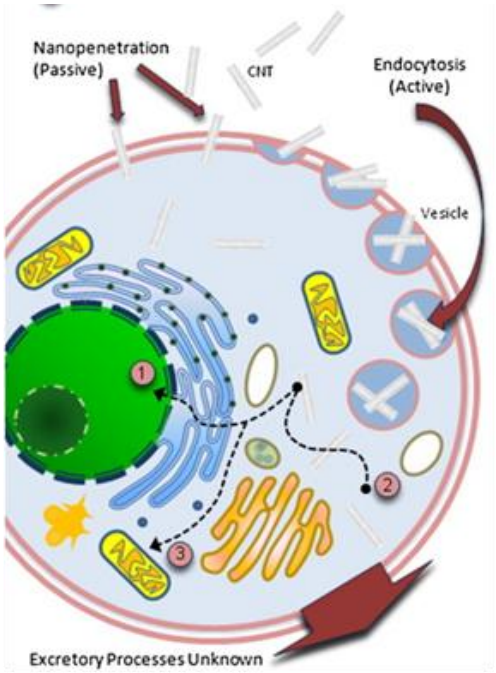

Figure1.3: Possible mechanisms for CNT uptake are receptor-mediated endocytosis and nanopenetration. From Firme and Bandaru [34].

1.3.Mechanisms of health effects

1.3.1. Chronic inflammation and oxidative stress

Inflammation is the host response to internal and environmental assaults [35]. It is a physiological process designed to defend the body against tissue damage [36]. The process entails chemical signals that initiate and maintain the condition to battle the infection, and to repair the damage. A large number of cell types from both innate and adaptive immune systems take part during an inflammatory response. Leukocytes (neutrophils, monocytes and

eosinophiles) are the first cells to be recruited to the affected site. Cytokines and chemokines are "early-response" chemical signals involved in activation of leukocytes and recruitment of downstream effectors cells. Leukocytes can produce more cytokines and chemokines, and thereby recruit various inflammatory cells to site of damage. When levels of leukocytes turn low, chemical factors will recruit monocytes, differentiating into macrophages, and will migrate to the site of damage. Macrophages are the key source of growth factors and cytokines that influencing cells of the local microenvironment to maintain tissue integrity and homeostasis [36]. Failure to control key mediators of the defense response, may lead to chronic inflammation and potentially to pathogenesis [35]. A chronic inflammatory process can stimulate cytokines and chemokines to contribute to the development of cancer [37]. The link between inflammation and cancer is not completely understood. However, chronic inflammation provokes DNA damage, survival of damaged cells, increased cell proliferation and tumor development [38].

Chronic inflammation may lead to generation of ROS/RNS and lipid peroxidation (LPO) both from endogenous and exogenous sources [38]. Example of an endogenous source is during aerobic metabolism in all tissues, where reactive oxygen species play a key role in normal cellular functions. In a pro-inflammatory microenvironment the action of inflammatory cytokines and cells may generate more ROS/RNS resulting in a cascade of signaling events [35].The microenvironment during chronic inflammation consists of inflammatory cells, reactive oxygen intermediates, DNA damage and growth factors [38-39]. Various enzymes responsible for the production of these intermediates are NADPH oxidase, inducible nitric oxide synthase (iNOS) and myeloperoxidase (MPO) [39]. ROS and RNS can cause damage of macromolecules e.i., DNA, RNA, lipids and proteins. ROS, RNS and LPO can alter signaling molecules, enzymes and proteins involved in normal cellular functions such as transcription factors nuclear factor kappa-B (NF-κB), iNOS and cyclooxygenase-2 (COX-2). Furthermore, ROS/RNS have been shown to activate many other transcription factors, induce cell death (apoptosis/necrosis), change mitogenic signals, influence cell growth and signaling cascades. Various types of reactive species are generated during normal and inflammatory conditions, and $\bullet O_2^-$ is considered as the main ROS [38]. NADPH oxidase is activated after ingestion or phagocytosis of foreign pathogens or components, and oxygen is reduced by one electron. A family of enzymes known as superoxide dismutase (SOD) dismutates $\bullet O_2^-$ into H_2O_2. H_2O_2 may further create $\bullet$OH radicals, known to be very reactive and consequently directly react with DNA resulting in DNA strand breaks and base modifications. 8-Hydroxydeoxyguanosine (8-OHdG) is a DNA damage related to OH radicals [40]. During inflammation activation of transcription factor NF-κB by cytokines will induce iNOS [39]. Expression of the enzyme iNOS drives the production of nitric oxide (NO$\bullet$). NO$\bullet$ is very reactive and has been suggested to promote deamination of DNA bases, production of carcinogenic N-nitrosamines and induction of single-strand breakage of DNA. The inflammatory mediator NO$\bullet$, has indicated to inhibit DNA repair through inhibition of key DNA repair enzymes [41].

The cyclooxygenases COX-1 and COX-2 are entailed in the production of prostaglandins from arachidonic acid.COX-1 is the constitutive enzyme, while the COX-2 protein is the

inducible isoform, responding to growth factors, tumor promoters, hormones, bacterial endotoxin, and cytokines [42]). Several signaling pathways are involved in the induction of COX-2, and also several transcription binding elements for NF-κB are found in its promoter. Up-regulation of NF-κB would result in constitutive expression of COX-2 in cells *in vitro* [43]. The tumor necrosis factor alpha (TNF-α) is a central pro-inflammatory cytokine that plays an important role in inflammation. TNF-α has been implicated to induce cellular growth, mediate proliferation and induce production of ROS/RNS via multiple signaling pathways. TNF-α also regulates expression of multiple pro-inflammatory proteins, among them interleukin-1beta (IL-1β), interleukin-6 (IL-6), interleukin-8 (IL-8), COX-2 and NF-κB. Activation of both pro- and anti-inflammatory mediators takes place during an inflammatory response. NF-κB is known as the pro-inflammatory transcription factor induced by pro-inflammatory cytokines, chemokines, oxidative stress, DNA-damaging agents, infectious agents and pollutants [44-45] , as figure 1.4 illustrates.

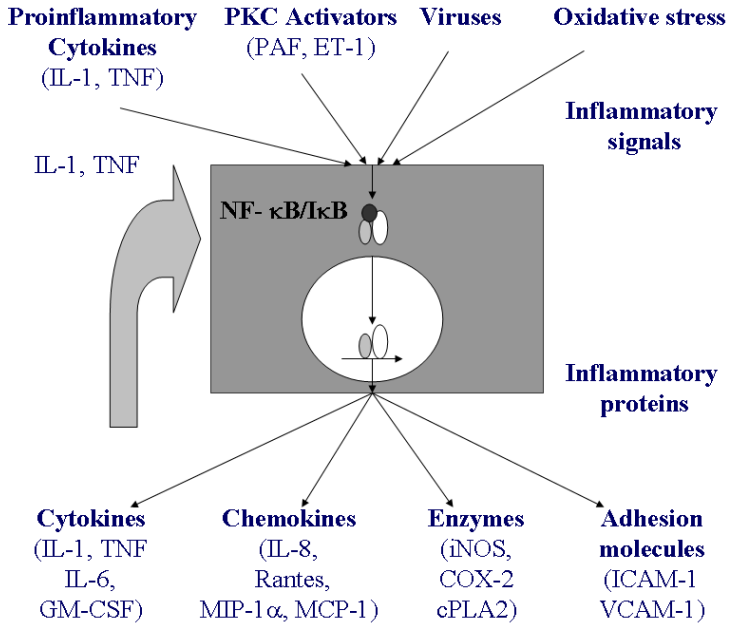

Figure 1.4: Inflammation and NF-κB. Activating factors of NF-κB are: cytokines, PKC activators, infectious agents or oxidative stress. NF-κB may respond by expressing inflammatory mediators, such as; cytokines, chemokines, enzymes and adhesion molecules. Potent mediators of NF-κB e.g. TNF-α and IL-1, may form a positive loop resulting in persistence of NF-κB activity and reactivity. From Bours et al. [44].

Activation of NF-κB occurs after activation of IκB-kinase (inhibitor of kappa B) through two pathways. The "canonical" pathway stimulated by microbial products and proinflammatory cytokines, results in activation of RelA or cRel components. The other pathway is activated by cytokines involved in the TNF-family-lymphotoxin β, CD40 ligand, B cell activating factor together with receptor activation of NF-κB which leads to activation of RelB/ p52 complexes. NF-κB activity is tightly controlled by inhibitory protein IκB-α/β. IKKβ kinases regulate the activation of canonical pathway and entail the IKKγ subunit. The other pathway mentioned, requires IKKα kinases for activation. The result of phosporylation is

ubiquitination of the inhibitory protein in such a way that NF-κB is free to migrate from cytosol into the nucleus for transcription of various genes [44]. The activity of NF-κB has generally been identified in response to important pro-inflammatory cytokines involved in chronic inflammatory conditions e.g. IL-1. The link between NF-κB and inflammation is not easy to understand, though pro- and anti-inflammatory mediator functioning simultaneously, and their balance will decide the effect.

In order to avoid prolong inflammation, the process of apoptosis (programmed cell death) which is an essential mechanism, is an important factor. NF-κB activation is necessary for apoptosis to occur. During acute inflammation NF-κB has confirmed a pro-apoptotic function towards neutrophils, this may indicate an anti-inflammatory process for NF-κB [46]. Controversially, NF-κB has also demonstrated an inhibiting function of pathogen -induced apoptosis in macrophages (*in vitro*) [47]. Figure 1.5 illustrates the role of NF-κB in the process of apoptosis.

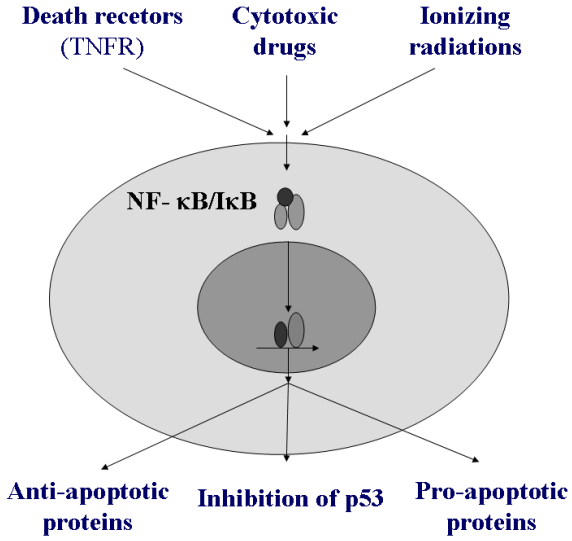

Figure 1.5: Pro-apoptotic signals activate the transcription of NF-κB and NF-κB regulates the expression of anti- and pro-apoptotic proteins. P53 is also inhibited by NF-κB. From Bours et al. [44].

The IL-1 family comprised of several cytokines including IL-1α, IL-1β and Interleukin 1 receptor antagonist (IL1-Ra), has a central role in regulating the innate immune response [48]). Cytokines of the IL-1 family exert their inflammatory effects through both receptor and nuclear interactions. The IL-1Ra binds competitively to the same receptor as IL-1β and thereby suppresses the pro-inflammatory actions of IL-1β. IL-1β, also termed the fever molecule, is an important pro-inflammatory cytokine that regulates the expression of a number of genes involved in the inflammatory process e.g.COX-2, iNOS, most cytokines, chemokines and adhesion molecules [49]). IL-1β is probably a key player during systemic inflammation, though it is a secreted cytokine. Secretion of IL-1β takes place when cytosolic bulk precursors are cleaved and transferred into specific secretory lysosomes [48]. A co-localization among IL-1β and procaspase-1 together with intracellular cysteine protease

occurs in the lysosomes. Proteins called "IL-1β inflammasome" functions to convert procaspase- 1 into active caspase-1. Caspase-1 cleaves inactive IL-1β precursor to a mature, secreted and active cytokine. IL-1β may reduce apoptosis, by altering the ratio of anti-apoptotic/pro-apoptotic genes (BCL-2/BAX), but excess levels of IL-1β may cause mutations in tumor protein 53 (TP53) and possibly higher risk of cancer [50]. In the microenvironment-derived IL-1β many cells are involved, where key players are blood monocytes, tissue macrophages and dendritic cells, but lung epithelial cells can also respond to this cytokine. IL-1 itself could also induce its own gene expression [51].

IL-6 belongs to the cytokine family named " the interleukin-6 type cytokines" [52]). The cytokines belonging to this family have a bilateral effect, acting both pro-inflammatory and anti-inflammatory properties. They are involved in the haematopoiesis, acute as well as inflammatory responses. Proteins in this subfamily function as ligands to an IL-6 receptor complex. IL-6 type cytokines direct their effect through the signal-transducers glycoprotein 130, Leukemia inhibitory factor (LIF) receptor and Oncostatin M (OSM) receptor, which mediate activation of cascades [Janus kinase/ signal transducer and activator of transcription (JAK/STAT) and mitogen-activated protein kinase (MAPK)]. A soluble, non signaling, type receptor also exists where IL-6 binds to the membrane receptor β-chain – gp130 resulting in a cellular signal. IL-6 stimulates generation of acute phase proteins (hepatic) and has demonstrated stimulation of an anti inflammatory mediator i.e. generation of IL-1Ra [53].

Two major groups of chemokines exist, called α (C-X-C) and β (CC) [37]. IL-8, belongs to the C-X-C chemokine family, and is a central activator and chemoattractant for netutrophils [54]. Various normal and tumor cells have demonstrated production of IL-8. Different stimuli induce the generation of IL-8. Three promoters are involved in the constitutive expression of IL-8. First, the promoter for activator protein-1 (AP-1)-like factors, second the promoter for NF-κB-like factors, and third the promoter for NF-IL-6-like factors [55]. Mutations in AP-1 and NF-κB binding sites damage also the promoters' ability to constitutively express IL-8. However, mutations in the NF-IL-6 binding site retained some promoter function. IL-8 is also regulated by MAPK. MAP kinases are important mediators that transduce signals into the nucleus from the cell-membrane [56]. Exposure to particles may be a stress factor for cells through induction of oxidants that has indicated to result in the release of IL-8 [57]. Inflammatory cytokines may contribute to the up-regulation of IL-8 expression. The expression of IL-8 can be induced by many cytokines such as TNF-α and IL-1. A relation between oxidative stress and expression of IL-8 has been demonstrated in airway epithelial cells [56].

ROS/RNS have been demonstrated to directly react with DNA and pose DNA damage such as base deletions, base modifications, chromosomal gains or losses and microsatellite instability. Furthermore, ROS/RNS have the capability to induce pro-inflammatory reactions by activating various transcription factors such as NF-κB which will further induce expression of multiple inflammatory genes such as *IL1B*, *IL6*, *IL8* and *COX-2*. The ROS/RNS may also affect apoptosis. Inhibition of apoptosis may promote neoplastic development from

inflammatory cells. Local generation of ROS/RNS has been related with accumulation of TP53 which occurs as a result of cellular stress and DNA damage. ROS/RNS are also capable to damage mitochondria which will lead to a release of cytochrome C and an induction of pro-apoptotic signaling molecules such as B-cell lymphoma 2 (Bcl-2). The intrinsic mechanism of ROS induced apoptosis causes damage to the mitochondria followed by a discharge of cytochrome C into the cytoplasm [38].

ROS/RNS may also activate cell signaling pathways regulated by MAPKs and extracellular signal regulated kinases (ERK). These genes are involved in inflammatory influx, inhibition of apoptosis and cell proliferation. TP53 is another gene which is also affected by ROS/RNS. Figure 1.6 depicts some of the cellular mechanisms triggered by ROS/RNS. TP53 is found to be very sensitive toward DNA damage. The apoptotic response of TP53 is also indirectly stimulated by enhanced levels of ROS. TP53 has the ability to regulate oxidative stress, by decreasing the level of intracellular ROS in the absence of acute stress. However, during maintained stress, the defensive function of TP53 will change to induce apoptosis.

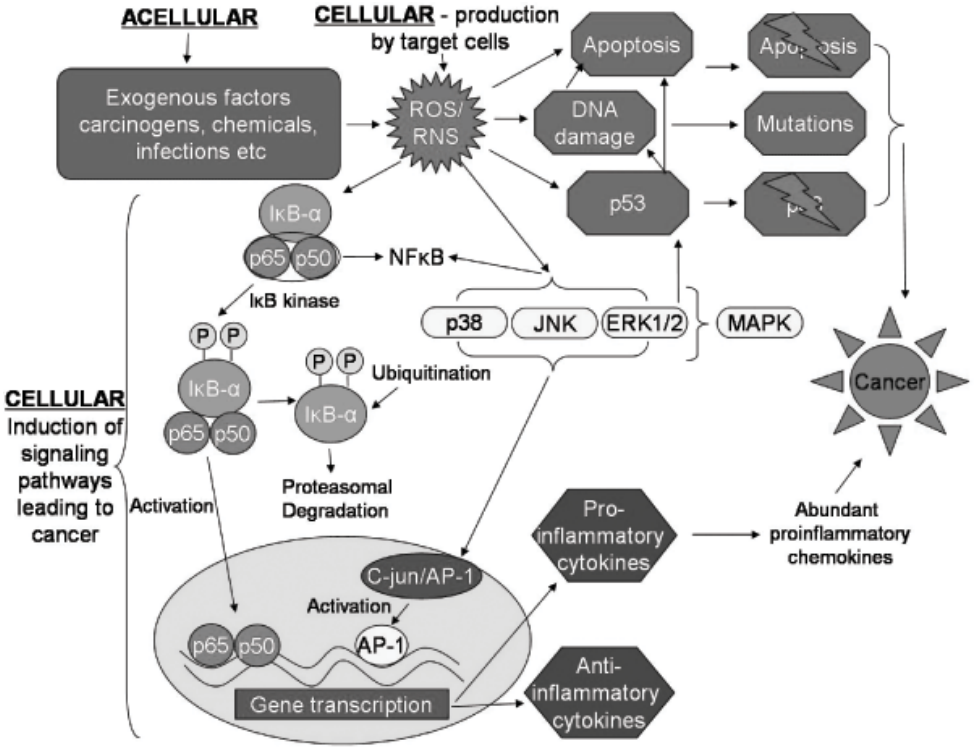

Figure 1.6: Illustration of important mechanisms and pathways induced by the production of oxidative stress following stimulation of cytotoxic or genotoxic insults e.g. particles. From Azad et al. [38].

1.3.2. The role of CNTs in induction of oxidative stress

Particle exposure may enhance oxidative stress which further will increases the expression of many epidermal growth factor receptor (EGFR) ligands [58]. In relation to oxidants generated by particle components, radicals may be directly bound to particle surface or produced as free components in solutions. To cause cell signaling or genotoxic effects, oxidants formed by

particles must directly interact with or be in close contact with their target molecule e.g. DNA or receptor. Particles may also generate radicals in solutions e.g. particles may produce H_2O_2, OH, O_2^- and O_2. Both particles and an inflammatory process can cause cell proliferation through generation and secretion of oxidants [59]. Figure 1.7 illustrates the pathways induced by nanoparticles, such as MWCNT.

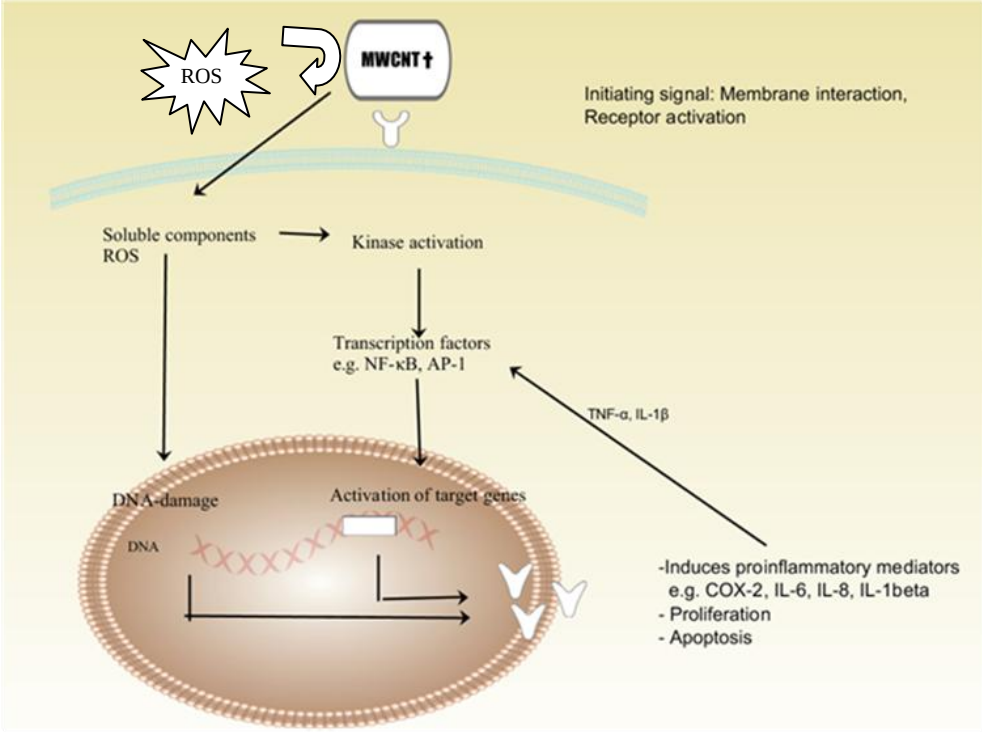

Figure 1.7: MWCNT-induced cellular effects. Initiating factors may be membrane interaction, formation of oxidative stress or activation of cellular membrane receptors (EGFR). Further potential intracellular effects could be activation of different kinases (MAPK) and activation of transcription factors. MAPK may also be stimulated by membrane receptors through interactions of oxidants, soluble metals, ligands and ROS/RNS generated by inflammatory cells. Activation of essential transcription further activates the transcription, mediating cellular effects. The direct formation of reactive oxygen species may among others cause damage to the DNA.

Different studies have considered the hypothesis whether an exposure to CNTs will result in the induction of ROS. The study by Reddy et al treated human embryonic kidney cells (HEK) with various concentration of MWCNT (10-100 µg/ml) and found that a concentration dependent cytotoxicity was associated with increased production of oxidative stress [60]. Similarly, the study by Ye et al. is demonstrating that MWCNTs (25-150 µg/ml) stimulate production of ROS, where the activation of NF-κB also seems to be involved in the cytokine production (IL-8) of human lung epithelial cells (A549) [57]. Contrary to the two mentioned studies, the study by Tsukahara and Haniu indicates a cellular uptake, decreased cell viability and increased LDH leakage without any significant generation of oxidative stress upon MWCNT exposure (0.1-30 µ/ml) to human bronchial epithelial cells (BEAS-2B). One obvious difference of this study compared to the two others is the low concentration range used. This study also made use of highly purified MWCNT without any presence of iron (potential hazard), and suggested that highly purified MWCT is not a potent induces of

ROS[61] Another study is verifying the hypothesis is Srivastava et.al who demonstrates the significant role of MWCNTs in both oxidative stress and apoptosis in human lung cell line A549. Both induction of apoptotic bodies, DNA fragmentation and increased caspase-3 activity were observed after exposure of MWCNTs (10 and 50 µg/ml), but with a delayed response (72 h). TP53, the pro-apoptotic component, was also found upregulated in the same study, after exposure to MWCNTs proving a role in apoptosis of MWCNTs at higher concentrations[62]. A summary of mechanistic health effects after particle exposure is illustrated in figure 1.8.

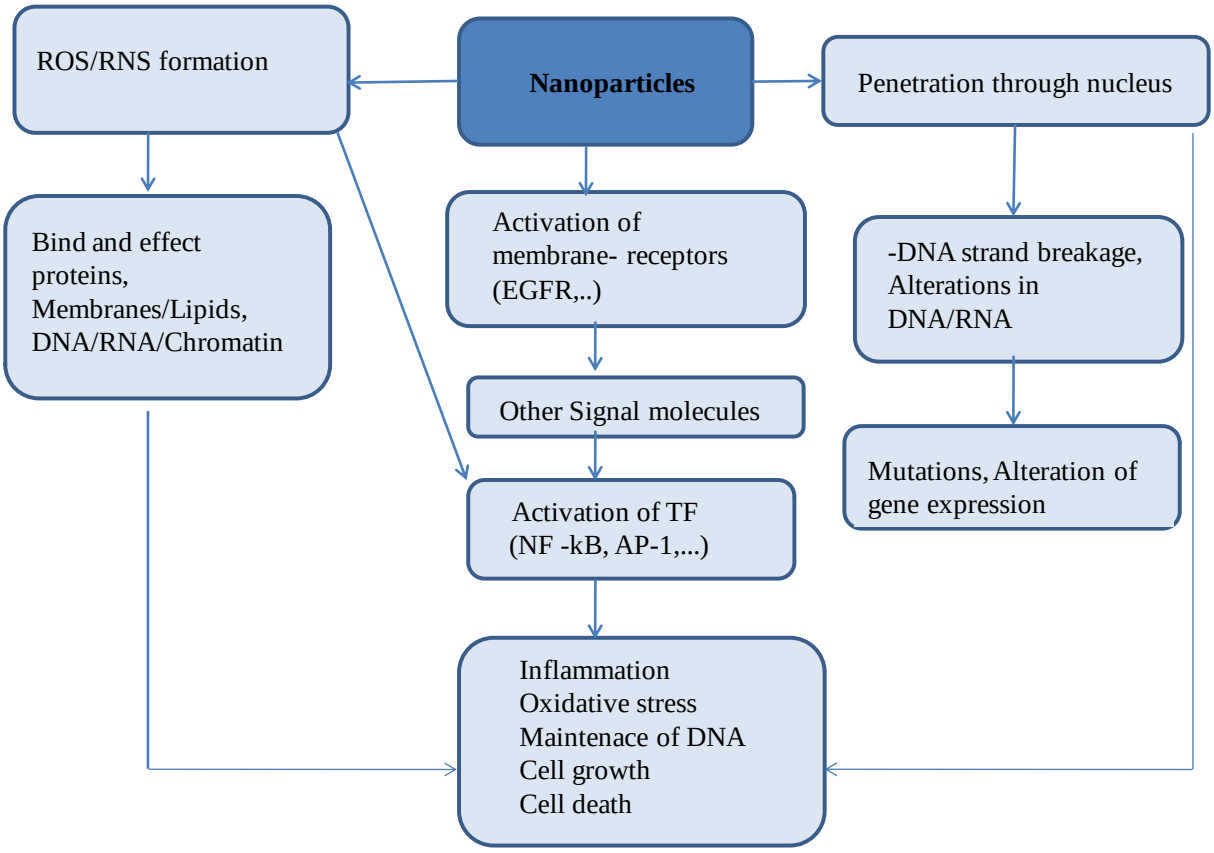

Figure 1.8: Paradigm of the fate of nanoparticles (NP). The main response to NP is oxidative stress (ROS/RNS). ROS may cause direct effect or activate transcription factors. MAPK may also activate the transcription factors with aid of epidermal growth factor receptors (EGFR) activation (direct NP exposure or NP stimulation of EGFR ligand expression). NP may interact with DNA if penetrated though the nucleus. All pathways may result in alteration of important genes (modified from Mühlfeld et al. [58])

1.4. Cell death

The process of cell death is generally divided into apoptosis and necrosis. Figure 1.9 illustrates schematic the differences between the two processes.

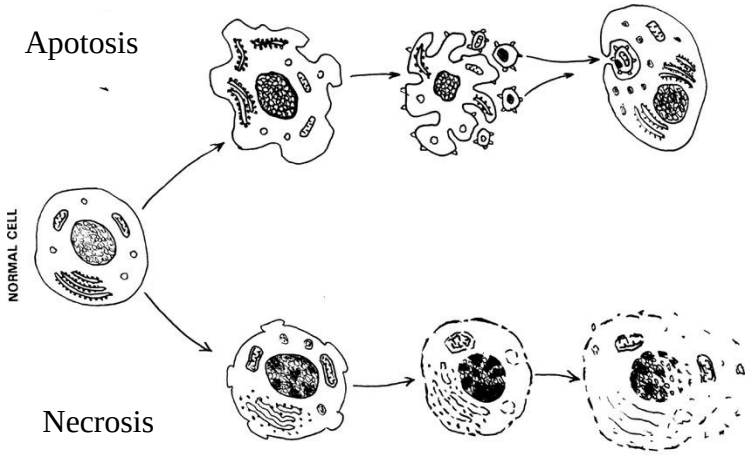

Figure 1.9: Steps of the apoptotic and necrotic cell death process. From van der Meer, et al. [63].

1.4.1. Necrosis

Exposure to toxicants can result in damage to the plasma membrane and further alterations of important biomolecules [64]. Lost control of the intracellular ionic balance, imbibe water, and lyse could be some consequences. Results could also be loss of ATP or membrane pumps, disturbance of the optimal pH and damage to the mitochondria. The process of necrosis is an uncontrolled cell death, resulting in release of intracellular constituents and strong inflammatory response [65].

1.4.2. Apoptosis

Apoptosis, the programmed cell death, is a process characterized by nuclear condensation, blebbing of the plasma membrane, and breakdown or fragmentation of DNA, Golgi, endoplasmic reticulum (ER) and mitochondria (formation of apoptoic bodies) [66]. The cell disposal is strictly controlled and neighboring cells stay unaffected during the process [67].Apoptosis is from the outside recognized as lonely cells that shrink and deformate. With their unique characteristics, the cells are tagged for phagocytes to rapidly engulf them from the milieu before any leakage of cell contents to surrounding environment causing inflammation may occur. Various proteins from the mitochondrial intermembrane space e.g. cytochrome c, are released [67]. Cytochrome c, found in the mitochondria, is capable of stimulating the caspase-activating complex where activation of cystein-aspartat proteases (caspases) is vital in the apoptotic process. The initiator caspases (caspase-2, -8, -9, and -10) are activated by adoptor molecules and function by cleaving and activating effector pro-

caspases. Activation of effector caspases (caspase-3,-6,and -7) cleaves many proteins resulting in the specific morphologies and characteristics of apoptosis. Cell stress or cell damage may trigger the apoptotic pathway directly by targeting mitochondria or indirectly by the caspase-8 mediated cleavage of the inactive cytosolic protein BID (BH-3 protein family). [67].

Mutations in genes regulating the apoptosis such as TP53 may result in deregulation of apoptosis and possibly cancer [65]. The TP53 has an important functions such as a transcription factor regulating the expressions of crucial genes [68]). One response to TP53 is the induction of apoptosis by stimulating expression of apoptotic genes involved in both extrinsic and intrinsic pathways (e.g Bcl-2, BAX). TP53 seems to include a transcriptional function and an independent-transcriptional (cytoplasmic) function, where both may advance the apoptotic response. PUMA, and important mediator of apoptosis, promotes apoptosis when over expressed (encode the BH3-domain proteins) and may act as a link between the transcriptional and the cytoplasmic function of TP53.

1.5. Biological effects of particle exposure in the lung

Lungs are exposed to particles in two ways; inhalation or through the bloodstream. The large surface area of the lungs causes exposure to pathogens, pollutants, oxidants, gases and toxicants from inhaled air [38]. The lungs are protected by surfactants, antioxidants, epithelium, alveolar macrophages, dendritic cells, the mucocilliary escalator, and secretory immunoglobulins [58]) .

Inflammation of the lung is regarded central to development of adverse health effects associated with particle exposure. Several studies have documented contribution of fine particles to disorders of the respiratory system, such as chronic obstructive pulmonary disease (COPD) and asthma together with cardiovascular and metabolic diseases that are consequences of systemic effects [69]. Inhaled particles are deposited differently in the respiratory organs depending on their size, shape or other properties [13]). Diffusional motion influences deposition according to particle dynamics (size, shape or other dynamic alterations due to breathing), geometry of the airways and alveolar structures, and breathing pattern. Inhaled particles not deposited in the upper airways are deposited in the alveoli by an increasing rate as the particle size decreases below 500 nm in diameter. But the different parts of the lungs contain a maximal limit of deposition within a specific diameter (Figure 1.10).

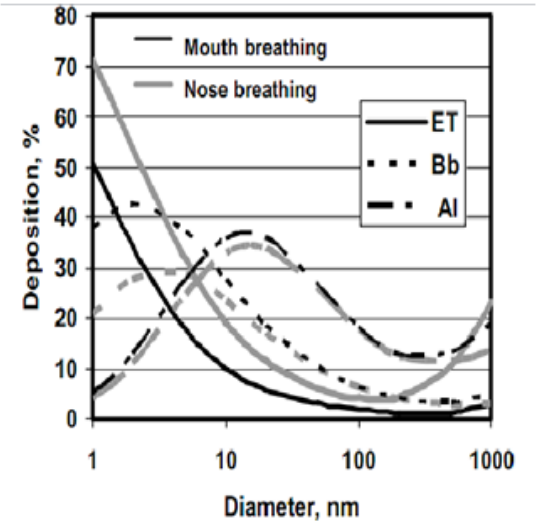

Figure 1.10: Deposition of inhaled NP with diameter between 1-100 nm from nose and mouth breathing in the extra thoracic airways (ET), the bronchial airways (Bb) and the alveolar region (Al) during breathing at rest, predicted by ICRP 66 model (ICRP, 1994). From Borm et al.[13].

The fate of particles also depends on their solubility. Highly water soluble particles are generally non-toxic and deposit early in the respiratory system whereas insoluble particles can penetrate deeply into the alveolar space. Highly insoluble particles have potential to cross the epithelial barrier, translocate and cause toxicity to distant compartments through the bloodstream. Insoluble particles can persist in the lungs for a long period of time [13]. Insolubility has proved to affect normal clearance mechanisms of the lung during inflammation and fibrosis. In the lungs, particles lead to secretion of various inflammatory mediators, e.g. cytokines, growth factors, ROS/RNS etc [57].

Diffusion is the main transport mechanism for NPs and therefore CNTs have the potential to penetrate deeply, in the alveolar regions of lung [70]. In the alveoli, the particle may come in contact with protein surfactants and may be transferred from the airspace to the hypophase. In the hypophase, NP may interact with proteins, be phagocytized by alveolar macrophages, bound to epithelial surface proteins, ingested by epithelial cells (endocytosis), translocated over the alveolar epithelium (paracellular transport) or localized in the interstitial space

Huczko et al. tested various types of MWCNTs exposed to Guinea pigs (intratracheal instillation: single dose of 15 mg) for a period of 90 days. This study experienced pathogenic results, e.i., obliterating bronchiolitis, desquamative interstitial pneumonia (with mild fibrosis around bronchioli), increase in resistance to pulmonary dilation and infiltration of bronchoalveolar space by inflammatory cells, emphysema and alveolar exudation were demonstrated [71]. Effects demonstrated to depend on the type of MWCNT together with duration of exposure [71]. Grubek-Jaworska et al. performed a similar study (*in vivo*) testing effects of four types of MWCNTs and SWCNTs exposed to Guinea pigs (intratracheal instillation: single dose of 12.5 mg) respectively for three months. All test materials caused pneumonitis with an interstitial non-specific focal reaction with little fibrosis. Amount of IL-8

in the bronchoalveolar lavage fluids was enhanced for one type of CNTs. A second type of CNT indicated increased amount of macrophages, lymphocytes and neutrophils and a third type showed elevated levels of macrophages and eosinophils. Most deposits of CNTs were found in the bronchioli. The authors suggested the physical structure and insolubility of CNTs to be causes to observed pathogenic effects [72].

Previous studies, mainly in rodents, indicate lung toxicity as a cause of exposure to CNT (mostly SWCNTs), with premature growth of fibrosis and granulomas, hypertrophy of epithelial cells, and following functional weakening [12]. SWCNTs are found more toxic compared to MWCNTs for alveolar macrophages, controversially a few studies obtain no cytotoxic effect after exposure to SWCNTs [73].

1.6.The hypothesis and project objectives

Inhalation is the main exposure route concerning particle exposure, where the lung epithelium serves as an important first line of defense. Inhaled particles may induce cellular responses in the epithelial cells of the lung including development and maintenance of a chronic inflammation. Chronic inflammation as a result of inhalation of the fiber-like compounds such as asbestos has been shown to lead to several adverse health effects in the lung including fibrosis and cancer. Due to the structural similarities with asbestos, carbon nanotubes particularly multiwalled carbon nanotubes may lead to the similar adverse effects following exposure of lung cells. The published toxicological studies with MWCNTs have shown that these CNTs may induce oxidative stress, inflammation, DNA damage and cell death. However, it has been hypothesized that responses may vary between CNTs produced by different producers, different methods and even varying from batch to batch from the same producer.

The objectives of this study were to investigate the cellular responses, and some of the molecular mechanisms involved in CNT exposure, using MWCNTs manufactured in Norway (MWCNT-NO), and in Japan (MWCNT-JP). It was also aimed to compare these effects with a known asbestos fiber (crocidolite) and an oxidative agent (hydrogen peroxide). Two human lung epithelial cell lines were used as an *in vitro* model system to investigate cellular endpoints such as cytotoxicity, apoptosis and changes in gene expression of inflammatory and apoptotic genes following the exposures. An outline of the experimental design of the project objectives is given in figure 1.11.

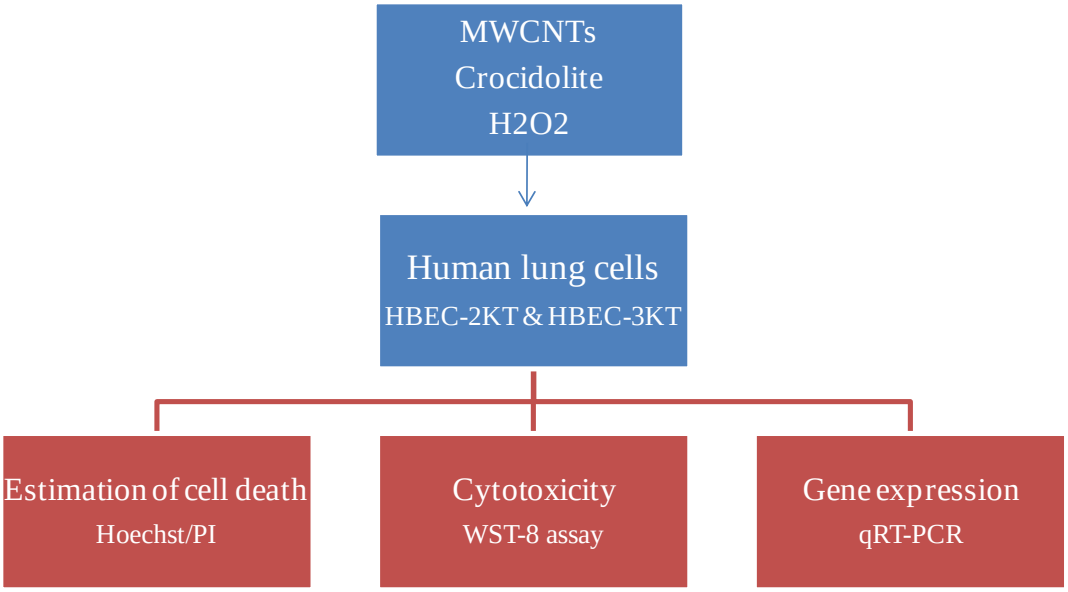

Figure 1.11: Outline of the project process and methods

2.Materials and Methods

The complete list of various kits, instruments, chemicals and solutions are included in Appendix I.

2.1.Culture of Human Bronchial Epithelial Cells (HBECs)

The Human Bronchial Epithelial Cells (HBECs) used in this thesis were immortalized through the expression of two genes, human telomerase reverse transcriptase (*hTERT)* and cyclin dependent kinase (*Cdk4*) [74]. The cells, HBEC-2KT and HBEC-3KT, were kindly provided by Dr. Minna J.D (Hamon Center for Therapeutic Oncology Research, Texas, USA). The cells were obtained from non-cancer lung tissue from two individuals, with the age 68 and 65 years respectively. Furthermore, both the individuals were exposed to cigarette smoking (see Appendix I). Cells were immortalized by transfection with retroviral constructs of *cdk4* (to hinder premature growth arrest and prevent stress) and hTERT, (to bypass telomere dependent senescence) to achieve continuously growing cultures. These immortalized cells include few genetic alterations, do not have a malignant phenotype, contain an intact p53 checkpoint pathway, and are valuable cells for understanding the pathogenesis of respiratory diseases [74].

Cells were incubated in 5 % CO_2 at 37ºC, they were kept in logarithmic growth and split twice a week. Furthermore, the cells were kept in collagen-coated 100-mm cell culture dishes, to facilitate attachments, and cultured in LHC-9 medium supplemented with 1 % Penicillin-Streptomycin. Cell morphology can be viewed in figure 2.1.

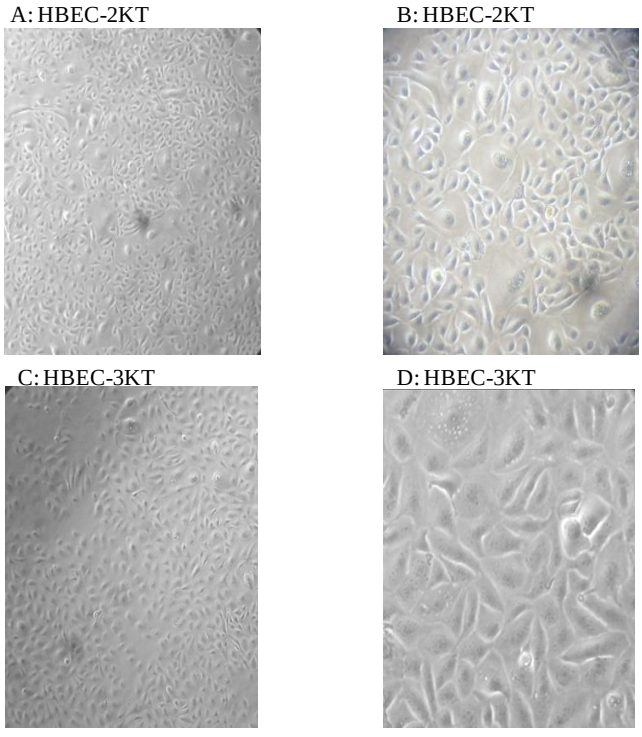

Figure 2.1: Cell morphology observed in light microscopy

2.2.Test materials

Two samples of MWCNTs and crocidolite asbestos and H_2O_2 were used during this study (see Appendix I).

The Norwegian MWCNT (Oslo, Norway), is abbreviated as MWCNT-NO. MWCNT-NO is prepared by the Arc discharge method [75] and has not been subjected to cytotoxicological experiments previously. Grossly physical characterization was performed by Scientist Asbjørn Skogstad (National Institute of Occupational Health, Oslo, Norway) using Scanning Electron Microscopy (SEM). Characterization supplied by the manufacturer is listed in table 2.1. A second MWCNT, supplied by MITSUI & Co. (MWNT-7, lot # 05072001K28, Tokyo, Japan), is used as reference and abbreviated as MWCNT-JP. MWCNT-JP is manufactured by chemical vapor deposition (CVD) [76], and has previously been subjected to various toxicity studies [27, 30, 77].Characterisations from two previous studies, are illustarted in table 2.1. Grossly physical characterisation was performed by Asbjørn Skogstad using SEM.

Table 2.1: Characterization of multiwalled carbon nanotubes.

Characterization of multiwalled carbon nanotubes		
Source	MWCNT-NO	MWCNT-JP
Diameter supplied by the manufacturer (nm, mean±SEM)		40-50
Diameter supplied by Poland et al. [27] (nm, mean±SEM)		84.89 ± 1.9
Mean length as supplied by the manufacturer (µm)		13
Percentage fibers greater than 20 µm		11.54
Diameter supplied by authors (nm, mean±SD)		88 ± 5
Mean length as supplied by Asakura et al. [77] (µm, mean ± SD)		5 ± 4.5
Percentage fibers greater than 5 µm		38.9
Diameter supplied by the manufacturer (nm, mean±SEM)	26.7 ± 3.7	
[Min,Max] interval of diameter (nm)	[2, 67]	
Mean length as supplied by the manufacturer (µm, mean ± SEM)	1.4 ± 0.1	
[Min,Max] interval of length (µm)	[0.2, 5.4]	

UICC Crocidolite Asbestos, supplied by Medical Research Counsling (England), is well known and used as a reference biopersistent fiber. Hydrogen peroxide (H_2O_2) supplied by Sigma –Aldrich (Steinheim, Germany), is a positive control as an oxidative agent known to cause ROS.

2.2.1. Handling of test materials

MWCNTs are hydrophobic materials that tend to aggregate/agglomerate [77]. To help disperse these aggregates/agglomerates into isolated fibers or prevent further aggregation, the NMs can be suspended in a suitable dispersion medium (DM) or solvent followed by ultrasonication.

2.2.2. Dispersion medium

A well tested DM was used for this study [25]. This DM is tested to be non-toxic and provides a lower degree of agglomeration for various test materials e.g. MWCNTs. The

contents of this DM were made to function as a “lung fluid mimic”, meaning to mimic the expected environment or status of lungs that aggregated/agglomerated fibers can meet (*in vivo*). The DM used consisted of PBS including various ingredients, briefly described in Porter, et al [25]. The premade dispersion medium was filtered through a 0, 45 µM/ 0, 20 filter, vortexed for 3x5 seconds and briefly utrasonicated for 2x30 (6W output and 20 % duty cycle) seconds before use.

2.2.3. Dispersion of test material

The three fibers MWCNTs and crocidolite were adequately weighed out, and suspensions of MWCNTs and crocidolite were made in DM (1 mg/ml). A couple drops of Tween 80 were added to avoid aggregation and increase the solubility of long and highly aggregated materials. A three-step sonication -process was in minimum applied to disperse test materials. The probe sonicator was thoroughly cleaned (with 70% ethanol and distilled water), before samples were ultrasonicated (6w output and 20 % duty cycle) for 3x5min at 4°C (samples were placed in ice).

Figure 2.2 illustrates the effect of dispersion medium (DM), Tween 80 and ultrasonication procedure on MWCNTs to avoid aggregation and disperse the test material.

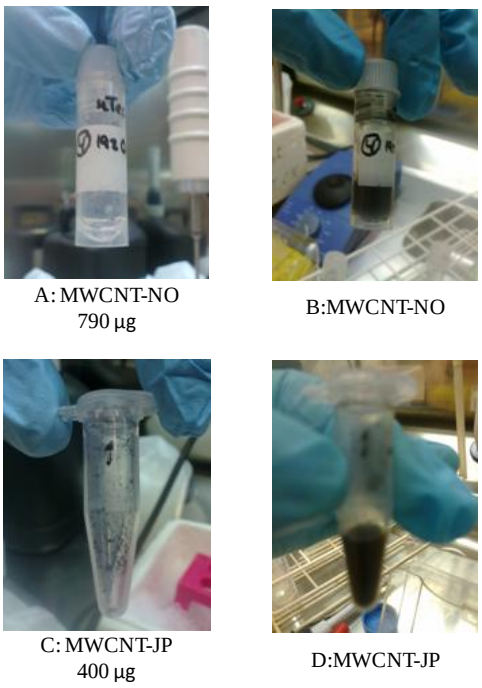

Figure 2.2: Before and after images, showing good dispersion of agglomerated (790 µg) MWCNT-NO (A-B) and (400 µg) MWCNT-JP (C-D) into dispersed fibers in dispersion medium after 3x5 min ultrasonication .

2.3.Cell culture

2.3.1. Cytotoxicity (WST-8) assay

Cells (HBEC2-KT and HBEC3-KT) were pre-cultured ($5x10^3$ cells/well) 24 hours before exposure in a 96-well dish (*i.e.* incubated at 37°C, 5% CO_2). Various cell densities ($5x10^2$, $1x10^3$, $2x10^3$, $3x10^3$, $4x10^3$, $5x10^3$, $1x10^4$ and $2x10^4$ cells/well) were cultured in the same 96-well dish, for a standard curve (See figure A2.1 in Appendix II). The standard curve will inform about the growth phase for the two different cell lines without any exposure. Each well, contained a total volume of 100 µL cell suspension.

It is important that the culture medium contains small or no amounts of phenol red, due to risk of interruption with later absorbance measurements.

2.3.2. Hoechst/ propidium iodide staining for apoptotic and necrotic cells

Cells (HBEC2-KT and HBEC3-KT) were pre-cultured ($1,1x10^5$ cells/ well) 24 hours before exposure in 12-well dishes and incubated (*i.e.* incubated at 37°C, 5% CO_2) for cell attachment to wells. Each well, contained a total volume of 900 µL cell suspension.

2.3.3. Determination of Gene Expression

In advance of RNA isolation, both cell lines were seeded in 6- well plates (3,5 cm^2). Cell density was $3,0x10^5$ cells/ well for HBEC-3KT and $4,0x10^5$ cells/ well for HBEC-2KT.
Each well, contained a total volume of 2 ml cell suspension.

2.4.Exposure of cells to test materials

Adequate dilutions, of dispersed test materials, in growth medium (LHC-9) were prepared (µg/ml), where all samples included 10 % DM. The samples were thoroughly vortexed and made ready for exposure to cells (more detailed procedure, see [25],[26],[78]). Different dilutions of H_2O_2 in growth medium (µM), were prepared from a 30 % 1mM stock solution (8,8M) blended with dH_2O. Samples containing H_20_2 were under all circumstances kept at 4°C.

Amount of suspensions added for the different exposures in this study, were based on total area of the specific culture dish used, so that amount of particles/area remain constant for each dish.

2.4.1. Cytotoxicity/Cell viability assay

After 24 hour incubation, the medium from each well was gently removed, before cells were cultured with various concentrations of premade dilutions of dispersed test materials (100 µl). Each cell line was exposed to six different concentrations of every test material and three replicates were carried out for all the different concentrations The various concentrations of test materials used are illustrated in table 2.2.

Table 2.2: Different concentrations of test materials used in cytotoxicity assay

H_2O_2 (µM)	MWCNTs & Crocidolite (µg/ml)	MWCNT-JP (µg/ml)
Control (Unexposed)	Control (Unexposed)	Control (Unexposed)
5	5	0.1
10	10	0.5
20	20	1
40	50	2
100	100	10

After appropriate exposure-time (6, 24, 48 and 72 hours), phosphate buffered saline (PBS) was used to wash cell monolayers. The washing step was performed to remove dead cells including test materials that could interrupt later absorbance measurements (2x PBS for MWCNTs & crocidolite and 1x PBS for H_2O_2).

Cell viability was evaluated using the WST-8 Cell Counting Kit (SIGMA)

2.4.2. Hoechst/ propidium iodide staining for apoptotic and necrotic cells

After 24 hour pre-culturing, the medium from each well was gently removed, before cells were cultured with various concentrations of premade dilutions of dispersed test materials (900 µl) for 24 hours. As a positive control to detect apoptotic cell death, HBEC-2KT and HBEC-3KT were treated with Thapsigargin, and cultured for 96 hours.

The various concentrations of test materials used are illustrated in table 2.3. Each concentration is based on results from the cytotoxicity assay, where approximately 80 % cell viability (low cell death) was observed. Two replicates were carried out for all the different concentrations.

Table 2.3: Various concentrations of test materials for Hoechst/PI staining

Test material	Concentration
MWCNT-NO	1 (µg/ml)
MWCNT-NO	5 (µg/ml)
MWCNT-JP	0.5 (µg/ml)
Crocidolite	20 (µg/ml)
H_2O_2	5 (µM)
Thapsigargin	100 (nM)

After a suitable time of exposure (24 hour and 96 hour), cells were stained and smeared on cover slips to be analyzed with use of fluorescence microscopy.

2.4.3. Determination of Gene Expression

After 24 hour pre-culturing, the medium from each well was gently removed, before cells were cultured with various concentrations of premade dilutions of dispersed test materials (2,5 ml) for 24 hour.

All cells were exposed for 24 hours to various concentrations of testing materials, as table 2.4 indicates. Concentrations used are based on results received from previous cytotoxicity assays, where results of low cell death (20 %) were observed. Two replicates were carried out for all the different concentrations.

Table 2.4: Various concentrations of test materials for determination of gene expression

Test material	Concentration
MWCNT-NO	1 (µg/ml)
MWCNT-NO	5 (µg/ml)
MWCNT-JP	0.5 (µg/ml)
Crocidolite	50 (µg/ml)
H_2O_2	5 (µM)

After an appropriate time of exposure, each well was washed 3x PBS (2 ml) before plates were stored at -80°C, and made ready for RNA isolation.

2.5. Cytotoxicity evaluation

Cytotoxicity assay

For determination of cell viability, an absorbance based methods was used; the WST-8 Cell Counting Kit. This colorimetric assay measures the dehydrogenase activity of metabolically active cells.

Hoechst/PI staining

For determination of apoptotic cell death, Hoechst 33342 and propidium iodide staining, was used. By this method changes in cell morphology are detected by fluorescence microscopy.

2.5.1. Cell viability

Determination of cell viability, a preliminary experiment for this study, was performed before initiation of further experimental tests of interest could take place. The purpose was to define an appropriate dose as well as the exposure time of each test material, for both cell lines. A dose which leads to 70-80 % viability was of great interest. The timeframe is also important when examining the various test materials for viability. Different levels of confluence can be estimated after various periods of time, e.g. 6… 24, 48 and 72 hours.

The estimated doses and periods of time were used for further experimental studies.

WST-8 Cell counting kit

The WST-8 Cell Counting Kit assay (WST-8/CCK-8 assay) is a highly sensitive assay for determination of viable cells in various cytotoxicity experiments. The WST-8 assay makes

use of the tetrazolium salt WST-8 [2-(2-methoxy-4- nitrophenyl)-3-(4-nitrophenyl)-5-(2,4-disulfophenyl)-2H-tetrazolium, monosodium salt]. The dehydrogenase enzymes in viable cells will reduce WST-8 to the water-soluble formazan dye (yellow colour). The chemical reduction is caused by existence of an electron carrier. 1-Methoxy PMS (1-Methoxy-5-methylphenazinium) is the electron mediator which receives electrons from the viable cell and further transfers this electron to WST-8.

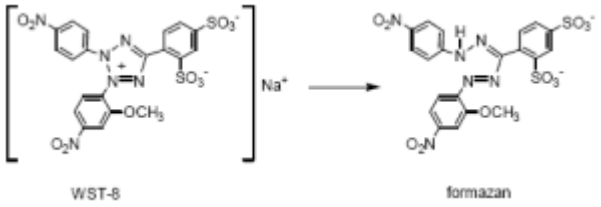

Figure 2.3: Structures of WST-8 and WST-8 formazan, the chemical reduction caused by dehydrogenase enzymes (From SIGMA).

The amount of yellow formazan dye generated is directly proportional to the number of viable cells. An absorbance at 460 nm is found to be proportional to the number of living cells in the medium. Determination of viable cells can therefore be decided with use of a known calibration curve for WST-8 formazan.

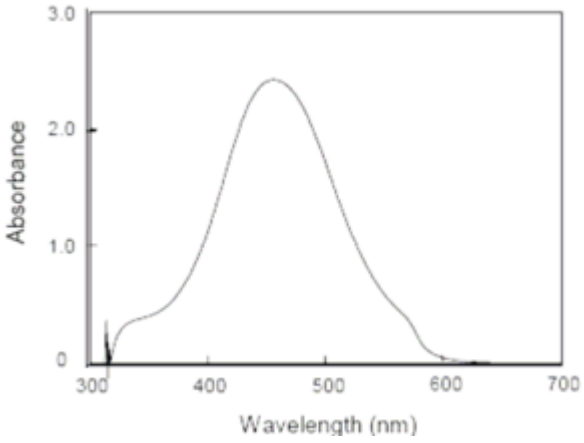

Figure 2.4: Absorption spectrum of WST-8 formazan (from SIGMA)

A specific procedure from the WST-8 Cytotoxicity Assay protocol was followed. For WST-8 Cytotoxicity Assay protocols, see URL;

http://www.dojindo.com/newimages/CCK-8TechnicalInformation.pdf

Absorbance was measured after 6, 24, 48 and 72 hours with a Modulus Microplate Multimode Reader. After Chromophore development (4 hours), OD measurement (450 nm with reference wavelength on 750 nm) was performed.

2.5.2. Hoechst/ propidium iodide (PI) staining for apoptotic and necrotic cells

Changes in the nuclear morphology and alterations of the plasma membrane are associated with cell death. Changes in cell morphologies can be detected with the use of microscopic methods. In this study, existence of apoptotic and necrotic cells were determined with fluorescence microscopy. Different stains were used to distinguish dead and viable cells. Hoechst stains the DNA in all cells (viable and dead) emitting blue fluorescence light, where apoptotic cells can be characterized by their condensated nucleus. Propidium iodid (PI) binds to DNA and emits red fluorescence light. However, the dye is unable to penetrate an intact cell membrane, resulting in detection of cells undergoing necrotic cell death.

Procedure for staining, smearing and visualizing apoptotic and necrotic cells on cover slips

Cell suspensions from every well were transferred to separate centrifuge tubes (~ 900 µl). Each well was washed 2x with PBS (250 µl). Cells were trypsinised (90 µl) at 37°C, 5% CO_2 until all cells were in suspension, and transferred to their respective tubes.

Cells ($1{,}1x10^5$ cells/ tube) were stained (20 µl) with propidium iodide (PI, 0,5 mg/ml) and Hoechst 33342 (1 mg/ml) for 30 minutes. The samples were centrifuged at 1200 rpm for 10 minutes. Supernatant was discarded and the collected pellet was suspended in 10 µl fetal bovine serum (FBS) 10 µl. Smears were made on micro slides from the suspended cells and air dried. Evaluation of cell death was performed using a fluorescence microscope. Cells containing distinct condensed nucleus, were assumed as apoptotic. The amount of apoptotic and necrotic cells were determined as a fraction of the total number of dead cells (see Appendix V.2).

2.6. Procedure for the determination of gene expressions

2.6.1. RNA isolation from cells

RNA extraction was performed for later conversion into cDNA (complementary DNA). The isolation process was executed in a cell culture bench with use of basic sterile techniques to avoid presence of RNase (ribonucleases) that may degrade RNA.

Isol-RNA Lysis Reagent (1 ml/ well) containing phenol and guanidine thiocyanate, was used to facilitate lysis of cells and to inhibit RNases. Cell suspension was homogenized with Isol-RNA Lysis Reagent by pipetting up and down several times. Through the lysis process cells were disrupted while the integrity of RNA was maintained. Cell suspensions were transferred over to separate RNase free micro centrifuge tubes by 5 minutes incubation at room temperature.

Chloroform solution (0,2 ml) was added to the sample, and mixed by vigorously shaking the tubes for 15 seconds and incubated for 2-3 minutes at room temperature. The homogenates were then centrifuged at 12 000 x g for 15 minutes at 4°C. A biphasic mixture was formed, with an aqueous phase containing the RNA (colorless) and an organic phase containing proteins (red). The two phases were separated by an interphase (white) containing DNA.

The aqueous phase, containing the RNA, was transferred into new RNase free tubes. RNA was precipitated with 0.5 ml isopropanol, followed by vigorous mixing, and 10 min incubation at room temperature. Another round of centrifugation at 12°000 g for 15 minutes at 4 °C was carried out to collect precipitated RNA.

The supernatant was discarded and the collected pellet was carefully cleaned with 75 % EtOH in Diethyl pyrocarbonate treated water (DEPC-water that is RNase free). After the cleaning step, all samples were centrifuged at 12 000 g for 5 minutes at 4 °C.

The supernatant was carefully discarded and the pellet was air dried for 15-20 minutes, to remove all traces of EtOH. DEPC water (10 µl) was added to re-dissolve the dried pellet and incubated at 65°C for 10 minutes. After mixing and collecting the RNA by a brief centrifugation the samples were placed in ice, and stored at -80°C.

Prior to cDNA synthesis to start, RNA concentration was measured on a Biophotometer (Eppendorf) with an absorbance at 260 nm and 280 nm for each sample, by diluting RNA (1 µl) with tris-EDTA (TE)- buffer (80 µl). The ratio OD_{260}/OD_{280} indicates the purity of the sample, where a ratio around 2 is estimated to be clean and of good quality.

2.6.2. cDNA Template synthesis (Reverse Transcription)

cDNA is created from mRNA template to a DNA copy in a reaction using the enzyme reverse transcriptase. Reverse transcriptase catalyze the addition of new nucleotides by hybridizing complementary oligo(dT) primers to an existing poly(A) tail of RNA and further synthesize a single strand of cDNA.

The previous extracted RNA from both cell lines in the following experiment was incubated at 65 °C for 10 minutes and reverse transcribed by the aid of qScript cDNA Synthesis Kit. The kit contains the novel qScript Reaction Mix, including a mix of oligo(dT), random primers and the qScript reverse transcriptase. This mix was blended together with RNA template (1µg), while kept in ice. The samples were run in the thermal cycler by the following schedule; 22°C for 5 min, 42°C for 30 minutes, 85°C for 5 minutes and 4°C for hold. The cDNA was diluted in TE-buffer (80 µl) to a final concentration of 10 ng/µl. All cDNA samples were stored at –20°C .

For reaction protocol, see URL:

http://www.quantabio.com/pdf/manual/95047%20(qScriptT%20cDNA%20Synthesis%20Kit%20PPS).pdf

2.6.3. Quantitative real-time PCR

Quantitative reverse transcriptase polymerase chain reaction (qRT-PCR) is an alternative to the standard PCR procedure quantifying DNA or RNA. With the use of sequence primers, the relative number of copies of DNA or RNA sequences can be determined. Quantification is possible if one measure the amount of amplified product at each cycle in the reaction with use of a fluorescent reporter

qRT-PCR can be divided into three steps . denaturation, annealing and extension.

1. The denaturation step is normally performed at 95°C. Undesired structures e.g. double stranded DNA (dsDNA) and DNA primer complexes will be removed by disturbing the non-covalent interactions between the two strands.
2. Annealing, also called hybridization, is when the primer binds the complementary sequence in the template. Primer length and GC-content are important factors when finding the optimal temperature for this reaction.
3. During the extension step DNA polymerase perform primer extension, by incorporating 3'-deoxy 5'- triphosphatases (dNTPs), and the complementary strand for cDNA is produced. Extension step is often combined with the annealing step, using 60°C as the temperature, when an amplicon in qRT-PCR is small.

Each reaction or cycle requires optimal conditions. A general reaction mixture contains a forward and reverse primer, dNTPs, a heat-stable polymerase, reaction buffer, divalent cations and cDNA template. The three steps briefly described constitute one cycle and is generally run for 40 cycles. If one or several components become depleted the reaction will terminate.

The qRT-PCR reaction is monitored during its' exponential phase that permits determination of the initial target to a high degree of certainty. In qRT-PCR, the amount of product after each cycle can be followed by monitoring the fluorescence of either a fluorescent probe or a DNA-binding dye e.g. SYBR Green, used for this study. The fluorescent signal from SYBR Green binds nonspecifically to double stranded DNA (dsDNA) that is present, and is directly proportional to the amount of product generated in the exponential phase of the reaction.

Gene regulation patterns between samples can, quantitatively through qRT-PCR be monitored by assessing the relative abundance of a transcript as it occurs in real time. If gene expression is high, amplification will be illustrated in earlier cycles. Furthermore, if expression is low the amplification will be illustrated in later cycles.

A reference gene, also called a endogene control, is necessary when comparing different samples in order to achieve accurate expression profiling of selected genes. Different samples generally contain different amounts of biological material, and the cDNA quality between samples may vary. Variation can be a result of different degrees of sample degradation or variation in the efficiency of cDNA synthesis. The reference gene, a housekeeping gene, is measured in the same sample to normalize for any possible variations in the cDNA input. This will allow accurate comparison of the expression of the gene of interest between different samples. The selected reference gene is assumed to be equally expressed in different samples from various tissues, including cell lines of various exposures.

With use of an instrument that combines thermal cycling with scanning capability, changes in fluorescence can be monitored during the reaction.

Protocol

Five different genes encoding cyclooxygenase-2 (COX-2), interleukin-1beta (IL1β), interleukin 6 (IL6), interleukin 8 (IL8) and tumor protein p53 (TP53) were analyzed for gene expression by qRT-PCR. HBEC-2KT and HBEC-3KT cells were exposed for four different test materials during two different exposure periods (see table 2.4). RNA was extracted and synthesized to cDNA and the cDNA template was used to analyze the expressions of the respective gene of interest for both cell lines (HBEC-2KT and HBEC-3KT). Stock solution of cDNA (10 ng/ µl) was diluted, in microfiltered water, into different concentrations depending on the gene to be analyzed. The concentration is set by optimizing its C_q value until a value in the range between 20 and 30 cycles is obtained. The amount of cDNA used in qRT-PCR were 25 ng (1.25 ng/ µl) for *COX-2*, *IL1B* and *IL6* and 5 ng (0.25 ng/ µl) for *IL8* and *TP53*.For the chosen reference gene, *ACTB*, 2.5 ng (0.125 ng/ µl).

To circumvent amplification of any DNA contamination, PCR primers were designed to span introns. All primers, ordered from Thermo Fisher Scientific, were designed using the Primer 3 program and PREMIER Biosoft international web page (http://frodo.wi.mit.edu/primer3/ and http://www.premierbiosoft.com/jsp/marketing/FreeToolLogin.jsp?PID=1). The sequences were checked for specificity by BLAST search. For further details regarding the primers, see Table 2.5

Table 2.5: Primers used for quantitative real-time polymerase chain reaction (qRT-PCR)

Primer	Sequence (5'→3')	bp	% GC	Tm°C	Product size (bp)
Actb forward *Homo sapiens*	GCG AGA AGA TGA CCC AGA TCA	21,00	52,38	53,75	76
Actb reverse *Homo sapiens*	GAT AGC ACA GCC TGG ATA GCAA	22,00	50,00	54,32	
Cox-2 forward *Homo sapiens*	ATC ACA GGC TTC CAT TGA CC	20,00	50,00	52,01	176
Cox-2 reverse *Homo sapiens*	CAG GAT ACA GCT CCA CAG CA	20,00	55,00	53,62	
Il1b forward *Homo sapiens*	ATG GCC CTA AAC AGA TGA AGT	21,00	51,00	42,86	153
Il1b reverse *Homo sapiens*	GCA TCT TCC TCA GCT TGT CC	20,00	52,88	55,00	
Il6 forward *Homo sapiens*	CCT TCC AAA GAT GGC TGA AA	20,00	45,00	50,09	70
Il6 reverse *Homo sapiens*	TTT CAC CAG GCA AGT CTC CT	20,00	50,00	52,91	
Il8 forward *Homo sapiens*	CTG CGC CAA CAC AGA AAT TA	20,00	45,00	51,33	81
Il8 reverse *Homo sapiens*	CTC TGC ACC CAG TTT TCC TT	20,00	50,00	52,17	
Tp53 forward *Homo sapiens*	CCA TCC TCA CCA TCA TCA CA	20,00	50,00	53,92	78
Tp53 reverse *Homo sapiens*	CAC AAA CAC GCA CCT CAA AG	20,00	50,00	55,24	

The reaction mixture used contained a forward and reverse primer, Perfecta SYBR Green Mastermix and micro filtered water. The reagents of the mastermix are included to dilute samples of DNA template and are illustrated in table 2.6.

Table 2.6::Mastermix solution for one sample

Reagents	**X1**
dH2O	4.6 µl
2 x Perfecta SYBR Green FastMix	10 µl
Primer up (25 pmol/µl)	0.2 µl
Primer down (25 pmol/µl)	0.2 µl
(Diluted cDNA)	(5 µl)
Total	20 µl

A serial dilution of a template, with a sample expressing target gene of interest to a high extent, was included to determine whether the qRT-PCR was optimized. The results can be used to generate a standard curve see figure 2.6. A linear standard curve, a high amplification efficiency and consistency across replicate reactions are important aspects of an optimized reaction. The cell-line A549 was exposed to 15 ng/ ml *TNFA* for 1 hour, was in this experiment used to make a standard curve (Figure 2.6). The dilution series for the reference gene, *ACTB*, was 12.5 ng, 3.13 ng,0,78 ng ,0.195 ng and 0.049 ng. The dilution series for each target genes was 50 ng, 12.5 ng, 3.13 ng, 0.78 ng and 0.195 ng.

All diluted cDNA samples including a non template control consisting of water (5 µl) was added in parallels together with the mastermix solution (15 µl) to a clear 96- well dish.

The quantification was performed on ABI PRISM 7900 HT Sequence Detection System with its' respective SDS 2.2 software guided through procedures shown in table 2.7.

Table 2.7: Different steps of quantitative real-time PCR (qRT-PCR)

Step	**Temperature (°C)**	**Time period**	
Initial denaturation of DNA and activation of Taq DNA	95	2 min.	
Denaturation of DNA	95	5 sec.	} 40 cycles
Annealing and extension of primers	60	30 sec.	
Dissociation	95	15 sec.	
	60	15 sec.	
	95	15 sec.	

2.6.4. Gene Expression Data Analysis

Data analysis was performed with aid of the SDS 2.2 software. A standard curve, amplification plot and melting curve was generated for each gene tested. The amplification plot is illustrated in figure 2.5. The X-axis illustrates the PCR cycles while Y-axis illustrates the intensity of the fluorescence, measured as ΔRn. In the exponential phase, the PCR doubles for each cycle. The stationary phase takes place when there are no more amplicons produced and thus the increase of the PCR product declines. C_q- value (Threshold cycle) is designated by a fractional number of PCR-cycles, where the curve reaches a particular threshold fluorescence signal level. The ΔRn threshold was for this report set to 1 (must be above the background level and before the stationary phase). Optimal C_q values are in the range between 20 and 30 cycles. For calculations used, see Appendix V.3

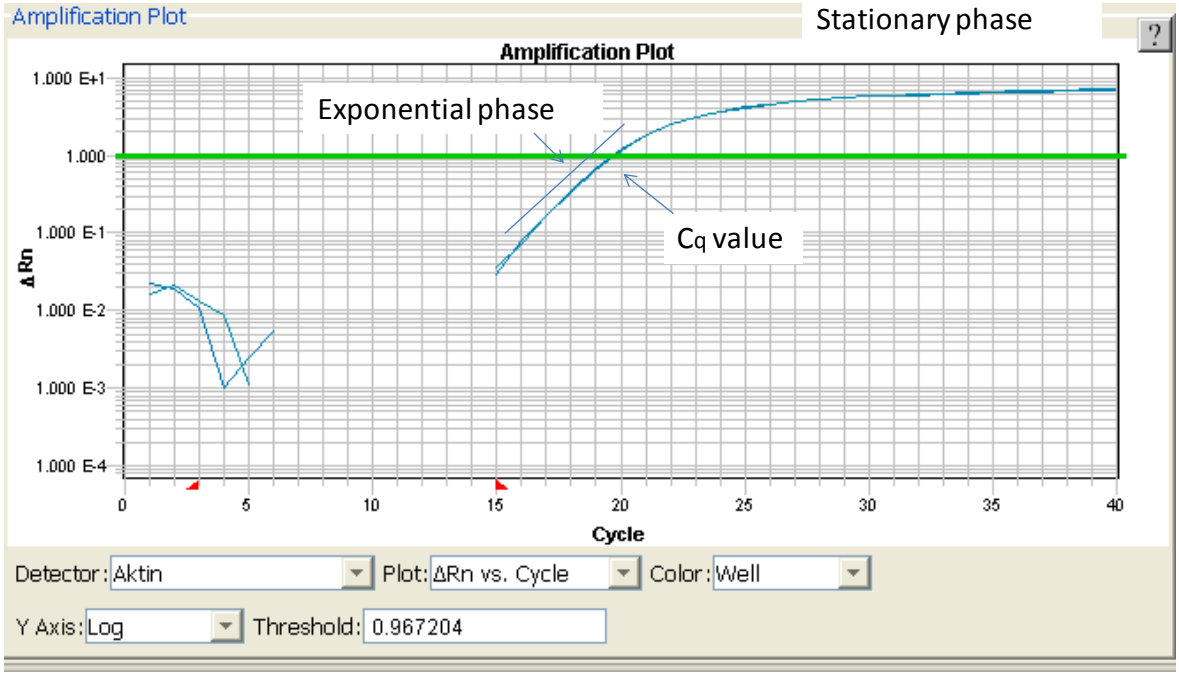

Figure 2.5: Amplification plot where the C_q-value, exponential phase and stationary phase is included

Figure 2.6 illustrates the standard curve. The optimal slope of the standard curve is -3.33 (efficiency at 100 %) indicating a perfect doubling of the PCR product per cycle. A slope between -3.3 and -3.6 is normal to accept. The negative sign indicates that a low amount of template claims more PCR-cycles to reach the set threshold compared to a high amount of template.

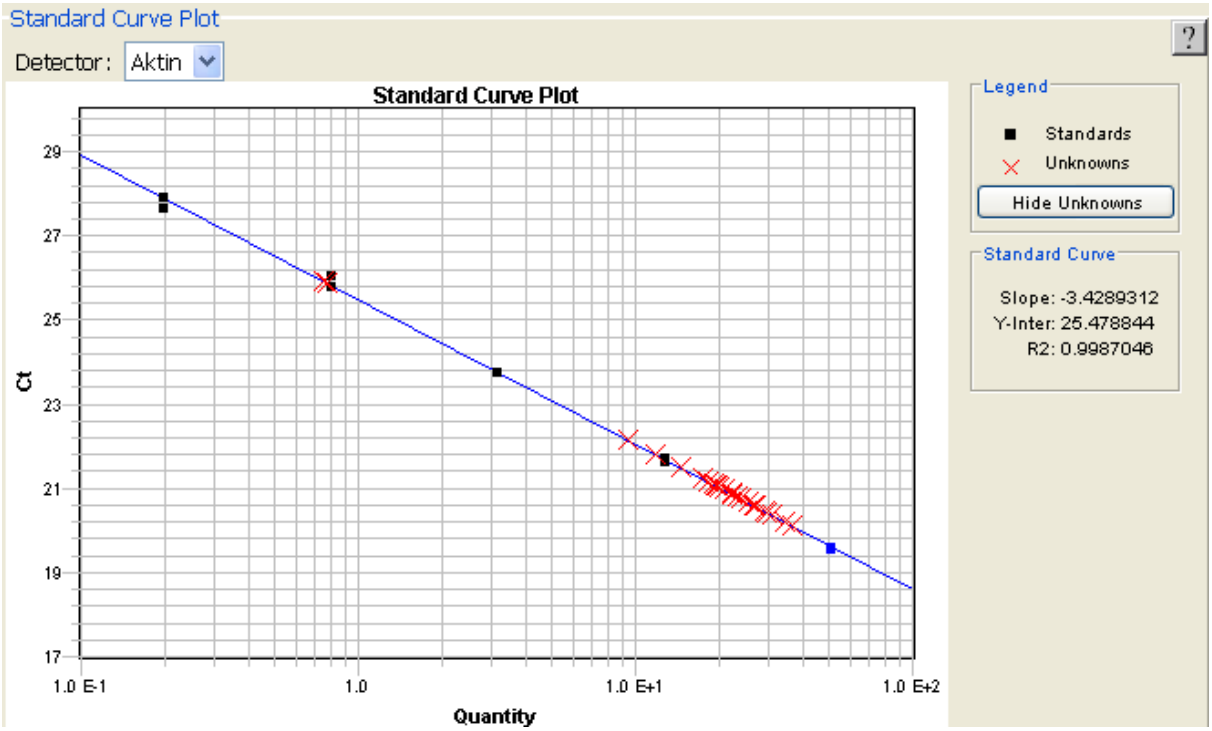

Figure 2.6: Standard curve with Cq (= Ct) values on the x-axis and quantity on the y-axis. The red cross illustrates the quantity to the test samples in relation to the standard samples

The melting curve (not shown) can be used to identify specific reaction products from non-specific products.

2.7.General human cell culture experiments

2.7.1. Coating of dishes or plates with pure bovine collagen

Purified Collagen solution for cell culture dissolved in 0.012 N HCl (2.7 mg/ml) was diluted in HBS to a total concentration of 0.03 mg/ml. Appropriate amounts were dispersed so it covered the dish to be coated. The coated dish was kept inside a cell culture bench for 2 hours, before the coating procedure was finished. The Collagen solution was thereafter removed, and the dish was washed with PBS .

2.7.2. Thawing of cells from liquid nitrogen storage

Protocol:

- Acquired ampoule containing the desired cell line was collected from liquid nitrogen storage.
- The ampoule was further thawed in a water-bath on 37°C.
- Cell suspension was transferred over to a centrifuge-tube (10 ml) and PBS (5 ml) was added.
- The suspension was then whirled down at 1000 rpm for 4 minutes and the supernatant was discarded in order to eliminate rests of dimethyl sulphoxide (DMSO).
- Cells (the pellet) where resuspended in culture media (~3 ml) and transferred to a 100 mm Petri dish (total of 8 ml LHC-9 media).

2.7.3. Maintenance and preparation of epithelial cell cultures

Cells were re-plated when level of confluence (70-80 %) was attained. Trypsin was used to degrade cell adhesion molecules anchored to the Petri dish. Trypsination is helpful when re-plaiting and maintaining the cell culture. The protocol used is thorough described below;

- Culture media covering the cells was discarded before cells were washed 2x with PBS (10 ml for a 100 mm Petri dish).
- Trypsin (1 ml of 1x dilution) was added to the Petri dish before located in a humidified incubator (*i.e.* at 37°C, 5% CO_2) until cells were in suspension.
- Trypsination was ended by adding complete culture media (5ml of LHC-9). The culture media was flushed over the dish to separate cells from each other and to thoroughly wash the Petri dish.
- Cells in suspension were further transferred to a centrifuge-tube/Falcon-tube before cells were whirled down at 1000 rpm for 4 minutes.
- The supernatant was discarded before cells were re-suspended in LHC-9 media (3-5 ml).
- When used for experiments, cells were counted and distributed to appropriate dishes in specific numbers. A small amount of cell suspension was stained with Trypan blue 0.4 % (10 µl cell suspensions in 10 µl Trypan blue) before cell counting. Trypan blue is useful when distinguishing between viable and dead cells. Viable cells shows out as lightning cells, while dead cells are blue due to permeated cell membranes.
- When not used in experiments, cells were maintained by distribution into diluted concentrations to new 100 mm Petri dishes.

2.7.4. Freezing of cells in liquid nitrogen

Storage of the human cell lines were carried out in liquid nitrogen, where cells were suspended in DMSO. DMSO helps preventing any crystallization and lysis of cell membranes.

Protocol used for freezing of cells:

After cells reached confluence, they were trypsinated as described in section 2.7.3 “Maintenance of cells”, whirled down and resuspended in AF (500 µl, antibiotic freeze media).

Cell suspension was transferred to a freeze- ampoule before DMSO (500 µl) was added to the ampoule.

The ampoule was primary placed in -80°C for 4-6 hours before storage in the liquid nitrogen tank. This process is performed to let the freezing process occur gradually.

2.8.Statistical analysis

In this section the focus is particularly on the description of the various statistical methods used. Data were analyzed on PASW Statistics 18 program (SPSS), using independent-sample t-test and paired sample t-test. Experiments were performed in triplicate, unless otherwise indicated, and $P< 0.05$ was considered significant.

Standard deviation is a measure of the distribution of individual scores around the mean, and the SE tells us the variability of the means [79]. Since all results during this report are based on mean values, and since indicating the uncertainty around this estimate of the mean measurement is required, the data during this report is presented as means ±SE (see Appendix V).

2.8.1. The t-distribution

In vitro cell culture experiments are subject to several small, random errors, however insignificant to systematic errors.

The t-distribution involves the distribution of the mean for smaller samples. The higher the sample size gets, the more the distribution will approach the normal distribution. When more than two samples exist, which is the case for this study, the analysis of variances will be essential (with use of the F distribution). All of these methods includes the assumption of normality existing [80].

2.8.2. P-values

After clarification of the distribution of a certain data, you could question whether the actual results were distributed as predicted [81]. A statistical hypothesis could here be useful to formulate, to understand what to expect from a specific experiment. The simplest hypothesis is the so called *null hypothesis,* estimating that the new result makes no difference achieving a more extreme result than the observed one. According to this hypothesis, the probability for various possible results of the test could be calculated before evaluating the significance of the particular result. The probability value is based on the amount of evidence towards the null hypothesis. If the calculated probability is below a set of boundary of 5 %, the hypothesis can be rejected while accepting the result of the experiment to be *significant*. A probability value of 5 % means that there is only a 5 % chance that the results are similar to the observed results. If the probability is below a set of boundary of 1% the result of the experiment can be called *highly significant [81]*.

2.8.3. Paired data

Paired tests are of value if the same cell-line is studied more than one time or when dealing with two different groups of cell-lines matching individually [80]. When dealing with paired data, the interest is in the variability within paired samples. By using the paired t-test, a P-value for the comparisons of the means can be calculated. The paired t-test was during this

report used when comparing one exposed sample against the unexposed sample in the same cell line and in the same experiment.

2.8.4. Independent data

Independent tests are valuable when comparing two independent groups of observations or when comparing samples from different experiments [80]. In an independent test the mean difference between groups is interesting and the variability is of importance. The independent t-test was performed, when comparing the difference between two types of test materials or when comparing two different cell lines.

All responses in present report are essentially relied on certain p-values, were a significant value is believed to mean a response and a non-significant value is believed to indicate no effect. Two possible errors exist when results are based on p-values, called Type I and Type II errors. The Type I error, is what you call a "false positive result, which is when rejecting the null hypothesis that appear to be true. Contrary, the Type II error is the "false negative finding" that emerges when receiving a non significant value as the null hypothesis is not true [82].

3.Results

3.1.Visualization of MWCNTs by Scanning Electron Microscopy (SEM)

Scanning Electron Microscopy was used to visually assess dry MWCNTs. The SEM images of the two MWCNTs tested in present study are shown in figure 3.1.Visual examination of MWCNTs showed long "fiber-like" structures. The structure of MWCNT from Japan (designated as MWCNT-JP) was observed longer and more isolated compared to MWCNTs from Norway (designated as MWCNT-NO). The SEM images also showed that MWCNT from Norway contained traces of unknown non-fiber like contaminants that were not further characterized.

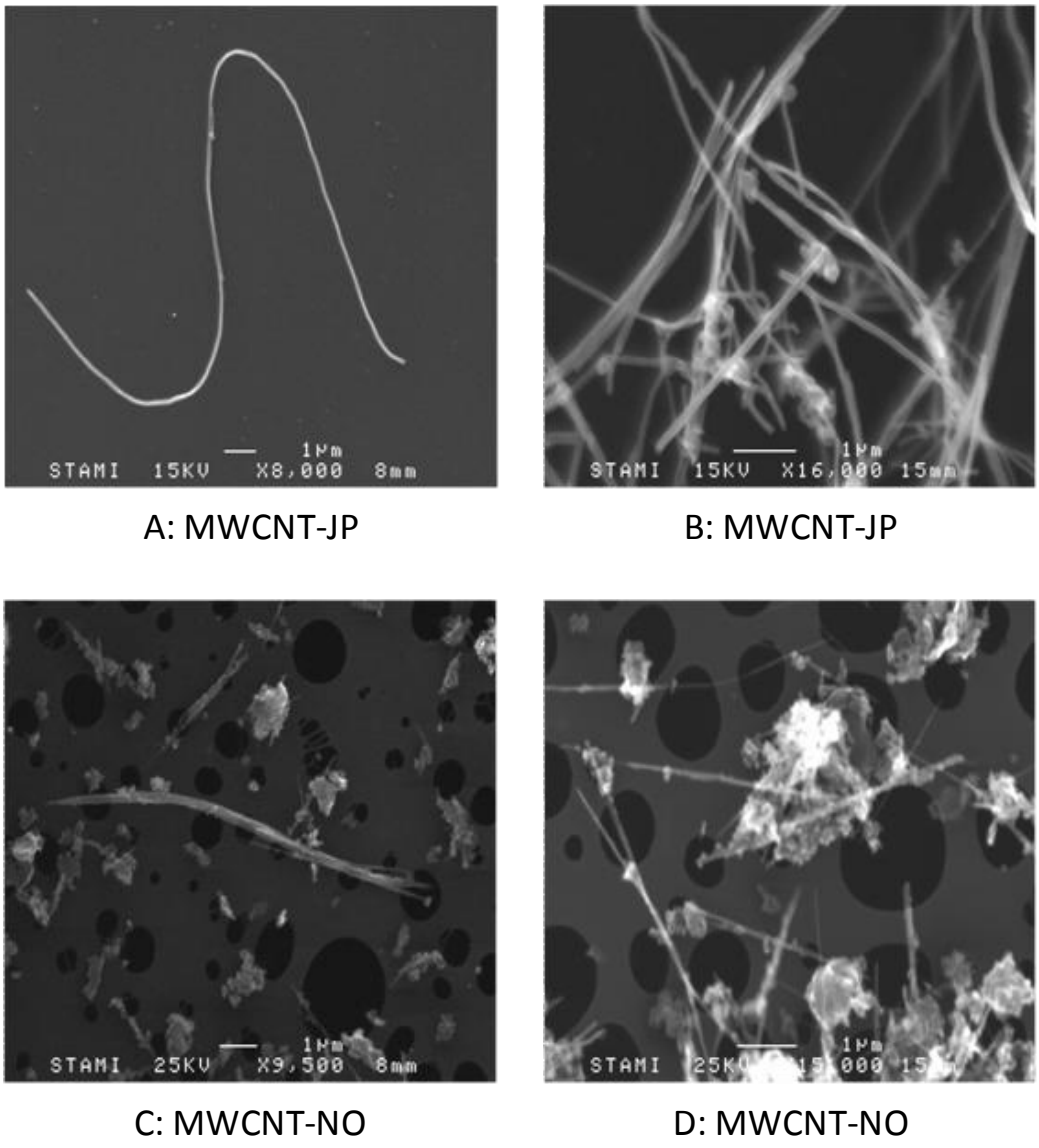

Figure 3.1: SEM images, showing dry MWCNTs. Fibers were sent through a grid (copper grid) and electrons were scanned. Bar indicates 1µm.

3.2.Determination of cytotoxic effects in human lung cells

The cytotoxic effects of the MWCNT particles, Crocidilite and H_2O_2 were studied in two human bronchial epithelial cell lines designated as HBEC-2KT and HBEC-3KT. The detailed characteristics of cell lines, the WST-8 cytotoxicity assay and experimental procedures are described in materials and methods. For supplementary raw data, see A6.1-5 in Appendix VI.

3.2.1. Cytotoxicity of MWCNT-NO

The MWCNT-NO, the CNT of focus for this study, is unknown and has not been previously subjected to any cytotoxicological experiments. The cell viability decreased both with increasing concentrations of the MWCNTs and duration of time (Figure 3.2). The cytotoxic effects were slightly different in the two cell-lines. HBEC-2KT cell line seemed to some extent be more sensitive than HBEC-3KT following exposure to MWCNT-NO for some doses (Figure 3.2). Some concentrations were statistically significant (indicated by *) compared to control (unexposed cells), especially after exposure to 50 and 100 µg/ml MWCNT-NO.

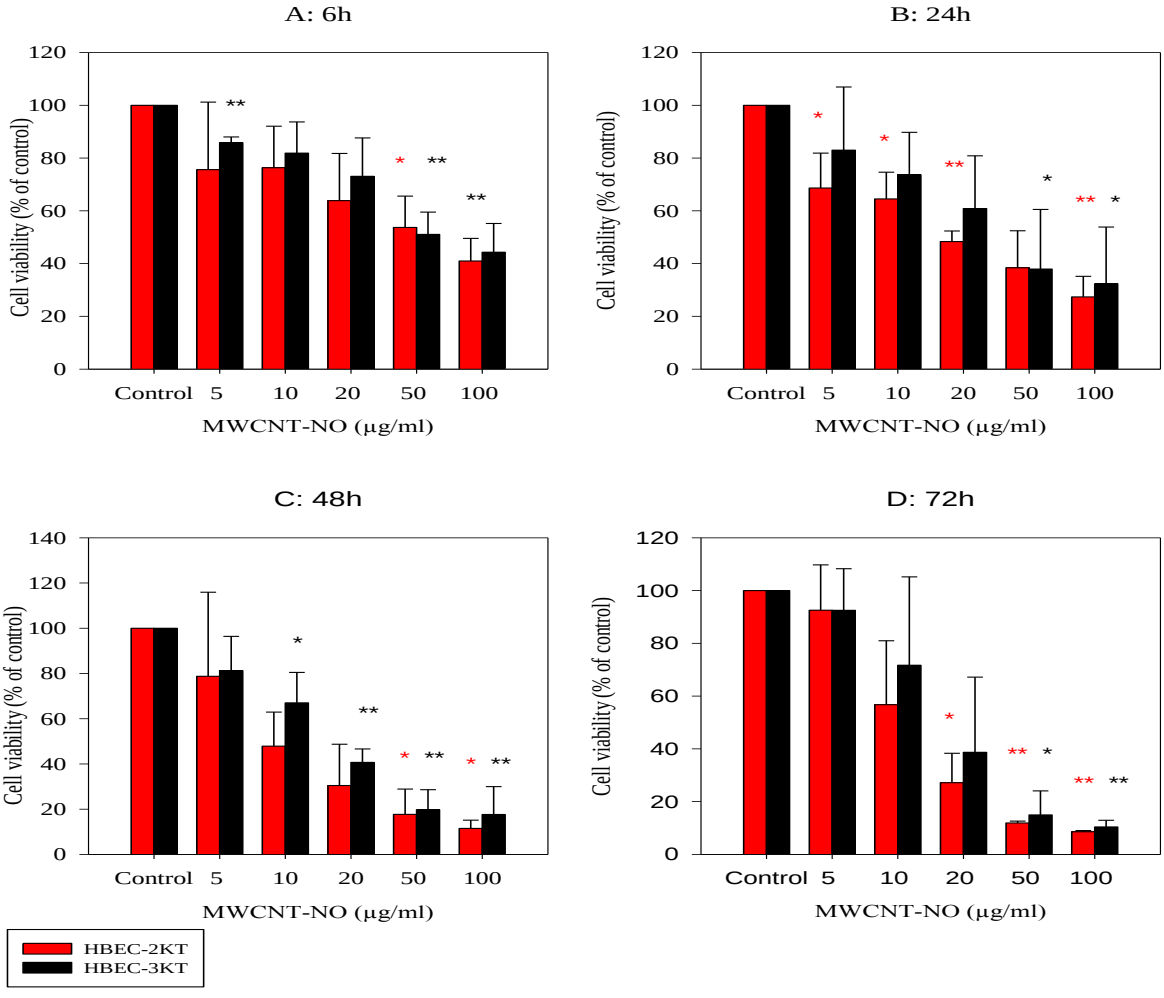

*Figure 3.2: Cell viability of HBEC-2KT and HBEC-3KT, exposed for increasing concentrations of MWCNT-NO for 6h (A), 24h (B), 48h (C) and 72h (D). asterix (*) represents samples which are significantly different from the control samples(Cell viability(%) = 100 x ($OD_{exposed}$/$OD_{control}$). Statistical analysis is performed with the Student's t-test for paired samples. Error bars= SE; *, $p< 0.05$;**, $p<0.01$*

3.2.2. Cytotoxicity of MWCNT-JP

MWCNT-JP, a well known CNT, has previously been subject of some toxicity studies. Effects of MWCNT-JP are therefore valuable when comparing the effects with that of MWCNT-NO. Similar to the results from the MWCNT-NO, the data implied that cell viability decreased both with increasing dose and exposure time (Figure. 3.3). The LC_{50} threshold was found to be after 24 hour exposure to all concentrations of this MWCNT. Little if at all, variation in toxicity between the two cell lines were observed. However, exposure time periods of 48 and 72 hours were extremely toxic and therefore excluded from further experiments. Additionally, the doses had to be reduced as shown in Figure 3.4. The new and reduced doses indicated that cell viability decreased both with increasing dose and exposure time (Figure 3.4). Statistically significant effects were seen for doses higher than 0.5 ug/ml (Figure 3.4 A and B). No considerable individual differences in cell survival were observed between the two cell lines.

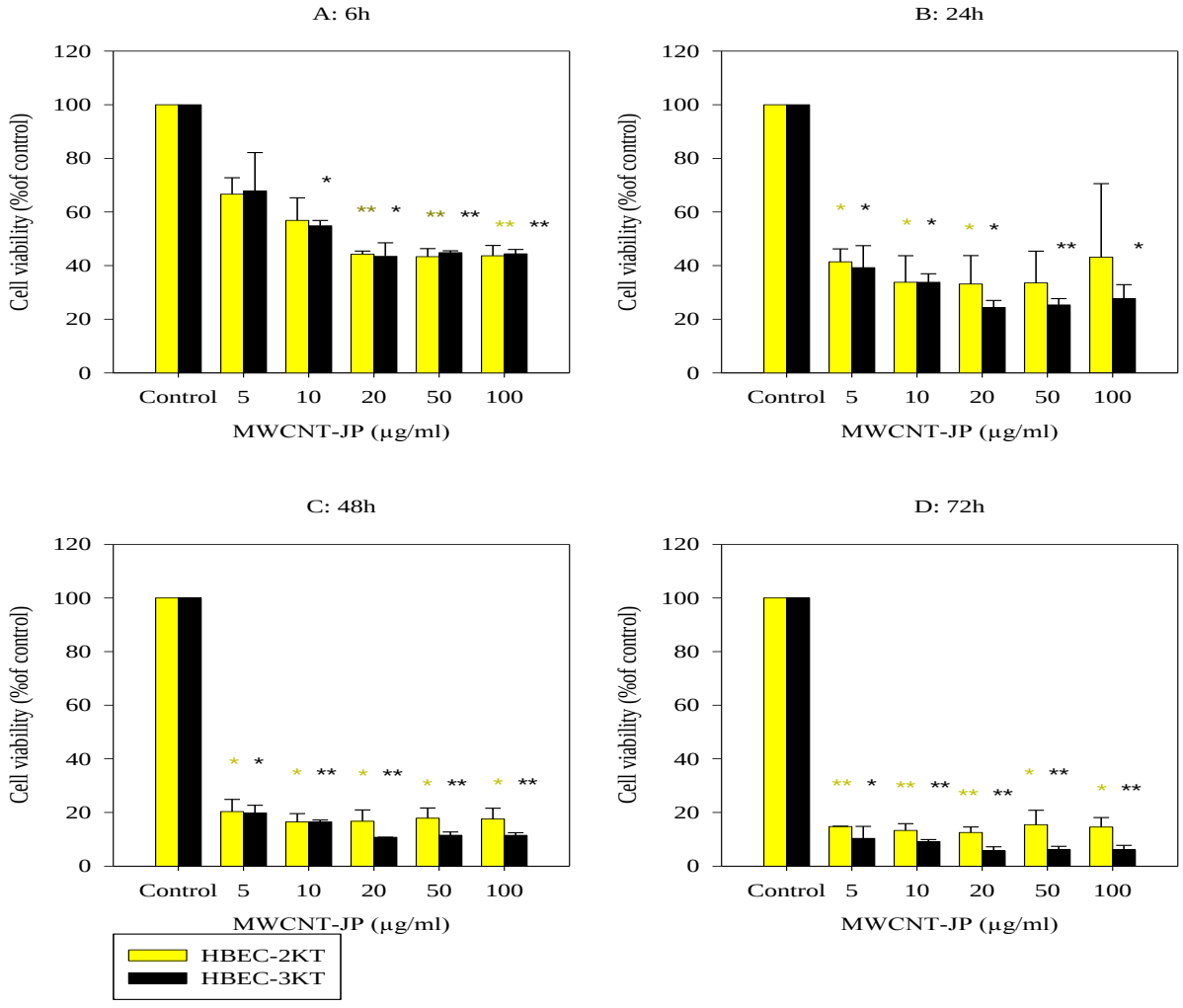

*Figure 3.3: Cell viability of HBEC-2KT and HBEC-3KT, exposed for increasing concentrations of (5-100 µg/ml) of MWCNT-JP for 6h (A), 24h (B), 48h (C) and 72h (D). asterix (*) represents samples which are significantly different from the control samples (Cell viability(%) = 100 x ($OD_{exposed}$ /$OD_{control}$). Statistical analysis is performed with the Student's t-test for paired samples. Error bars= SE; *, p< 0.05;**, p<0.01*

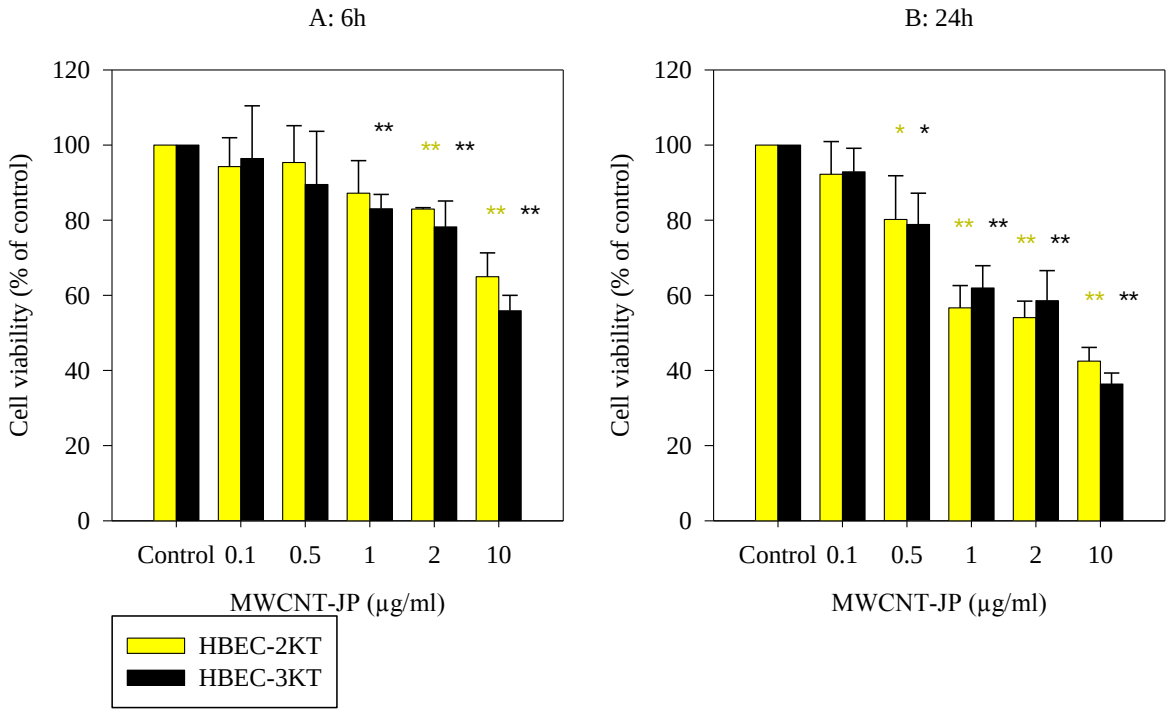

*Figure 3.4: Cell viability of HBEC-2KT and HBEC-3KT, exposed for increasing concentrations of (0,1-10 µg/ml) of MWCNT-JP for 6h (A) or 24h (B). asterix (*) represents samples which are significantly different from the control samples (Cell viability(%) = 100 x ($OD_{exposed}$ /$OD_{control}$).Statistical analysis is performed with the Student's t-test for paired samples. Error bars= SE; *, p< 0.05;**, p<0.01*

3.2.3. Cytotoxicity of crocidolite

CNTs contain a needle-like fiber shape that has been compared with asbestos. The crocidolite, known as blue asbestos, is well known and was used as a positive control for fiber-toxic effects. The results in Figure 3.5 show a dose and time dependent decrease in cell viability after exposure to crocidolite. Some individual variations have also been registered. The statistically significant toxic effects are, for most concentrations observed after exposure for 24 hours or longer (Figure. 3.5 B). However, the most significant effects are observed at the higher concentrations where the LC_{50} threshold is observed after 48 hours (Figure. 3.5 C) and 72 hours (Figure. 3.5 D).

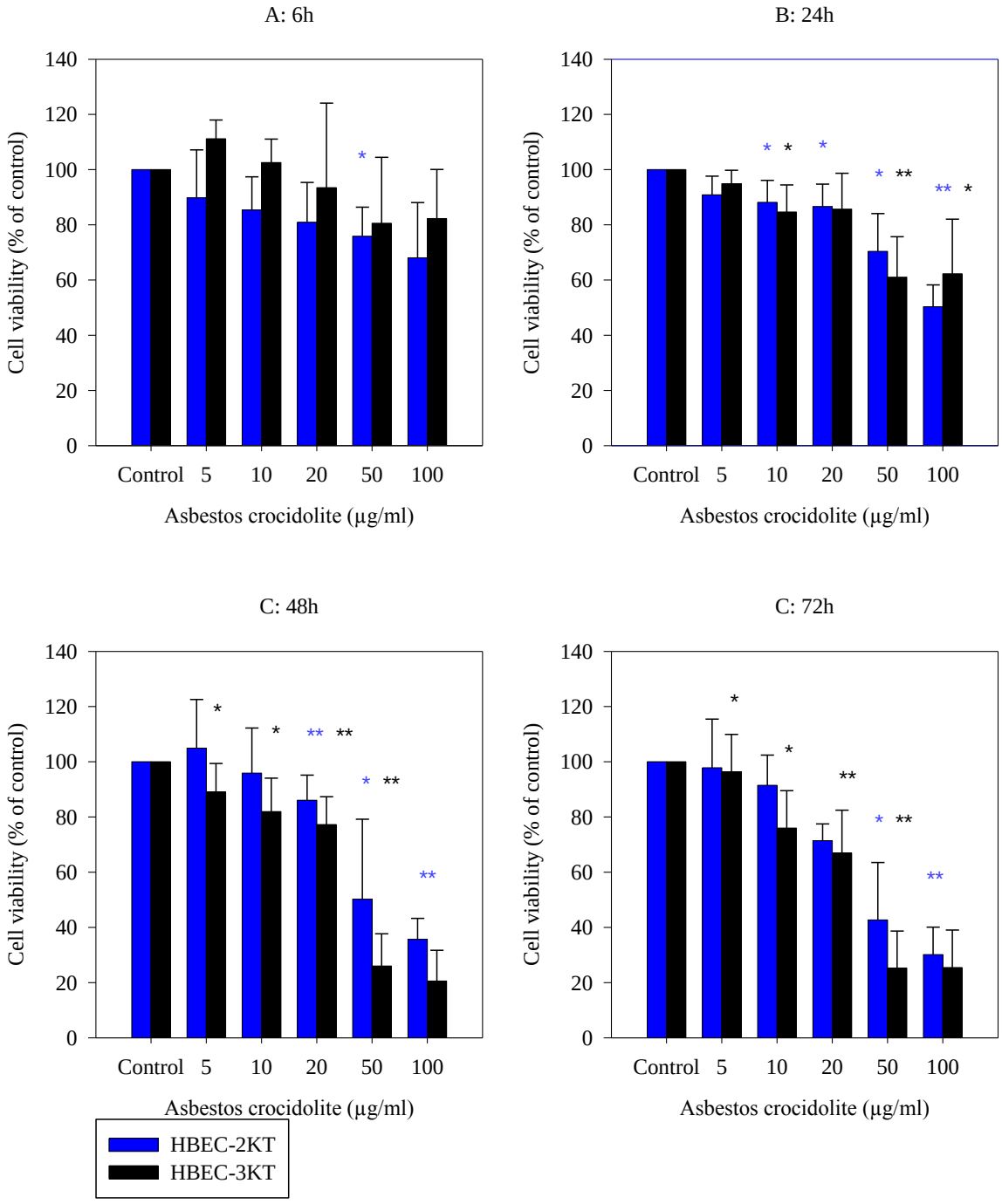

*Figure 3.5: Cell viability of HBEC-2KT and HBEC-3KT, exposed for increasing concentrations of asbestos crocidolite for 6h (A), 24h (B), 48h (C) and 72h (D) asterix (*) represents samples which are significantly different from the control samples(Cell viability(%) = 100 x ($OD_{exposed}$ /$OD_{control}$) Statistical analysis is performed with the Student's t-test for paired samples. Error bars= SE; *, p< 0.05;**, p<0.01*

3.2.4. Cytotoxicity of hydrogen peroxide (H_2O_2)

Hydrogen peroxide was included, not as a non-fiber or as a non-NP control, but as an oxidative agent known to cause ROS. As shown in figure 3.6, a dose dependent decrease in

cell survival was observed in cells exposed to all concentrations of H_2O_2. Very few variations between the two cell lines were observed, but HBEC-3KT is the most sensitive after 24 hour (Figure. 3.6 B) and HBEC-2KT is essentially the most sensitive after 72 hour (Figure. 3.6 D) exposure. Cell viability did not fall below the LC_{50} threshold for any of the concentrations or any of the time periods.

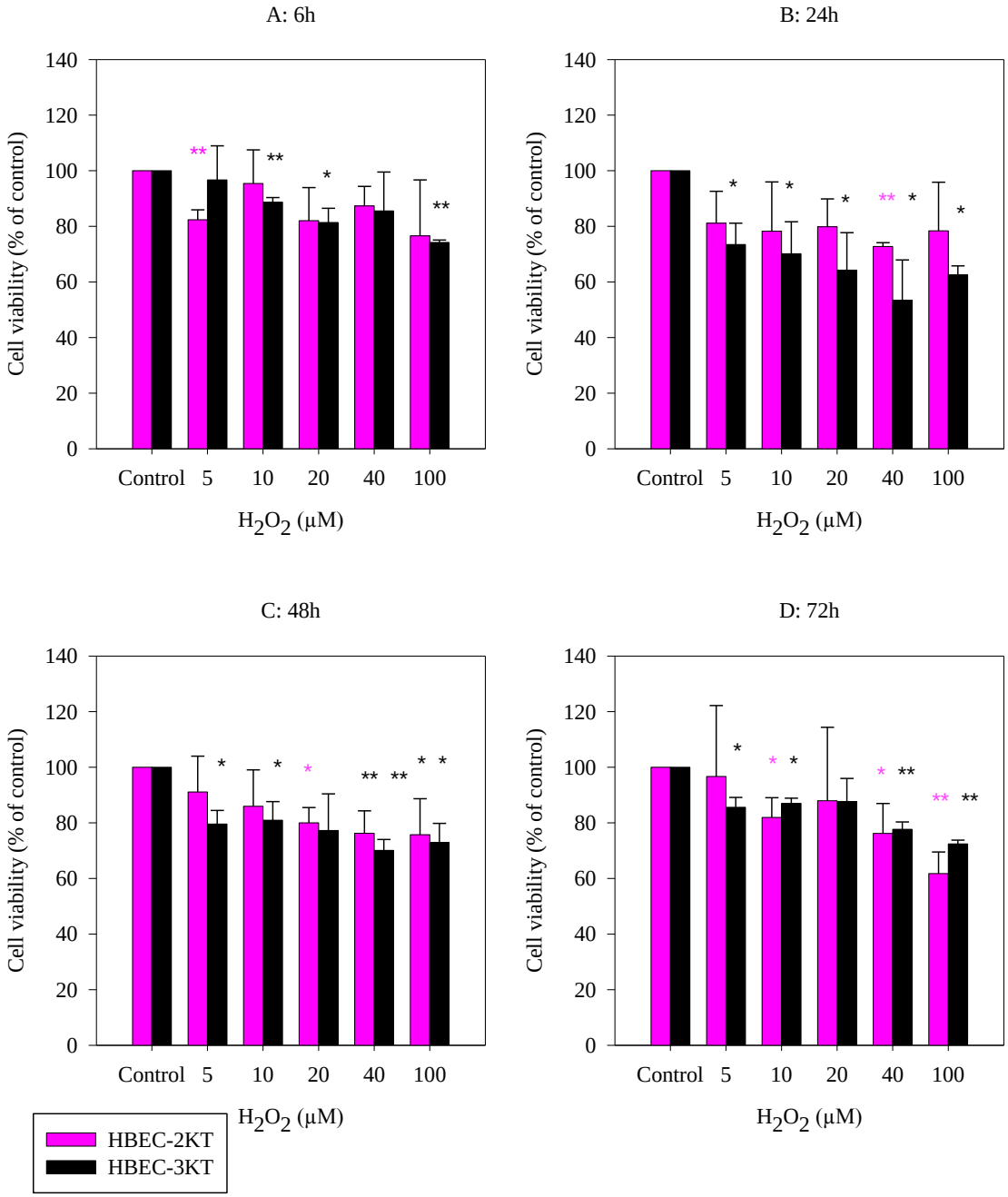

*Figure 3.6: Cell viability of HBEC-2KT and HBEC-3KT, exposed for increasing concentrations of H_2O_2 for 6h (A), 24h (B), 48h (C) and 72h (D), asterix(*) represents samples which are significantly different from the control samples (Cell viability (%) = 100 x ($OD_{exposed}$ /$OD_{control}$)Statistical analysis is performed with the Student's t-test for paired samples. Error bars= SE; *, p< 0.05;**, p<0.01*

3.2.5. Comparison of toxicity of MWCNTs and crocidolite

The cytotoxic effects of the three fiber-like compounds were compared in the two cell lines using dose-response results from 24 hour exposure (Figure 3.7). For HBEC-2KT cell line (Fig. 3.7 A) the significant effects were observed between MWCNT-JP and crocidolite after all exposure time periods, except for the highest dose. A statistically significant difference in cell death was observed between MWCNT-NO and MWCNT-JP after exposure to 10 µg/ml ($P<0.05$, Student's t-test for unrelated samples). For the HBEC-3KT cells a significant effect was also seen between MWCNT-NO and MWCNT-JP after exposure to 10 µg/ml (Fig. 3.7 B). Significant effects between MWCNT-NO and crocidolite were also found after exposure to 10, 20, 50 and 100 µg/ml (Fig. 3.7 B). Significant differences between MWCNT-JP and crocidolite were seen for 10, 20 and 50 µg/ml doses. Taken together MWCNT-JP was more toxic than MWCNT-NO and crocidolite asbestos was less toxic than all the three fibers.

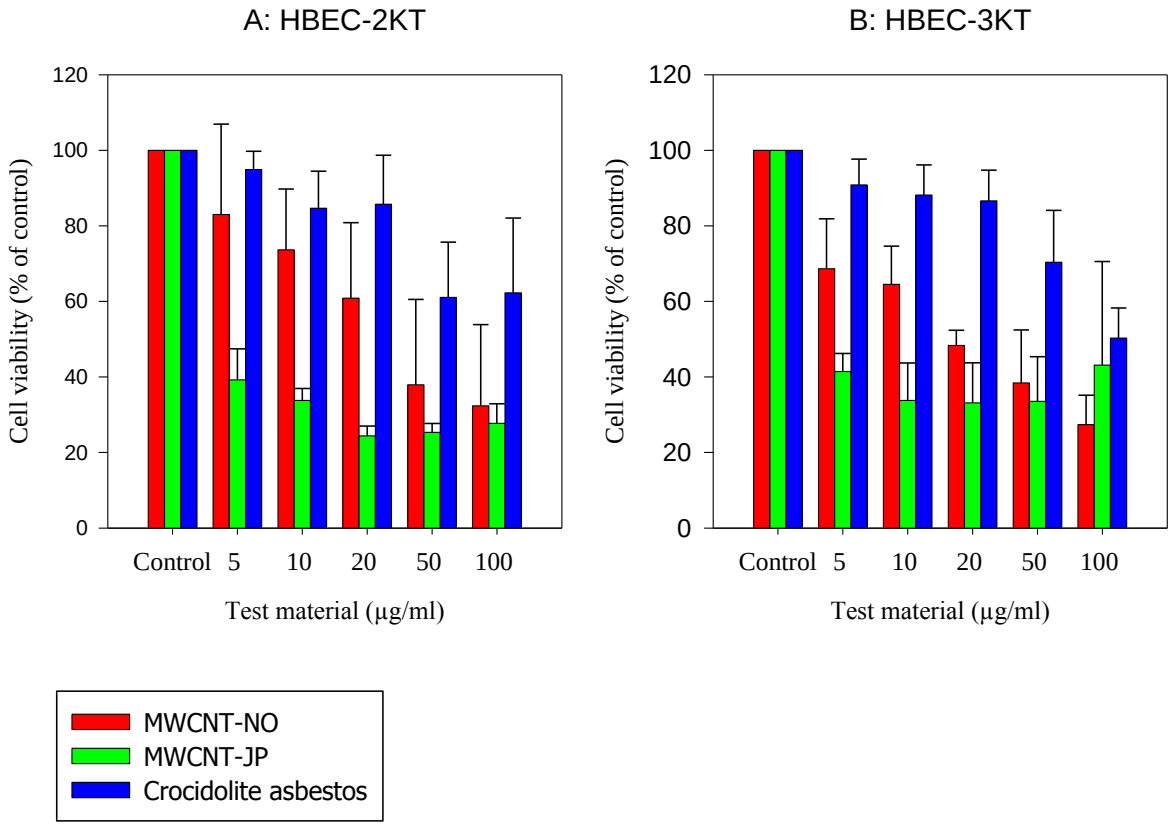

Figure 3.7: Cell viability of MWCNT-NO, MWCNT-JP and crocidolite after 24 hours exposure in HBEC-2KT (A) and HBEC-3KT (B) (Cell viability (%) = 100 x ($OD_{exposed}/OD_{control}$).

3.2.6. Determination of doses and exposure time for apoptosis and gene expression studies

The dose-response results from the cytotoxicity experiments were used to choose suitable doses for apoptosis and gene expression experiments. Doses which gave low toxicity (70-80% viability) in the toxicity assays were preferred since these may not have many adverse effects on cellular function. The 24 hour exposure was chosen for further studies, since the results were observed to have less variation. For the MWCNT-NO, which is the main focus in the experiments, it was determined to use the concentrations 1 and 5 µg/ml for fluorescence

microscopy (apoptosis). For the MWCNT-JP particles, the concentration used was 0.5µg/ml, 20 µg/ml for crocidolite, and 5 µM for H_2O_2. Based on the results from the cytotoxicity assays (Figure 3.7), these concentrations seemed to have similar toxicity after a 24 hours exposure (about 20–30 % cell death). For the qRT-PCR analysis of gene expression following doses were used: For the MWCNT-NO, 1 and 5 µg/ml, for the MWCNT-JP particles, the concentration used was 0.5µg/ml, for Crocidolite 50 µg/ml and for H_2O_2 5 µM.

3.3. Analysis of apoptotic cell death

To study apoptosis, the HBEC-2KT and HBEC-3KT cells were cultured with various concentrations of test materials for 24 hours. After exposure, cells were stained with Hoechst 33432 and propidium iodide (PI) dyes. Thapsigargin (TG) a known apoptosis-inducing chemical, was included as a positive control.

In this assay, using a fluorescence microscope, the nucleus of live cells is stained blue (Figure. 3.8), necrotic cells are stained red (rectangle cells in Figure 3.9 A and B), and the nucleus of apoptotic cells are also stained blue but with intense spots (encircled cells in Figure.3.10 A and B). The dead cells comprise of both necrotic and apoptotic cells.

Figure 3.8 shows example photographs from fluorescence microscopy from the two cell lines; unexposed (Figure 3.8 A and B).The unexposed control cells, contained a portion of necrotic cells, but not cells that morphologically look like apoptotic cells.

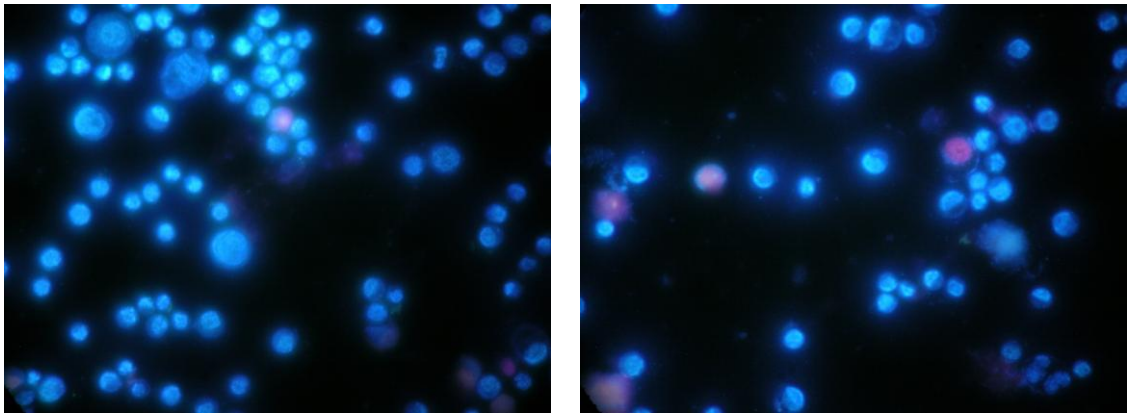

A: HBEC-2KT: Control B: HBEC-3KT: Control

Figure 3.8: Viability of unexposed HBECs in cell culture. Cells were stained with PI and Hoechst 33342. Viability was estimated with fluorescence microscopy.

Figure 3.9 shows examples of photographs from the fluorescence microscopy from the two cell lines, exposed to 5 µg/ml MWCNT-NO (Fig. 3.9 A and B), with examples of necrotic cells.

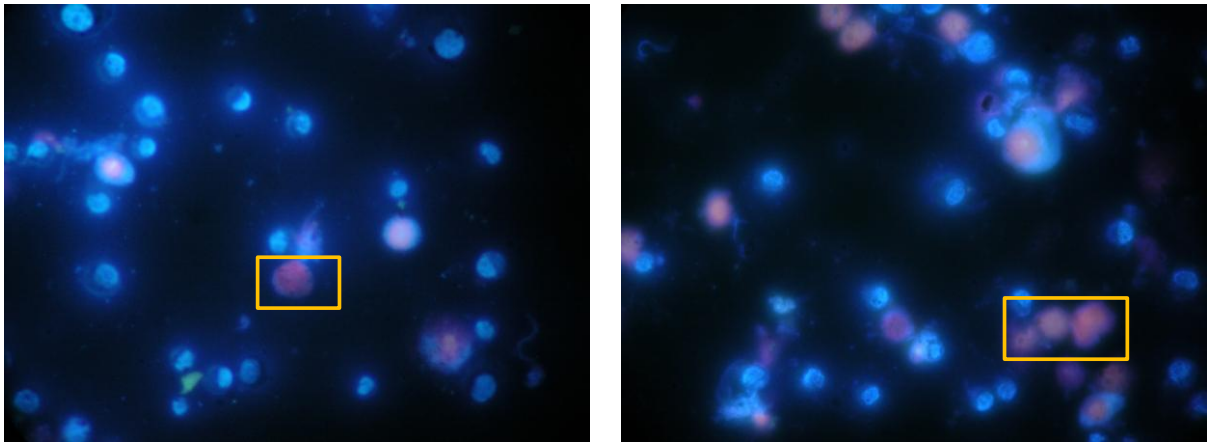

A: HBEC-2KT: MWCNT-NO (5µg/ml) B: HBEC-3KT: MWCNT-NO(5µg/ml)

Figure 3.9: Viability of HBECs exposed for MWCNT-NO (5 µg/ml) for 24 hours. Cells were stained with PI and Hoechst 33342. Viability was estimated with fluorescence microscopy. Rectangle cells illustrate necrotic cells.

Figure 3.10 shows two examples of photographs from the fluorescence microscopy from the two cell lines, exposed to 100 nM TG (Figure 3.10 A and B), with examples of cells that morphologically looks like apoptotic cells (encircled).

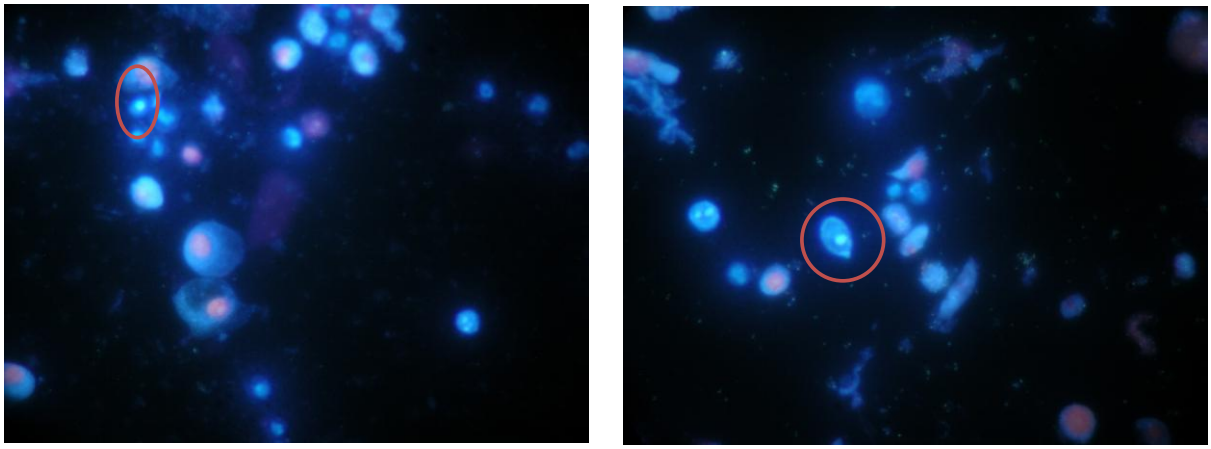

A: HBEC-2KT: TG (100 nM) B: HBEC-3KT: TG (100 nM)

Figure 3.10: Viability of HBECs exposed for Thapsigargin (100 nM) for 96 hours. Cells were stained with PI and Hoechst 33342. Viability was estimated with fluorescence microscopy. Encircled cells indicate apoptotic cells

Figure 3.11 illustrates a number of dead cells, after an exposure to various test materials. The highest concentration of MWCNT-NO (5 µg/ml) demonstrated the highest cell death, however, the fraction of apoptotic cells was low and it seemed that the test materials induced cell death through necrosis. TG was mainly the only compound inducing apoptosis in these cells, however, only after a 96 hours exposure. The details are shown in table A3.3 in Appendix III. Figure 3.11 verifies that the estimated concentrations of test materials from the cytotoxicity experiment result in a 70-80% viability, for both cell-lines. The portion of dead cells (necrosis) in the controls, are slightly too high after counting approximately 300 cells/slide.

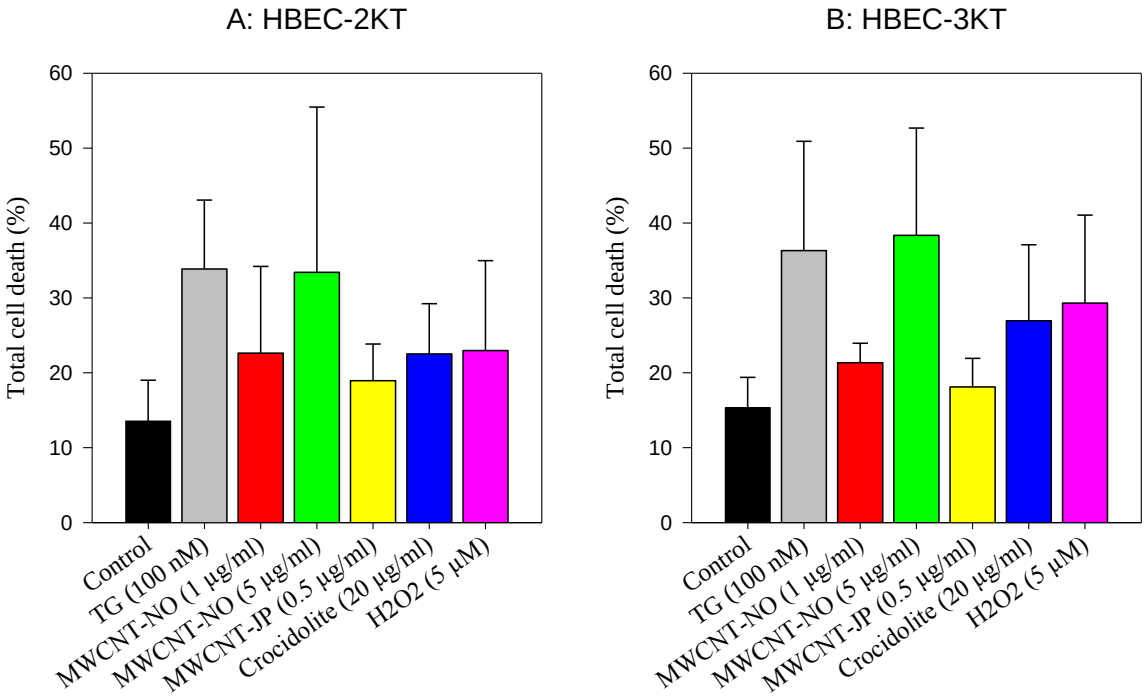

Figure 3.11: Total Cell death (%) after exposure to various test materials. (Tot cell death in exposed samples (%) = (apoptotic + necrotic cells)/tot. number of cells) x 100)

3.4. Analysis of gene expression

HBEC-2KT and HBEC-3KT were cultured with various concentrations of test materials estimated from the cytotoxicity experiment following a 24 hours exposure. Extraction of RNA and reverse transcription into cDNA were performed before gene expressions of *PTGS2 (COX-2)*, *IL1B*, *IL6*, *IL8* and *TP53* were analyzed with qRT-PCR. The data were then normalized to the expression levels for each gene in control (unexposed) cells in order to compare the expression of various genes to each other. The fold changes in expression (increase or decrease) of genes after exposure to MWCNTs, crocidolite and H_2O_2 is shown in Figure 3.12 and Figure 3.13. The figure of relative expression for both cell-lines, is found in figure A4.1 in Appendix IV and detailed data are found in supplementary tables A6.6-7 in Appendix VI.

For the HBEC-2KT cells, there was a statistically significant induction (12.54 ± 1.95) in expression of *COX-2* (Figure 3.12A, $p< 0.05$) in the crocidolite exposed cells compared to the control cells.

For *COX-2* and *ILB*, there are indications of a gradual induction in expression with increasing concentrations of MWCNT-NO, although they were not statistically significant (Figure 3.12-A&B).The exposure for MWCNT-JP had no effect on the expression of genes, except a slight induction in the expression of *IL6* (Figure 3.12 C). The expression of *IL1B*, *IL6* and *IL8* seemed to be influenced after crocidolite exposure. Exposure to H_2O_2 indicated also a trend with a slight increase in expression of *IL6*. The expression of *TP53* gene was not observed to be influenced by any of the tested compounds (Figure 3.12 E).

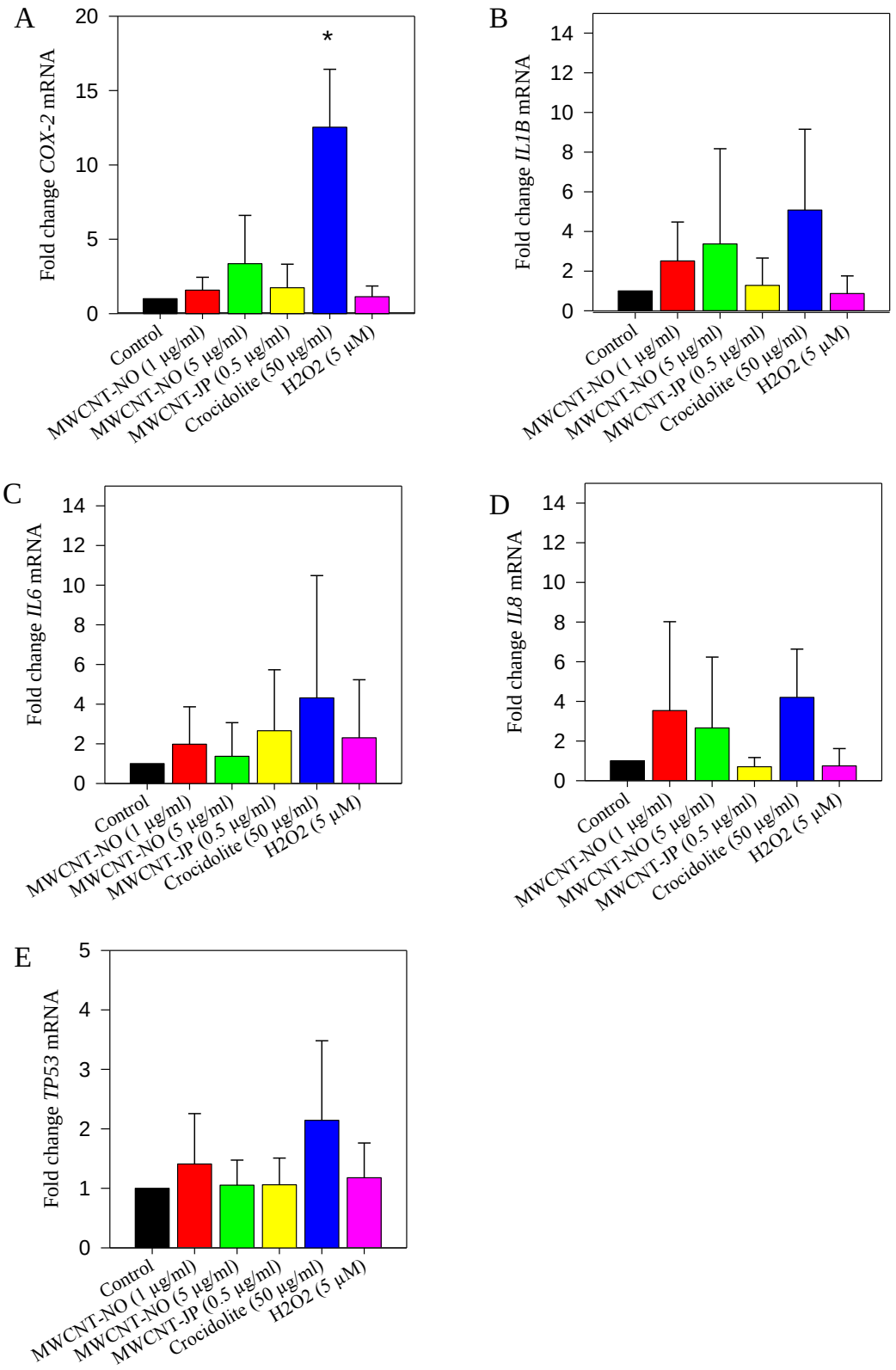

*Figure 3.12: The expression of the COX-2 (1), IL1B (2),IL6 (3), IL8 (4) & TP53 (5) in HBEC-2KT, normalized in proportion to the endogen control ACTB. [Fold change= (relative expression)$_{exposed}$/(relative expression)$_{control}$ where Relative expression= $2^{(-\Delta Cq)}$ x 10^4] asterix (*) represents samples which are significantly different from the control samples Statistical analysis is performed with the Student's t-test for paired samples. Error bars= SE; *, p< 0.05;**, p<0.01*

The comparison of expression of various genes in HBEC-3KT is shown in figure 3.13. In HBEC-3KT cells exposed to MWCNT-NO, statistical significant inductions ($p<0.05$) in *IL6 (4.4±0.68)* and *IL8 (4.67±1.56)* expressions (5µg/ml) were observed compared to control cells (Figure 3.13- C and D).

In HBEC-3KT cells exposed to crocidolite, a statistical significant induction was shown ($p<0.05$) in the expression of *IL1B* compared to un-exposed control cells (8.65 ±0.82) (Figure 3.13-B).

Indications on some trends are observed when analyzing the various gene expressions in HBEC-3KT. As to the *IL1B, IL6* and *IL8,* we observed an indication of a gradual induction in expression with increasing concentrations of MWCNT-NO, although not statistically significant (Figure 3.13-B,C &D). There is also a non-significant increased expression of *IL1B, IL6* and *IL8* after exposure for MWCNT-JP and crocidolite (Figure 3.13-B, C and D). No changes in expression of any of the tested genes were observed after exposure to H_2O_2 (Figure 3.13). In relation to the HBEC-2KT cells there were no significant changes in *TP53* expression after exposure to any of the test-materials observed for HBEC-3KT cells as well (Figure 3.13)

Few individual differences exist when analyzing the fold increase in mRNA expression in exposed cells compared to unexposed control cells in each cell line, as indicated in figure 3.14. There are significant differences in the expression of *COX-2 (Figure 3.14 B)* and *IL6* (Figure 3.14 C) between the cell lines following exposure to crocidolite and (5µg/ml) MWCNT-NO ($p<0.05$, independent student's t-test).

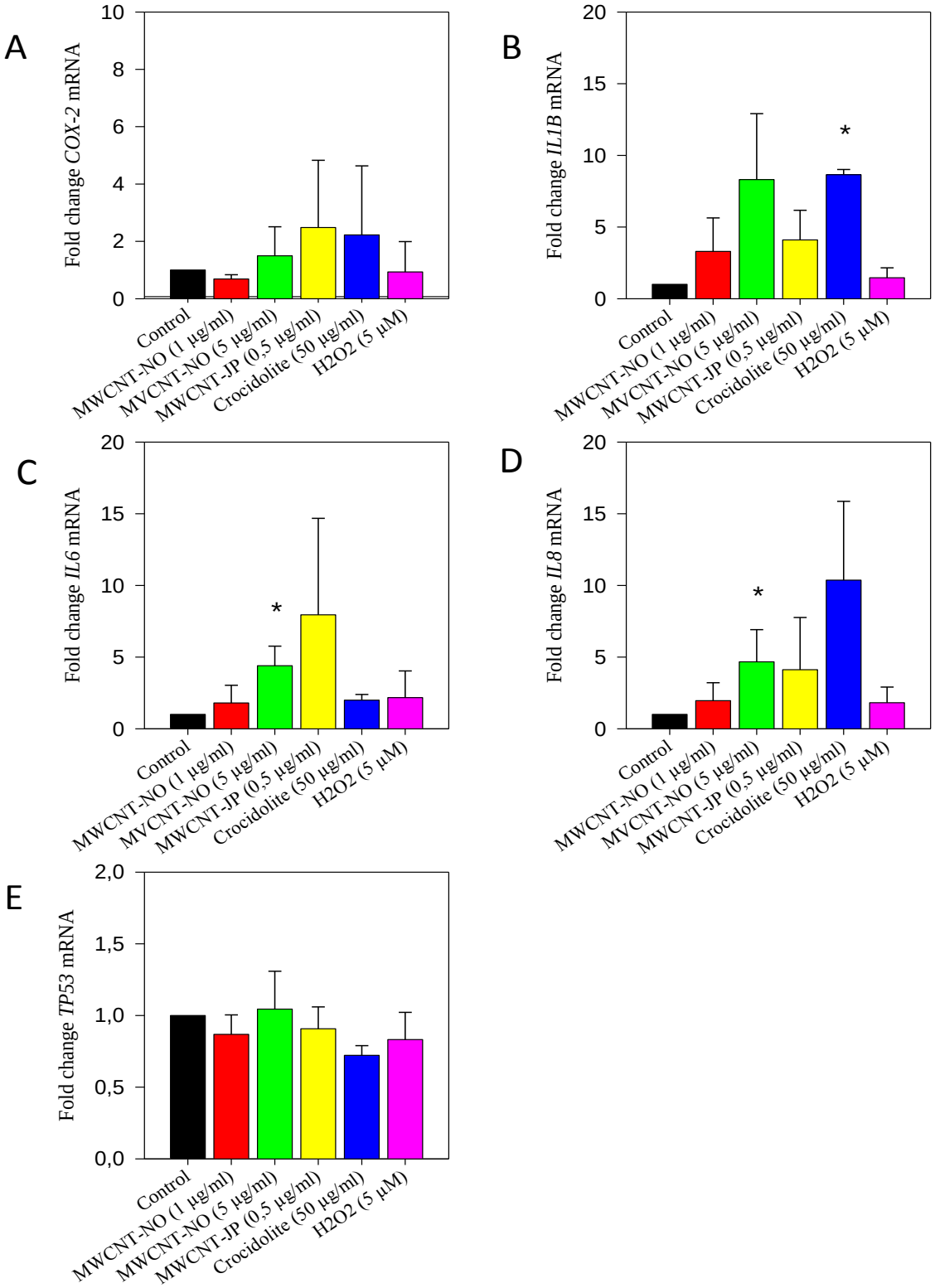

*Figure 3.13: The expression of the COX-2 (1), IL1B (2),IL6 (3), IL8 (4) & TP53 (5) in HBEC-3KT, normalized in proportion to the endogen control ACTB. [Fold change= (relative expression)$_{exposed}$/(relative expression)$_{control}$ where Relative expression= $2^{(-\Delta Cq)}$ x 10^4] asterix (*) represents samples which are significantly different from the control samples Statistical analysis is performed with the Student's t-test for paired samples. Error bars= SE; *, p< 0.05;**, p<0.01*

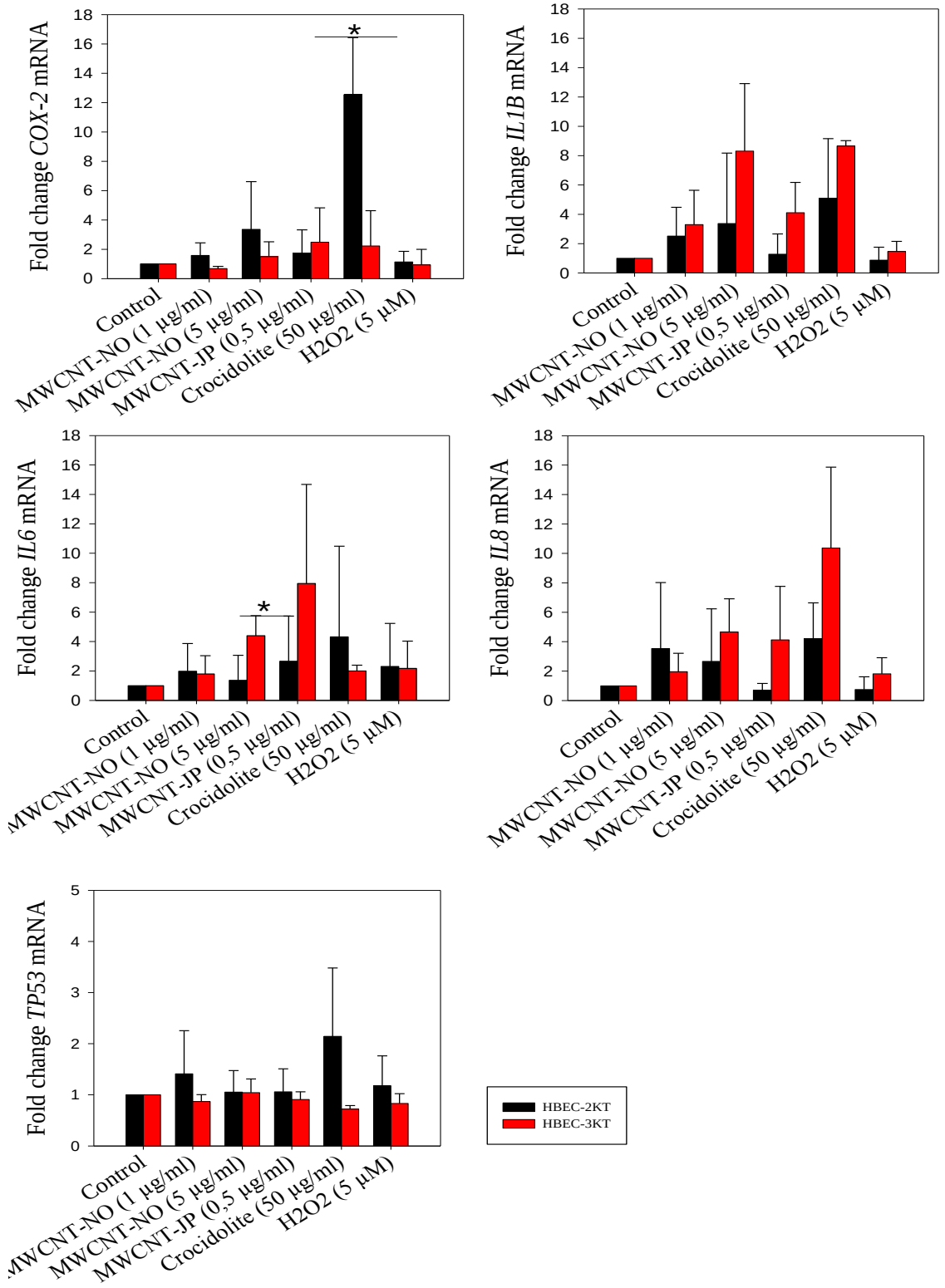

*Figure 3.14: Comparison between HBEC-2KT and HBEC-3KT on the mRNA expression of COX-2, IL1B, IL6, IL8, and TP53. normalized in proportion to the endogen control ACTB. [Fold change= (relative expression)$_{exposed}$ /(relative expression)$_{control}$ where Relative expression= $2^{(-\Delta Cq)}$ x 10^4] asterix (*) represents samples which are significantly different from the control samples Statistical analysis is performed with the Student's t-test for independent samples. Error bars= SE; *, p< 0.05;**, p<0.01*

4.Discussion

4.1.The cell culture model

In this study two cell lines of epithelial origin derived from normal human lung were used. Epithelial cells are commonly used for *in vitro* exposure studies since the bronchial epithelium functions as an important first line of defense. The immortalized human bronchial epithelial cells (HBECs) used in present study, provide a suitable model to study the molecular mechanisms as well [74]. These cells are immortalized with *hTERT* and *Cdk4,* and include minimal disturbance in normal cellular pathways [83-84]. Although an in *vitro* system will not represent the situation *in vivo,* the system is helpful when investigating mechanisms behind cellular toxicity. [85]. A drawback may be that high exposure levels used *in vitro* may not represent a real exposure on the bronchial surface, in the alveolar compartments or in blood. Further, there are several experimental factors affecting the results *in vitro,* depending on type of cells and assays that are used [86].

4.2. Characterization and dispersion of the MWCNTs

MWCNTs from two different sources were tested and their morphology was grossly characterized by scanning electron microscopy. Previous studies have thoroughly characterized the morphology of MWCNT-JP (supplied by Mitsui & Co) using various equipments e.g. transmission electron microscopy (TEM). The study of Poland et al. describes the presence of MWCNTs mainly in the range 10-20 µm, and a portion with long and straight fibers, > 20 µm [27]. However, some other studies that have characterized MWCNTs from the same source (Mitsui & Co) show a substantially shorter fiber length [77]. The SEM images obtained by us indicate that the MWCNT-JP could be within the same length range as reported by Poland et al (Figure 3.1 A), and the fiber length of MWCNT-JP appeared to be longer than MWCNT-NO, which are in accordance with previous literature and manufacture information (Table 2.1). However, estimation of size cannot be reliably determined for any of the MWCNTs. Bundling between fibers was observed for both sources of MWCNTs, and this could illustrate the phenomena of aggregation and agglomeration or presence of other contaminations. Previous studies have indicated presence of some metals e.g. Ni, Co, Na and Fe which may be used as catalysts for MWCNT during synthesis [27, 77, 87]. The SEM images of MWCNT-NO did, however, illustrate a substantially higher proportion of clumps with thin needle-like fibers in between. Whether this indicates impurities or high degree of agglomeration is unknown and a better characterization is needed with e.g. TEM, and DLS.

The insoluble and electrostatic properties of CNTs may result in formation of aggregates and agglomerates in aqueous solutions [27]. The tendency of CNTs to agglomerate has demonstrated to influence their toxicity both *in vivo* and *in vitro.* An *in vivo* study has shown that formation of CNT (MWCNT) agglomerates resulted in lesions mainly localized to the upper respiratory system, while isolated particles reach the alveolar spaces where granuloma formation was observed [11]. Similarly, an *in vitro* study reported the influence of agglomeration regarding CNTs (SWCNTs) toxicity, where individually dispersed CNTs were more toxic than CNT aggregates [88].

4.3. Cytotoxicity experiments

To estimate the cytotoxic dose for each test material, cells were treated with various doses of each test material. In our studies we used concentrations ranging from 0.5-100 µg/ml MWCNT, which previously have been used in various studies and seemed to work well. The uptake of particles by the cells is an important factor for toxic response. Based on results from the study of Hirano et al. regarding association or uptake of MWCNT in human lung BEAS-2B cells, the time of exposure for further experiments in this thesis was chosen to be 24 hours. The study of Hirano et al. demonstrated that uptake of MWCNTs reached the maximum after 10 hrs [89].

There are large variations in the doses used in various studies depending on cell type used. One example is a study using fibroblasts treated with 40-400 ug/ml where a significant cytotoxic effect was not seen before 72 h [90]. Another study on human bronchial epithelial cells (BEAS-2B cells) reported a significant toxicity after 24 hours with an IC_{50} (concentration of nanoparticles to induce 50 % cell mortality) at 12 µg/ml [89].

4.3.1. MWCNTs

A dose and time dependent reduction in cell viability was observed after MWCNT-NO treatment for all time and doses but the effect was much higher after 48 and 72 hours (Figure 3.2). The reduction in cell viability was statistically significant for the highest concentrations.

Similarly, a dose and time dependent reduction in cell viability was seen for MWCNT-JP (Figure 3.3). However, the effect seemed to be significant following 48 hour exposure of MWCNT-JP compared to MWCNT-NO. With use of substantially lower concentrations for MWCNT-JP, the dose-time dependent reduction of cell viability was still observed (Figure 3.4). This observation demonstrates that very low concentrations of MWCNT-JP are needed to affect the viability of bronchial epithelial cells. Small variations between the cell-lines were observed, which may indicate that the effect is associated to the type of MWCNT.

4.3.2. Crocidolite

Crocidolite belongs to the group of amphibole asbestos, including a high content if iron [91]. Crocidolite is observed to generate reactive oxygen species that may be linked to cell injury. Asbestos fibers have also confirmed to be biologically active in various cell types, where the lung epithelial cells are the first cells that come into contact with fibers [91].With increasing time, the reduction of cell viability was observed, essentially for the highest concentrations after crocidolite exposure (Figure 3.5). The LC_{50} threshold (the lethal concentration, resulting in a 50 % of cell death) observed after 48 hours, was more apparent for the HBEC-3KT cell line.

4.3.3. Hydogene peroxide (H_2O_2)

The hydrogen peroxide, the oxidative agent known to cause ROS, induced a dose-dependent reduction without any dramatic effects on the cell viability (Figure 3.6). Neither concentrations nor various time periods indicated to fall below the LC_{50} threshold following H_2O treatment. The dose-time effect seemed to include a similar trend in reduction for 24, 48 and 72 hours.

4.3.4. Comparison of toxicity of MWCNTs

The cytotoxicity was found substantially higher for MWCNT-JP exposed cells than for MWCNT-NO exposed cells. At a lower dose-range the cytotoxicity of MWCNT-JP increases much faster than for MWCNT-NO, especially following 48 hour exposure. This implies that the dose-dependent response of cells to MWCNT-NO and MWCNT-JP differs. The various responses observed between the two sources of MWCNTs are supported by the results of Hu et al[19]. The study of Hu et al. demonstrated that CNTs with various size and shape (both SWCNT and MWCNT) may have different cytotoxic responses *in vitro* [19]. It is interesting to note that the response to asbestos seems to be more delayed, since asbestos demonstrates an increased response after 48 and 72 hours. In regard to whether MWCNT induce asbestos like effects or not, it was shown that the cell viability was higher for asbestos treated cells than for MWCNT treated cells, even at relatively high concentrations following a 24 hours exposure (Figure 3.7). These differences could be due to structural differences, where previous studies have experienced that the fiber characteristics of MWCNT have played an important role in the cytotoxicity [92].

All together, the results indicate that the CNTs were more toxic compared to asbestos: MWCNT-JP > MWCNT-NO > crocidolite.

A more toxic response for MWCNT (especially MWCNT-JP) compared to crocidolite was observed in our experiments which is consistent with the results from the study by Hirano et al. Hirano et al. also observed that the IC_{50} value of 10 µg/ml MWCNT was less than 1/50 of crocidolite after 24 hour exposure in BEAS-2B cells [89].In our experiments we observed that LC_{50} values of MWCNT-NO were less than 1/5 of crocidolite and less than 1/20 for MWCNT-JP after 24 hour exposure, respectively. The study of Hirano et al. suggested the cytotoxic effect of MWCNT to derive from the interference of MWCNT with the plasma membrane function [89]. According to the study of Garza et al there is a correlation between the cytotoxicity and the production of ROS [93]. The toxicity of MWCNTs following 24 h exposure is much higher than (Figure 3.7) the cytotoxicity induced by the H_2O_2 (Figure 3.6 B). This may indicate an additional damage to the cells than already caused by ROS or that the fibers induce a prolonged ROS production.

4.4. Analysis of apoptotic cell death

The apoptotic/necrotic cell death was evaluated by staining cells with Hochest 33342, staining DNA in both viable and dead cells, and PI, staining DNA when membrane integrity is lost (necrotic cells). The percentage of cell death resulted from Hoechst/PI staining was comparable with the cytotoxicity results obtained in the WST assay.

The results from table A3.1 in Appendix III, illustrate that MWCNTs like asbestos and H_2O_2, may induce death mainly through the process of necrosis in the HBECs. However, Thapsigargin which inhibits the Ca^{2+}-ATPase in the membrane of the endoplasmatic reticulum [94], was more effective in inducing the process that morphologically looks like apoptosis in these cells. Still, the apoptotic event was delayed and not observed before a 96 h

exposure. Delayed apoptotic response observed in these HBEC cells correlates well with an earlier study carried out by Srivastava et al, where a significant number of apoptotic bodies were observed first after a 72 hour exposure of MWCNTs in A549 cells [62]. The same delayed response indicated to correspond with changes in mRNA and protein expressions, where transcriptional alterations were observed after 12 hours and translational alterations after 24 hours. Another explanation was suggested to be that post-translational alterations may take time which makes it logic that the apoptotic markers were not observed before 72 h [62]. However, another study experienced how rat lung epithelial cells treated with (5 µg/ml) MWCNTs underwent apoptosis rather than necrosis in a time period up to 36 hours. The cell death occurred after induction of oxidative stress that again stimulated transcription factor AP-1 and NF-κB before the release of cytochrome c [95]. It has been suggested that particles may interfere with intracellular proteins, DNA, and organelles, which may result in cell death via both apoptosis and necrosis. The study of Hu et al. has demonstrated that physical penetration of CNTs may result in an apoptotic and necrotic cell death via generations of ROS in various human cell lines [19].

The sensitivity of H_2O_2 treated cells (5 µM) appear to correlate with MWCNT-NO (1 µg/ml), MWCNT-JP and crocidolite (20 µg/ml) treated cells, where the various materials were observed to result in about 20-30 % cell death. Higher intensity of the PI-stained cells was observed at the higher concentrations of MWCNT-NO, illustrating an enhanced number of necrotic cells.

Apoptosis or necrosis are not the only mechanisms that may result in cell death. The study of Ding et al (2005) used MWCNT treated cells (human skin fribroblasts) and observed that the reduction in cell number was a result of apoptosis, necrosis and a possible G2/M block (Gap 2 phase / mitotic phase) resulting in reduced proliferation [96]. A hypothesis that particles affect cells during their division is possible, and an increased cell proliferation would therfore be detrimental.

4.5. Analysis of gene expression

The gene expression studies were performed using quantitative real-time PCR (qRT-PCR) after the isolation of RNA and synthesis of cDNA. qRT-PCR is considered as a well established method to measure the amount of mRNA expressed by the cells before and after exposure to the test materials. The expression of *COX-2, IL1B, IL6* and *IL8* were measured as markers of inflammation. Also, these genes are involved in a number of other cellular stress responses e.g. DNA damage and cell death [86]. The expression of *TP53* was investigated as a gene that is important for apoptosis.

4.5.1. Effects of MWCNT-NO

The gene expression experiments suggested that HBEC-3KT cells responded to the inflammatory stimuli of MWCNT-NO (5 µg/ml), though about a 5 fold increase of *IL6, IL8* and *IL1B* mRNAs was seen following a 24h exposure compared to unexposed control cells. The expression levels were correlated with increase in dose from 1 to 5 ug/ml of MWCNT-NO. IL-8 as a central activator and chemoattractant of neutrophils to site of inflammation

belongs to the group of pro-inflammatory chemokines [54]. Cellular stress is one condition that may stimulate the production of IL-8 [56]. The exposure of MWCNT in present the study might have resulted in cellular stress and therefore stimulation of *IL8*. The increase of *IL6* and *IL8* mRNAs can also correspond with the results of Hirano et al. which indicate an increase of the pro-inflammatory cytokines IL-6 and IL-8 in a MWCNT-dose dependent manner (1-10 µg/ml) for BEAS-2B cells (also human bronchial epithelial cells). However, a study by Herzog et al, analyzed the inflammatory response of tumor and primary human lung cells (A549 and NHBE) to SWCNT and found that the DPPC in the dispersion medium may affect IL-8 and IL-6 expression in A549 cells [97].

An increasing expression of *IL1B* after exposure of HBEC-2KT cells to MWCNT-NO was found. Whether this is an effect of particles or correlated with increased expression of *IL6* and *IL8* remains to be investigated. A study by Loitsch et al has suggested that either IL-1 or TNF-α may stimulate the production of the IL8 [56]. The production of IL-6 has also been indicated to be regulated by IL-1β [98].

4.5.2. Effects of MWCNT-JP

The release of inflammatory cytokines such as *IL6*, *IL8* together with *IL1B* for the HBEC-3KT cells indicated to increase after a treatment of MWCNT-JP (0.5 µg/ml). This tendency is similar to MWCNT-NO, and may illustrate similar inflammatory responses of the two different MWCNTs at least for HBEC-3KT cells. However, little changes in gene expression were observed for HBEC-2KT following MWCNT-JP treatment, which could be a result of individual variations and different defense mechanisms.

4.5.3. Effects of crocidolite asbestos

A hypothesis to be addressed in this thesis is whether the response seen for MWCNT exposure resembles that of crocidolite exposure. Crocidolite treated HBEC-2KTcells induced the expression of *PTGS2 (COX-2)* about 12 times after a 24 hour exposure compared to unexposed control cells. The induction of various pro-inflammatory mediators may be time-dependent, and since the expression only is measured after a 24 hour exposure, it is difficult to detect other mediators such as *IL1B*, that may already have been stimulated. The up-regulation of COX-2 may take several hours [99], which could be the effect seen in present report. COX-2 has shown to be a downstream target of IL-β signaling [100], but other signaling pathways may also affect its expression. This finding is in accordance with a previous study of Leyva and Roberts, that interestingly illustrates how epithelial cells release PGI_2 (product of arachidonic acid metabolism) after a crocidolite exposure. A release of the prostacyclin PGI_2 is an indicator of cell activation and inflammation, which is depends on the function of COX-2, and vitronectin receptors (VNR). The same study showed that crocidolite in addition required the presence of an RGD protein coating the fibers to induce PGI_2 (inflammation) [101].

IL-1β is involved in mediation of critical illnesses e.g. auto inflammatory diseases [48] and is regulated on various levels. There are many downstream targets of the IL-1β signaling. The asbestos in HBEC-3KT, resulted in nearly 8 times increase of *IL1B* mRNA levels following a

24 hour exposure to 50 µg/ml of crocidolite compared to unexposed control cells. An increased production of the pro-inflammatory cytokine *IL1B*, has previously been demonstrated in rat alveolar macrophages *in vitro* after an exposure to 25 µg/ml crocidolite, this could support the possibility of *IL1B* induction post-exposure to asbestos in epithelial cells as well [102].

A tendency towards increasing the *IL8* mRNA levels was seen in crocidolite-treated HBEC-3KT cells. The study of Herzog et al. observed no statistically significant response of neither IL-8 nor IL-6 for NHBE cells after a 24 hour exposure of crocidolite (0.20-50 µg/ml), however, following 48 hour exposure a small increase was seen [97]. The small induction of *IL8* in present study might be due to different exposure conditions or source of asbestos, and the cytokine induction could in addition be time-dependent, by occurring either at a later or an earlier stage than following 24 hour post exposure.

The expression of IL8 has been indicated to be stimulated by the induction of TNF-α and IL-1[56]. However, the study of Rosenthal et al (1994) experienced induction of IL-8 after crocidolite treatment in A549 and primary epithelial cells without presence of TNF-α or IL-1 *in vitro*, which demonstrated that asbestos fibers manage to directly stimulate the release of IL-8. The release of IL-8 is not stimulated by all types of particles, but certain physico-chemical attributes of fibers have indicated to play a crucial role regarding the IL-8 response which could be linked to fiber-like shape of MWCNTs [103]. Since the expression levels of both *IL1B* and *IL8* increase at the same time, it could illustrate that they are regulated through the same mechanism.

4.5.4. Effects of H_2O_2

The H_2O_2 reference seemed not to have any effect on any of the various inflammatory mediators tested after a 24 hour exposure for HBECs. One possible explanation could be the time-dependent factor, though H_2O_2 fast diffuses through the cellular membrane into the cell where it quickly interacts with cellular constituents and following inactivation by antioxidant molecules and enzymes before the 24 hour exposure [104] The intracellular level may only reach a certain amount of the applied H_2O_2 which depends on e.g. the cell type.

4.5.5. Comparison between the experiments

The analysis of gene expression in the HBEC cells after a 24 hour exposure resulted in induction of some of the inflammatory genes after an exposure for the three fibers (MWCNTs and crocidolite) and essentially MWCNT-NO and crocidolite treatment resulted in enhanced response on gene expression. The HBEC cell lines represent normal cells of the lung epithelium, and our results indicate that the two cell lines from different individuals principally respond in the same manner. However, as seen in figure 3.14 the *COX-2* and *IL6* mRNA expressions differed significantly between the two individuals, with an enhanced fold increase of *COX-2* for HBEC-2KT cells after crocidolite treatment, and increased fold increase of *IL6* for HBEC-3KT cells after MWCNT-NO treatment. The study of Levya and Roberts demonstrated how COX-2 induced PGI_2 production, whereas the same study also observed that crocidolite did not cause a cytotoxic effect [101]. In relation to our results, the

expression of *COX-2* for HBEC-2KT could also be induced by proteins coating the fibers similar to proteins that matched certain membrane receptors (e.g. VNR), which further induced the observed expression of *COX-2*. However, it should be noted that the culture medium used in our experiments was serum free. The significant *COX-2* difference observed could also be a result of a virtual early transcriptional expression of *COX-2* for HBEC-3KT. Levya and Roberts reported a transcriptional induction of COX-2 already 2 hours after an exposure in LA-4 lung epithelial cells, which could indicate various cells and fibers induce the expression at various time-periods [101]. Surface coating can similarly affect MWCNT uptake, where the membrane may have receptors for the specific adsorbed proteins and the MWCNT-bound proteins are able both to interact with the receptors and compete with existing free proteins, resulting in cellular responses. Observed individual differences can be caused by many factors of both environmental and genetic backgrounds e.g. different polymorphisms in pro-inflammatory genes or various epigenetic patterns [105-106].

HBECs demonstrated to be very susceptible to MWCNT-induced toxicity, especially MWCNT-JP. However, when measuring the transcriptional activity of inflammatory genes crocidolite and MWCNT-NO had significant inflammatory effects after 24 hour exposure.

The H_2O_2 treated cells did not respond differently in the expression of the few inflammatory genes or in the expression of TP53 after exposure to various compounds. However, the low expression of the *TP53* gene after a 24 hour exposure may correlate with low apoptotic fraction of cells observed in the apoptosis analysis. Ramirez et al. who generated the HBEC cells also experienced low levels of p53 expression before UV irradiation and a substantially increase after UV irradiation [74]. Our results indicate that particles may not induce expression of *TP53* following a 24 hour exposure. Up regulation of p53 has clearly been related to DNA damage, although expression of *TP53* was not observed in this study it cannot be excluded that DNA damage may not be involved.

It is also possible that the MWCNT-induced cellular effects may result from the association of MWCNT with cell membrane, resulting in damage to the cell membrane integrity [89]. This can be supported by the finding of the PI/Hoechst experiments, where MWCNT essentially induced cell death through the process of necrosis and loss of cell membrane integrity.

4.6.Methodological considerations

4.6.1. Handling of test materials

To help dispersion of the MWCNTs dissolved in DM, a sonication procedure together with a non-ionic surfactant Tween 80 were used. The tendency of CNTs to form large agglomerates points out the difficulty regarding the toxicity studies. To study the effect of inhaling MWCNTs, the fibers must be non-agglomerated and the use of an effective dispersion medium (DM) is essential. A well tested DM developed by Porter et al. was used in this thesis, mimicking components of the lung alveolar lining fluid (BAL fluid)[25].
Various assay components may interfere with the particles resulting in toxicity e.g. cell type, traces of metals, state of agglomeration, rate of dispersion or cell culture media [107]. The

surface of the nanoparticles includes a high capacity to adsorb proteins, and adsorption may subsequently mediate cellular responses [10]. Diapalmitoylphosphatidylcholine (DPPC), an important lung surfactant, is supplemented in the DM used for this thesis. Herzog et al (2009) demonstrated that a lung carcinoma cell line (A549) exposed to SWCNTs had an increased ROS production in the presence of DPPC [26].One suggestion of such an effect was that dispersion enhances the interaction between DPPC and CNTs which creates an hydrophilic particle coating and following alterations of the surface chemistry [26].The bioavailability toward traces of metals or other contaminating compounds may also be enhanced with the use of DPPC. In contrast, in another study MWCNTs dispersed in culture medium containing 1 % DPPC, neither result in cell membrane injury nor oxidative stress in A549 cells [108]. To assist dispersion of the MWCNTs dissolved in DM, a sonication procedure together with a non-ionic surfactant Tween 80 were included in our dispersion protocols. The effect of sonication has previously demonstrated to enhance particle dispersion resulting in a more homogenous solution [109].However, sonication can only facilitate a temporal suspension of the particles and particles may readily re-agglomerate [109].

The electrostatic nature of MWCNTs may negatively affect the concentrations in cytotoxicity experiments. Due to the static attribute of MWCNTs this made them adhere to the sonicator probe, cap and walls of the tube during handling. In addition, they were also quickly lost (dry powder) to the ambient air when removing the cap of the tube as described by Porter et al [25]. All these parameters may result in a lower concentration than assumed. The DM also contained the surfactant Tween 80 which may influence toxicity or the outcome of other experiments. A study by Geys et al. showed an apparent interaction between Tween 80 and CNTs. Furthermore, particles that were suspended in Tween 80 resulted in a decreased toxicity, where the outcome was cell-specific being more toxic in A549 tumor cells than in fully differentiated human bronchial epithelial cells.

The degree of agglomeration was not fully investigated i.e. using analytical instruments such as DLS and therefore may vary from experiment to experiment an also from sample to sample. MWCNT-JP seemed more electrostatic and harder to dissolve in the DM. In order to achieve a good homogenized solution an addition of Tween 80 was essential. This was not the case for MWCNT-NO which could be dispersed without Tween 80. In order, to have similar conditions Tween 80 was added to the MWCNT-NO samples as well. Tween 80 is a surfactant that may reduce the reactivity of MWCNT coating the reactive sites or affect particle uptake [24].

4.6.2. Choice of the cytotoxicity assay

The results obtained in this thesis may be influenced by several factors. Hirano et al. have commented on the effect of cell density on MWCNT cytotoxicity, where an enhanced cytotoxicity was connected to a low cell density and increased cell viability was linked to a high cell density [89]. Concentration is another crucial factor, where high concentrations (50-100 µg/ml) of particles seemed to fully cover the cells. Complete coverage may affect the cell growth condition e.g. the supply of light, oxygen or other essential nutrients. The adsorptive

nature of MWCNT (especially with a large surface area) may cause binding and elimination of important nutrients, cytokines or growth factors that are included in e.g. the culture media [110]. This property of MWCNT may therefore cause an indirect toxicity resulting in decreased cell viability, decreased metabolic activity, and hinder the rate of cell proliferation and metabolism. The consequence of such indirect toxicity may be false positive results instead of true particle toxicity. It is important to note that the colorimetric cytotoxic assay used in these experiments measure metabolic active cells which includes dying, damaged cells that still may be metabolically active and consequently cause false results [111]. Further factors influencing in vitro toxicity assays, may be physical form, diameter and length, coating, catalytic activity, acidity or alkalinity, magnetic properties, and dissolution [19, 23].
An enhanced number of *in vitro* toxicity studies have generated evidence that nanoparticles have the ability to interfere with assay components or detection systems [23]. To elucidate the cytotoxicity of various test materials in present study, cell viability through mitochondrial function was quantitatively assessed under exposed condition for the respective test materials (after 6, 24, 48 and 72 hours). To start with, two assays were tested: WST-8 and MTT. The WST-8 assay essentially indicates a dose-dependent decrease of the mitochondrial enzyme activity after 24 hours for the various test materials. The MTT-assay, on the other hand, which is based on the same principle as the WST assay but results in an insoluble reaction product, demonstrated varying results with large standard errors when measuring the cell survival (data not shown). Furthermore, an increase in viability after a 6 hour exposure was observed with the MTT assay, which implies enhanced proliferation after particle exposure. Pulskamp et al. suggests that disturbance of the MTT test may occur through attachment of CNTs to the insoluble MTT product. Unexpectedly the two assays gave divergent results concerning the effects of MWCNT-NO. Pulskamp et al similarly experienced divergent results of the MTT and the WST tests, after CNT exposure to A549 cells after 24 hour exposure. The study of Pulskamp et al. decided to verify the cytotoxicity assay with the use of PI and FACS analysis to measure the response of CNTs on the cell membrane integrity (detect apoptotic and necrotic cells). The results of PI/FACS verified that results of the WST assay were more reliable [112].

Interference of CNTs with the MTT also reported by Belyanskaya et al where reduction of MTT by SWCNT (oxidizing the substrate MTT) was detected, which resulted in cautionary conclusion to be careful when evaluating any result from MTT assay [113]. The two assays, MTT and WST, differ among other factors in relation to the optical detection (O.D. 450 nm for WST and 560 nm for MTT). Some NP includes optical properties which can disturb the detection system. NP may absorb and release light of various wavelengths, and further be capable of disturbing the signal intensity in assays with optical measurements [23]. The study of Hirano et al. determined the MWCNT concentration, and experienced a good correlation between increases in O.D at 640 nm and amounts of MWCNT [89]. This observation further strengthens the WST-assay when working with particles. Based on these reports we therefore decided to use WST-8 for toxicity experiments.

4.6.3. Fluorescence microscopic detection of cell death

The Hoechst/PI staining is a fast, well known method used to distinguish between apoptotic and necrotic cells. However, the procedure is based on visual cell counting, which in itself means a subjective judgment. The cell death obtained in these experiments may illustrate the real picture, but one should be aware that the study may depend on many experimental factors e.g. uncertainties when defining the morphology of an apoptotic cell, treatment of cells, the cell passage number, and the preparation of particles or the medium used. A factor to note from these results (see Figure 3.11), is the relative high proportion of death in the control cells which may be caused by mechanical damage from the staining procedure, trypsination procedure or during the cell culture process. An alternative method of quantification of the viability could involve automatic counting by flow cytometry.

4.6.4. qRT-PCR

During the RNA isolation from the cells treated with crocidolite and MWCNT-NO, there were some difficulties: the dose that actually should result in 80 % viability did not result in sufficient amount of RNA for cDNA synthesis and therefore lower doses were selected. During RNA isolation the quality of the RNA is important. The quality or the purity of RNA can be controlled by measuring on the RNA concentration, where an OD_{260}/OD_{280} ratio around 2 indicates pure RNA. Contamination (low OD_{260}/OD_{280} ratio) was observed when measuring the concentration of the little product received form cells treated with crocidolite and MWCNT-NO, which could indicate contamination from the particles. Samples with the low ratio were not included, samples mainly with a ratio between 1,8 and 2 were included. Another observation made during the separation of RNA was how the MWCNT-NO particles in contrast to MWCNT-JP where located in the interphase where the DNA exists (after chlorophorm was added), and possible interaction between MWCNT and DNA could occur.

5. Conclusion and future perspectives

In this study two human lung epithelial cell lines established from normal epithelial cells were used to investigate the biological responses after exposure to MWCNTs, asbestos and hydrogen peroxide. The results showed that the MWCNTs, especially MWCNT-JP, were more effective to reduce the number of viable cells as observed by the cytotoxicity assays. The cytotoxicity between fibrous compounds varied being highest for MWCNT-JP followed by MWCNT-NO and crocidolite, respectively. The dose and time dependent reduction in cell viability observed for MWCNTs was similar for both cell-lines. Further analysis of cell death by Hoechest/PI staining showed that the cell death essentially occurred through necrosis rather than apoptosis following exposure to MWCNTs, crocidolite and H_2O_2. The gene expression analysis showed that MWCNT-NO induced higher expressions of the inflammatory genes compared to MWCNT-JP. A similar dose-dependent trend in induction of *COX-2* and *IL1B* was observed in both cell lines whereas induction of *IL6* and *IL8* after MWCNT-NO exposure was only observed in HBEC-3KT. In HBEC-2KT cells, induction of *COX-2* was observed after treatment with crocidolite. In contrast to cytotoxicity assays Crocidolite was a more effective inducer of gene expression followed by MWCNT-NO and MWCNT-JP, respectively. There were no changes in the expression of *TP53* gene following exposure to any of the compounds.

Various physico-chemical properties, degree of aggregation/agglomeration, contaminants, length and diameter of CNTs may affect their biological responses. A more detailed characterization of the MWCNTs is needed in order to compare effects between different products. This could be achieved by using DLS and TEM. Furthermore, the low apoptosis observed in these cells should be confirmed by other methods such as flow-cytometri or caspase-3/7 assay. Additionally, the induction of gene expressions from this study needs to be verified at the protein level with use of e.g. ELISA or western blot. It would also be interesting to analyze different genes and transcription factors, such as NF-κB and AP-1 to see whether they are involved in the mechanisms of MWCNT- induced toxicity observed. One important hypothesis for particle mediated effects is their ability to form ROS. To achieve further insight to their mechanisms it would be interesting to detect ROS production in MWCNTs-stimulated HBECs with the use of e.g. the oxidant-sensitive dye DCFH-DA. It will also be helpful to verify the responses in many more cell lines and possibly in other cell types as exposure to MWCNTs also occurs through other routs than lungs. *In vitro* studies investigating the altered effects of inflammatory mediators should be verified in animal studies, though these models include the complexity of a whole animal and particularly the involvement of the immune system.

References

1. Warheit, D.B., *How Meaningful are the Results of Nanotoxicity Studies in the Absence of Adequate Material Characterization?* Toxicological Sciences, 2008. **101**(2): p. 183-185.
2. Shvedova, A., V. Kagan, and B. Fadeel, *Close Encounters of the Small Kind: Adverse Effects of Man-Made Materials Interfacing with the Nano-Cosmos of Biological Systems.* Annual Review of Pharmacology and Toxicology, 2010. **50**(1): p. 63-88.
3. Oberdorster, G. and G. Oberdörster, *Safety assessment for nanotechnology and nanomedicine: concepts of nanotoxicology.* Journal of internal medicine, 2010. **267**(1): p. 89-105.
4. Gwinn, M.R. and V. Vallyathan, *Nanoparticles: Health Effects—Pros and Cons.* Environ Health Perspect, 2006. **114**(12).
5. Rejeski, D. *The Project on Emerging Nanotechnologies*. 2011 [cited 2011 30.03.2011]; Available from: http://www.nanotechproject.org/.
6. Ostiguy, C., et al. *Health Effects of Nanoparticles*. 2008 [cited 2011 01.04.2011]; Available from: http://www.irsst.qc.ca/media/documents/PubIRSST/R-589.pdf.
7. Berube, D., et al., *Characteristics and classification of nanoparticles: Expert Delphi survey.* Nanotoxicology. **0**(0): p. 1-10.
8. Donaldson, K., et al., *Carbon nanotubes: a review of their properties in relation to pulmonary toxicology and workplace safety.* Toxicol Sci, 2006. **92**(1): p. 5-22.
9. Iijima, S., *Helical microtubules of graphitic carbon.* Nature, 1991: p. 354.
10. Ehrenberg, M.S., et al., *The influence of protein adsorption on nanoparticle association with cultured endothelial cells.* Biomaterials, 2009. **30**(4): p. 603-610.
11. Muller, J., et al., *Respiratory toxicity of multi-wall carbon nanotubes.* Toxicology and Applied Pharmacology, 2005. **207**(3): p. 221-231.
12. Rotoli, B.M., et al., *Non-functionalized multi-walled carbon nanotubes alter the paracellular permeability of human airway epithelial cells.* Toxicol Lett, 2008. **178**(2): p. 95-102.
13. Borm, P.J., et al., *The potential risks of nanomaterials: a review carried out for ECETOC.* Part Fibre Toxicol, 2006. **3**: p. 11.
14. Aitken, R.J., et al., *Manufacture and use of nanomaterials: current status in the UK and global trends.* Occupational Medicine, 2006. **56**(5): p. 300-306.
15. Aschberger, K., et al., *Review of carbon nanotubes toxicity and exposure--appraisal of human health risk assessment based on open literature.* Crit Rev Toxicol, 2010. **40**(9): p. 759-90.
16. Han, J.H., et al., *Monitoring Multiwalled Carbon Nanotube Exposure in Carbon Nanotube Research Facility.* Inhalation Toxicology, 2008. **20**(8): p. 741-749.
17. Jiang, J., et al., *Does Nanoparticle Activity Depend upon Size and Crystal Phase?* Nanotoxicology, 2008. **2**(1): p. 33-42.
18. Rivera Gil, P., et al., *Correlating Physico-Chemical with Toxicological Properties of Nanoparticles: The Present and the Future.* ACS Nano, 2010. **4**(10): p. 5527-5531.
19. Hu, X., et al., *In vitro evaluation of cytotoxicity of engineered carbon nanotubes in selected human cell lines.* The Science of the total environment, 2010. **408**(8): p. 1812-1817.
20. Peigney, A., et al., *Specific surface area of carbon nanotubes and bundles of carbon nanotubes.* Carbon, 2001. **39**(4): p. 507-514.
21. Muller, J., et al., *Clastogenic and aneugenic effects of multi-wall carbon nanotubes in epithelial cells.* Carcinogenesis, 2008. **29**(2): p. 427-433.
22. Yamashita, K., et al., *Carbon nanotubes elicit DNA damage and inflammatory response relative to their size and shape.* Inflammation, 2010. **33**(4): p. 276-80.
23. Kroll, A., et al., *Current in vitro methods in nanoparticle risk assessment: Limitations and challenges.* European journal of pharmaceutics and biopharmaceutics, 2009. **72**(2): p. 370-377.

24. Gratton, S.E., et al., *The effect of particle design on cellular internalization pathways.* Proc Natl Acad Sci U S A, 2008. **105**(33): p. 11613-8.
25. Porter, D., et al., *A biocompatible medium for nanoparticle dispersion.* Nanotoxicology, 2008. **2**(3): p. 144-154.
26. Herzog, E., et al., *Dispersion medium modulates oxidative stress response of human lung epithelial cells upon exposure to carbon nanomaterial samples.* Toxicology and Applied Pharmacology, 2009. **236**(3): p. 276-281.
27. Poland, C.A., et al., *Carbon nanotubes introduced into the abdominal cavity of mice show asbestos-like pathogenicity in a pilot study.* Nat Nano, 2008. **3**(7): p. 423-428.
28. Jaurand, M.-C., A. Renier, and J. Daubriac, *Mesothelioma: Do asbestos and carbon nanotubes pose the same health risk?* Particle and Fibre Toxicology, 2009. **6**(1): p. 1-14.
29. Oberdorster, G., J. Ferin, and B.E. Lehnert, *Correlation between particle size, in vivo particle persistence, and lung injury.* Environ Health Perspect, 1994. **102 Suppl 5**: p. 173-9.
30. Takagi, A., et al., *Induction of mesothelioma in p53+/- mouse by intraperitoneal application of multi-wall carbon nanotube.* J Toxicol Sci, 2008. **33**(1): p. 105-16.
31. Donaldson, K., et al., *Re: Induction of mesothelioma in p53+/- mouse by intraperitoneal application of multi-wall carbon nanotube.* J Toxicol Sci, 2008. **33**(3): p. 385; author reply 386-8.
32. Shimada, A., et al., *Translocation pathway of the intratracheally instilled ultrafine particles from the lung into the blood circulation in the mouse.* Toxicol Pathol, 2006. **34**(7): p. 949-57.
33. Chithrani, B.D. and W.C.W. Chan, *Elucidating the Mechanism of Cellular Uptake and Removal of Protein-Coated Gold Nanoparticles of Different Sizes and Shapes.* Nano Letters, 2007. **7**(6): p. 1542-1550.
34. Firme Iii, C.P. and P.R. Bandaru, *Toxicity issues in the application of carbon nanotubes to biological systems.* Nanomedicine: Nanotechnology, Biology and Medicine, 2010. **6**(2): p. 245-256.
35. Aggarwal, B.B., et al., *Inflammation and cancer: how hot is the link?* Biochem Pharmacol, 2006. **72**(11): p. 1605-21.
36. Coussens, L.M. and Z. Werb, *Inflammation and cancer.* Nature, 2002. **420**(6917): p. 860-7.
37. Balkwill, F. and A. Mantovani, *Inflammation and cancer: back to Virchow?* The Lancet, 2001. **357**(9255): p. 539-545.
38. Azad, N., Y. Rojanasakul, and V. Vallyathan, *Inflammation and lung cancer: roles of reactive oxygen/nitrogen species.* J Toxicol Environ Health B Crit Rev, 2008. **11**(1): p. 1-15.
39. Bartsch, H. and J. Nair, *Chronic inflammation and oxidative stress in the genesis and perpetuation of cancer: role of lipid peroxidation, DNA damage, and repair.* Langenbecks Arch Surg, 2006. **391**(5): p. 499-510.
40. Folkmann, J.K., et al., *Oxidatively damaged DNA in rats exposed by oral gavage to C60 fullerenes and single-walled carbon nanotubes.* Environ Health Perspect, 2009. **117**(5): p. 703-8.
41. Jaiswal, M., et al., *Human Ogg1, a protein involved in the repair of 8-oxoguanine, is inhibited by nitric oxide.* Cancer Res, 2001. **61**(17): p. 6388-93.
42. Smith, W.L., R.M. Garavito, and D.L. DeWitt, *Prostaglandin endoperoxide H synthases (cyclooxygenases)-1 and -2.* J Biol Chem, 1996. **271**(52): p. 33157-60.
43. Poligone, B. and A.S. Baldwin, *Positive and negative regulation of NF-kappaB by COX-2: roles of different prostaglandins.* J Biol Chem, 2001. **276**(42): p. 38658-64.
44. Bours, V., et al., *NF-kappaB activation in response to toxical and therapeutical agents: role in inflammation and cancer treatment.* Toxicology, 2000. **153**(1-3): p. 27-38.
45. Lawrence, T., *The nuclear factor NF-kappaB pathway in inflammation.* Cold Spring Harb Perspect Biol, 2009. **1**(6): p. a001651.

46. Greten, F.R., et al., *NF-kappaB is a negative regulator of IL-1beta secretion as revealed by genetic and pharmacological inhibition of IKKbeta.* Cell, 2007. **130**(5): p. 918-31.
47. Park, J.M., et al., *Signaling pathways and genes that inhibit pathogen-induced macrophage apoptosis--CREB and NF-kappaB as key regulators.* Immunity, 2005. **23**(3): p. 319-29.
48. Dinarello, C.A., *Immunological and inflammatory functions of the interleukin-1 family.* Annu Rev Immunol, 2009. **27**: p. 519-50.
49. Dinarello, C.A., *Interleukin-1beta.* Crit Care Med, 2005. **33**(12 Suppl): p. S460-2.
50. Hart, K., et al., *A combination of functional polymorphisms in the CASP8, MMP1, IL10 and SEPS1 genes affects risk of non-small cell lung cancer.* Lung Cancer, 2011. **71**(2): p. 123-9.
51. Schindler, R., P. Ghezzi, and C.A. Dinarello, *IL-1 INDUCES IL-1 .4. IFN-GAMMA SUPPRESSES IL-1 BUT NOT LIPOPOLYSACCHARIDE-INDUCED TRANSCRIPTION OF IL-1.* Journal of Immunology, 1990. **144**(6): p. 2216-2222.
52. Heinrich, P.C., et al., *Principles of interleukin (IL)-6-type cytokine signalling and its regulation.* Biochem J, 2003. **374**(Pt 1): p. 1-20.
53. Gabay, C., et al., *Interleukin 1 receptor antagonist (IL-1Ra) is an acute-phase protein.* J Clin Invest, 1997. **99**(12): p. 2930-40.
54. Xie, K., *Interleukin-8 and human cancer biology.* Cytokine Growth Factor Rev, 2001. **12**(4): p. 375-91.
55. Shi, Q., et al., *Regulation of interleukin-8 expression by tumor-associated stress factors.* J Interferon Cytokine Res, 2001. **21**(8): p. 553-66.
56. Loitsch, S.M., et al., *Reactive Oxygen Intermediates Are Involved in IL-8 Production Induced by Hyperosmotic Stress in Human Bronchial Epithelial Cells.* Biochemical and Biophysical Research Communications, 2000. **276**(2): p. 571-578.
57. Ye, S.F., et al., *ROS and NF-kappaB are involved in upregulation of IL-8 in A549 cells exposed to multi-walled carbon nanotubes.* Biochem Biophys Res Commun, 2009. **379**(2): p. 643-8.
58. Mühlfeld, C., et al., *Interactions of nanoparticles with pulmonary structures and cellular responses.* American Journal of Physiology - Lung Cellular and Molecular Physiology, 2008. **294**(5): p. L817-L829.
59. Knaapen, A.M., et al., *Inhaled particles and lung cancer. Part A: Mechanisms.* Int J Cancer, 2004. **109**(6): p. 799-809.
60. Reddy, A., et al., *Multi wall carbon nanotubes induce oxidative stress and cytotoxicity in human embryonic kidney (HEK293) cells.* Toxicology, 2010. **272**(1-3): p. 11-16.
61. Tsukahara, T. and H. Haniu, *Cellular cytotoxic response induced by highly purified multi-wall carbon nanotube in human lung cells.* Molecular and Cellular Biochemistry, 2011: p. 1-7.
62. Srivastava, R.K., et al., *Multi-walled carbon nanotubes induce oxidative stress and apoptosis in human lung cancer cell line-A549.* Nanotoxicology, 2010.
63. van der Meer, F.J., et al., *Apoptosis- and necrosis-induced changes in light attenuation measured by optical coherence tomography.* Lasers Med Sci, 2010. **25**(2): p. 259-67.
64. Lockshin, R.A. and Z. Zakeri, *Apoptosis, autophagy, and more.* The International Journal of Biochemistry & Cell Biology, 2004. **36**(12): p. 2405-2419.
65. Okada, H. and T.W. Mak, *Pathways of apoptotic and non-apoptotic death in tumour cells.* Nat Rev Cancer, 2004. **4**(8): p. 592-603.
66. Kerr, J.F., A.H. Wyllie, and A.R. Currie, *Apoptosis: a basic biological phenomenon with wide-ranging implications in tissue kinetics.* Br J Cancer, 1972. **26**(4): p. 239-57.
67. Taylor, R.C., S.P. Cullen, and S.J. Martin, *Apoptosis: controlled demolition at the cellular level.* Nat Rev Mol Cell Biol, 2008. **9**(3): p. 231-241.
68. Vousden, K.H. and D.P. Lane, *p53 in health and disease.* Nat Rev Mol Cell Biol, 2007. **8**(4): p. 275-283.
69. Dominici, F., et al., *Fine particulate air pollution and hospital admission for cardiovascular and respiratory diseases.* JAMA, 2006. **295**(10): p. 1127-34.

70. Muhlfeld, C., P. Gehr, and B. Rothen-Rutishauser, *Translocation and cellular entering mechanisms of nanoparticles in the respiratory tract.* Swiss Med Wkly, 2008. **138**(27-28): p. 387-91.
71. Huczko, A., et al., *Pulmonary Toxicity of 1-D Nanocarbon Materials.* Fullerenes, Nanotubes and Carbon Nanostructures, 2005. **13**(2): p. 141 - 145.
72. Grubek-Jaworska, H., et al., *Preliminary results on the pathogenic effects of intratracheal exposure to one-dimensional nanocarbons.* Carbon, 2006. **44**(6): p. 1057-1063.
73. Jia, G., et al., *Cytotoxicity of Carbon Nanomaterials: Single-Wall Nanotube, Multi-Wall Nanotube, and Fullerene.* Environmental Science & Technology, 2005. **39**(5): p. 1378-1383.
74. Ramirez, R.D., et al., *Immortalization of human bronchial epithelial cells in the absence of viral oncoproteins.* Cancer Res, 2004. **64**(24): p. 9027-34.
75. Li, H., et al., *Direct Synthesis of High Purity Single-Walled Carbon Nanotube Fibers by Arc Discharge.* The Journal of Physical Chemistry B, 2004. **108**(15): p. 4573-4575.
76. Kim, Y.A., et al., *Synthesis and structural characterization of thin multi-walled carbon nanotubes with a partially facetted cross section by a floating reactant method.* Carbon, 2005. **43**(11): p. 2243-2250.
77. Asakura, M., et al., *Genotoxicity and Cytotoxicity of Multi-wall Carbon Nanotubes in Cultured Chinese Hamster Lung Cells in Comparison with Chrysotile A Fibers.* Journal of occupational health, 2010. **52**(3): p. 9-20.
78. Sharma, C., et al., *Single-walled carbon nanotubes induces oxidative stress in rat lung epithelial cells.* Journal of Nanoscience and Nanotechnology, 2007. **7**(7): p. 2466-2472.
79. Streiner, D.L., *Maintaining standards: Differences between the standard deviation and standard error, and when to use each.* Canadian Journal of Psychiatry-Revue Canadienne De Psychiatrie, 1996. **41**(8): p. 498-502.
80. Altman, D.G. and J.M. Bland, *Standard deviations and standard errors.* BMJ, 2005. **331**(7521): p. 903.
81. Tailor, J.R., *An introduction to Error Analysis*. second ed, ed. A. McGuire. 1997, CA: University Science Books.
82. Altman, D.G., *Practical statistics for medical research*. 1991, CHAPMAN & HALL/CRC: London. p. 589.
83. Lundberg, A.S., et al., *Immortalization and transformation of primary human airway epithelial cells by gene transfer.* Oncogene, 2002. **21**(29): p. 4577-86.
84. Gazdar, A.F., B. Gao, and J.D. Minna, *Lung cancer cell lines: Useless artifacts or invaluable tools for medical science?* Lung Cancer, 2010. **68**(3): p. 309-18.
85. Rushton, E.K., et al., *Concept of assessing nanoparticle hazards considering nanoparticle dosemetric and chemical/biological response metrics.* J Toxicol Environ Health A, 2010. **73**(5): p. 445-61.
86. Mitschik, S., et al., *Effects of particulate matter on cytokine production in vitro: a comparative analysis of published studies.* Inhal Toxicol, 2008. **20**(4): p. 399-414.
87. Porter, D., et al., *Mouse pulmonary dose- and time course-responses induced by exposure to multi-walled carbon nanotubes.* Toxicology, 2010. **269**(2-3): p. 136-147.
88. Liu, S., et al., *Sharper and faster "nano darts" kill more bacteria: a study of antibacterial activity of individually dispersed pristine single-walled carbon nanotube.* ACS Nano, 2009. **3**(12): p. 3891-902.
89. Hirano, S., et al., *Uptake and cytotoxic effects of multi-walled carbon nanotubes in human bronchial epithelial cells.* Toxicol Appl Pharmacol, 2010. **249**(1): p. 8-15.
90. Patlolla, A., B. Knighten, and P. Tchounwou, *Multi-walled carbon nanotubes induce cytotoxicity, genotoxicity and apoptosis in normal human dermal fibroblast cells.* Ethn Dis, 2010. **20**(1 Suppl 1): p. S1-65-72.

91. Mossman, B.T., *Assessment of the pathogenic potential of asbestiform vs. nonasbestiform particulates (cleavage fragments) in in vitro (cell or organ culture) models and bioassays.* Regul Toxicol Pharmacol, 2008. **52**(1 Suppl): p. S200-3.
92. Kim, J.S., et al., *Determination of cytotoxicity attributed to multiwall carbon nanotubes (MWCNT) in normal human embryonic lung cell (WI-38) line.* J Toxicol Environ Health A, 2010. **73**(21-22): p. 1521-9.
93. Garza, K.M., K.F. Soto, and L.E. Murr, *Cytotoxicity and reactive oxygen species generation from aggregated carbon and carbonaceous nanoparticulate materials.* Int J Nanomedicine, 2008. **3**(1): p. 83-94.
94. Davidson, G.A. and R.J. Varhol, *Kinetics of thapsigargin-Ca(2+)-ATPase (sarcoplasmic reticulum) interaction reveals a two-step binding mechanism and picomolar inhibition.* J Biol Chem, 1995. **270**(20): p. 11731-4.
95. Ravichandran, P., et al., *Multiwalled carbon nanotubes activate NF-<i>κ</i>B and AP-1 signaling pathways to induce apoptosis in rat lung epithelial cells.* Apoptosis, 2010. **15**(12): p. 1507-1516.
96. Ding, L., et al., *Molecular characterization of the cytotoxic mechanism of multiwall carbon nanotubes and nano-onions on human skin fibroblast.* Nano Lett, 2005. **5**(12): p. 2448-64.
97. Herzog, E., et al., *SWCNT suppress inflammatory mediator responses in human lung epithelium in vitro.* Toxicology and Applied Pharmacology, 2009. **234**(3): p. 378-390.
98. Zheng, H., et al., *Resistance to fever induction and impaired acute-phase response in interleukin-1 beta-deficient mice.* Immunity, 1995. **3**(1): p. 9-19.
99. Mitchell, J.A., et al., *Induction of cyclo-oxygenase-2 by cytokines in human pulmonary epithelial cells: regulation by dexamethasone.* Br J Pharmacol, 1994. **113**(3): p. 1008-14.
100. Lin, C.H., et al., *Involvement of protein kinase C-gamma in IL-1beta-induced cyclooxygenase-2 expression in human pulmonary epithelial cells.* Mol Pharmacol, 2000. **57**(1): p. 36-43.
101. Leyva, F. and K. Roberts, *Crocidolite Induces Prostaglandin I₂ Release Mediated by Vitronectin Receptor and Cyclooxygenase-2 in Lung Cells.* Lung, 2010. **188**(2): p. 133-141.
102. Mongan, L.C., T. Jones, and G. Patrick, *CYTOKINE AND FREE RADICAL RESPONSES OF ALVEOLAR MACROPHAGES IN VITRO TO ASBESTOS FIBRES.* Cytokine, 2000. **12**(8): p. 1243-1247.
103. Rosenthal, G.J., et al., *Asbestos stimulates IL-8 production from human lung epithelial cells.* J Immunol, 1994. **153**(7): p. 3237-44.
104. Schröder, E. and P. Eaton, *Hydrogen peroxide as an endogenous mediator and exogenous tool in cardiovascular research: issues and considerations.* Current Opinion in Pharmacology, 2008. **8**(2): p. 153-159.
105. Hart, K., A. Haugen, and S. Zienolddiny, *Allele-specific induction of IL1B -31T/C promoter polymorphism by lung carcinogens.* Mutat Res, 2008. **656**(1-2): p. 14-8.
106. Sharma, S., T.K. Kelly, and P.A. Jones, *Epigenetics in cancer.* Carcinogenesis, 2010. **31**(1): p. 27-36.
107. Piret, J.P., et al., *Dispersion of multi-walled carbon nanotubes in biocompatible dispersants.* Journal of Nanoparticle Research, 2010. **12**(1): p. 75-82.
108. Tabet, L., et al., *Adverse effects of industrial multiwalled carbon nanotubes on human pulmonary cells.* J Toxicol Environ Health A, 2009. **72**(2): p. 60-73.
109. Murdock, R.C., et al., *Characterization of nanomaterial dispersion in solution prior to in vitro exposure using dynamic light scattering technique.* Toxicol Sci, 2008. **101**(2): p. 239-53.
110. Casey, A., et al., *Single walled carbon nanotubes induce indirect cytotoxicity by medium depletion in A549 lung cells.* Toxicol Lett, 2008. **179**(2): p. 78-84.
111. Roper, P.R. and B. Drewinko, *Comparison of in vitro methods to determine drug-induced cell lethality.* Cancer Res, 1976. **36**(7 PT 1): p. 2182-8.

112. Pulskamp, K., S. Diabate, and H.F. Krug, *Carbon nanotubes show no sign of acute toxicity but induce intracellular reactive oxygen species in dependence on contaminants.* Toxicol Lett, 2007. **168**(1): p. 58-74.
113. Belyanskaya, L., et al., *The reliability and limits of the MTT reduction assay for carbon nanotubes-cell interaction.* Carbon, 2007. **45**(13): p. 2643-2648.

Contents -Appendix

Appendix I

Cell lines

Cell line	Growth Medium	Tissue origin	Gender	Notes	Smoker
Human Bronchial Epithelial Cell (HBEC-3KT)	LHC-9 (serum-free) with Pit. Extract, in collagen-coated dishes	Lung, Immortalized	65 yr, F	NSCLC; informed consent	Yes
Human Bronchial Epithelial Cell (HBEC-2KT)	LHC-9 (serum-free) with Pit. Extract, in collagen-coated dishes	Lung, Immortalized	68 yr, M	No cancer; informed consent	Yes
Human lung adenocarcinoma epithelial cell line (A549)	DMEM /F12 w/10 % FBS	Lung	M	Lung adeno	Unknown

Test Material	Type	Company
MWCNT (XNRI MWNT-7, lot # 05072001K28)	Nanomaterials (NM), Positive control (MWCNT)	Mitsui & Co (Japan)
MWCNT	Nanomaterials (NM)	n-Tec (Norway)
UICC Crocidolite asbestos	Positive control (Fiber)	Medical Research Counsling (England)
Hydrogen peroxide (H_2O_2)	Positive control (ROS)	Sigma –Aldrich (Steinheim, Germany)
Thapsigargin (TG)	Positive control (apoptosis)	Sigma –Aldrich (Steinheim, Germany)

Kits

Biotium Inv:

Cell viability w/ MTT Cell Viability Assay kit

Quanta Bioscience:

cDNA synthesis w/qScript™ cDNA synthesis Kit

qRT-PCR w/ PerfeCTa SYBR Green master mix

Sigma-Aldrich

Cell viability w/ WST-8 Cell Counting Kit assay

Instruments

Instruments	Name
Automatic cell counting	InvitrogenTM Contess automated cell counter
Camera	Fugfilm las-4000 mini camara
Centrifuge	Eppendorf centrifuge 5702
Centrifuge	Sigma-26E
Cooler centrifuge	Sigma 4K15
Cooler centrifuge	Eppendorf centrigue 5417R
Fluorescene microscopy	Nikon Labophot
Heating block	Grant Instruments QBT2
Light microscope	Nikon Diaphoto (interphoto A/S)
Multimode Reader	Modulus Microplate Multimode Reader (Promega Corporation)
Real-time instrument	ABI Prism 7900HT Sequence Detection system with SDS2.2
Spectrophotometer	Eppendorf biophotmeter
Thermal cyclers	Perkin Elmer Cetus DNA Thermal Cycler 480 (Grant instruments)
Ultrasonicator	LabsonicM (Sartorius Stedium biotech)
Vortexer	Heidolphreax 2000
Water bath	Gesell

Chemicals

Chemicals	**Producer**
BSA	Sigma
Chloroform	Sigma
Collagen	Vitrogen 100
DMSO	Sigma
Dubecco's Modified Eagle Mediu	Gibco
EDTA (Triplex III)	Merck
Ethanol (rectified, absolute)	Kemetyl
FBS Fetal bovine serum	Gibco
Glucose	Sigma
HCl	Merck
HEPES	Sigma
Hoechst 33342	Sigma
Hydrogen peroxide	Sigma
Insulin	Sigma
Isol-RNA (Trizol)	5-Prime
KCl	Merck
Leibovitz's L-15 media	Invitrogen
LHC-9	Invitrogen
NaCl	Merck
NaHPO4*H_2O	Merck
Penicillin - Streptomyoci	Gibco
Phenol red	Sigma
Propane-2-ol (Isopropanol)	Merck
Propidium iodide (PI)	Merck
Selenium (Na_2SeO_3)	Sigma
Thasigargin	Sigma
Tris -base 7-9	Sigma
Trypan Blue dye 0,4 %	Invitrogen
Tween 80	Sigma

Cell culture media

Cell culture media	**Ingredients**
LHC-9	500 ml LHC-9, 5 ml PS
DMEM/ F12 w/ 10 % FBS	500 ml DMEM/F12, 7,5 ml HEPES, 625 µl insulin, 50 µl HC, 500 µl HC, 500 µl EGF 145 µl Selenium, 5 ml PS, 500 µl TF 50 ml FBS (10 %)

Solutions

All solutions are blended with ddH_2O and sterile filtered before use.

Name	Ingredients
AF (antobiotic freeze media)	76 % L15 media, 2 % 1M HEPES, 2 % PS, 20 % FBS
BSA (bovinle serum albumin) 1 mg/ml stock	100 mg BSA, 100 ml HBS
Collagen solution for petri dish coating 0,03 mg/ml	1 % collagen solution 3.13 mg/ml, 99 % HBS
DEPC	0.1 % DEPS in dH20
DM	PBS, 5.5 mM D-glucose , 0.6 mg/ml BSA, 0.01 mg/ml 1,2-dipalmitoyl-sn-glycero-3-phosphocholine (DPPC) diluted in ethanol (200 proof) (10 mg/ml)
DMSO (dimethyl sullphoxide) for cell culture storage	50 % L15 media, 2 % 1M HEPES, 8 % DMSO, 40 % FBS, EDTA
EDTA 0,5 M disodium dihydrate	9.3 g EDTA, 50 ml H_2O, pH adjusted to 8
EGF (epidermal growth factor) 10 µg/ml	200 µg EGF, 2ml BSA, 18 ml HBS
Etanol	75% EtOH i DEPC
FBS (fetal bovine serum)	Heat inactivated at 56°C for 45 minutes
HBS (HEPES buffered saline)	4.76 g HEPES, 7.07 g NaCl, 0,20g KCL, 1.70 g glucose, 1.94 g NaHPO4*H_2O, 1.04 ml 0,12 % phenol red, H_2O to 1 L
HC (hydrocortisone) 1 m'M	7.2 mg HC, 20 ml rectified ethanol
HEPES	238.3 g HEPES, 1 ml 0.12 % phenol red, in 1L d$H_2$0, adjusted to pH7.3
PBS (phosphate buffered saline)	7.07 g NaCl, 0.20 g KCl, 1.94 g $NaHPO_4$*H_2O, H_2O to 1L
Phenol red 125 mg/ml	125 g phenol , 360 µl ,1 M NaOH, 100 ml H20
TE buffer (Tris-EDTA buffer) 10 X, pH 8	100 mM Tris-Cl pH 8, 10 mM EDTA pH 8
TF (tranferrin) 5 mg/ml	500 mg transferrin, 10 ml BSA stock, 90 ml HBS
Tris -CL 1M pH 8, 1L	121.1 g Tris base, 42 ml HCl, H_2O to 1 L
Trypsin 1 %	50 mg Trypsin, 5 ml HBS
Thasigargin	100 µM in DMSO

Appendix II

Standard Curve

During the cytotoxicity experiment (WST-8-assay) various cell densities ($5x10^2$, $1x10^3$, $2x10^3$, $3x10^3$, $4x10^3$, $5x10^3$, $1x10^4$ and $2x10^4$ cells/well) were cultured in a 96-well dish, for a standard curve. The standard curve will inform about the growth phase for the two different cell lines without any exposure, see figure A2.1.

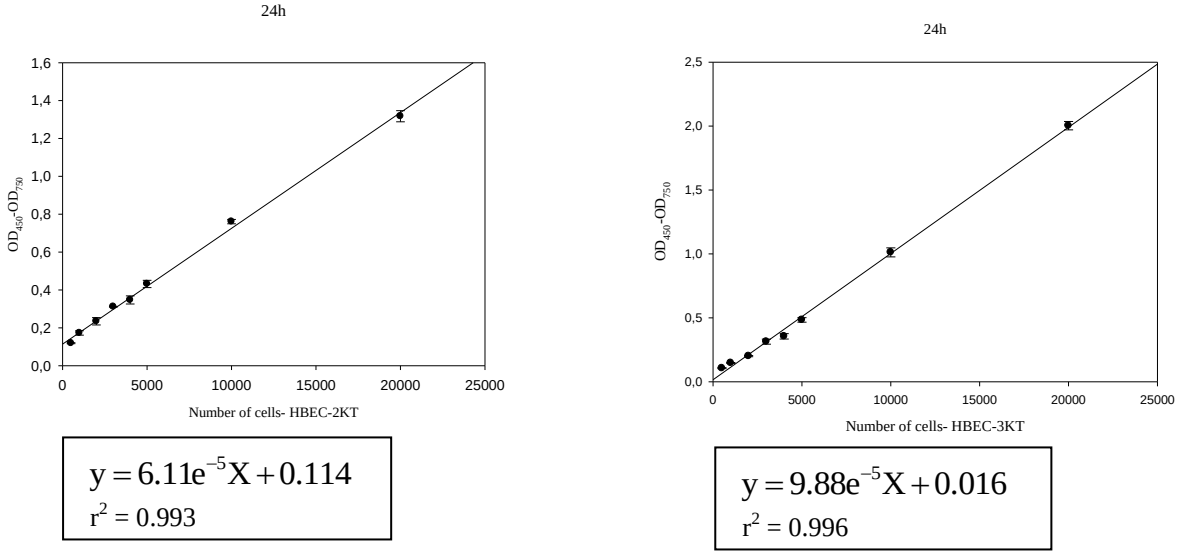

Figure A2.1: Standard curve – Illustration of the growth phase for the two cell lines, cultured for 24 hours

Appendix III

Fluorescence microscopic characterization of cells

HBEC-2KT and HBEC-3KT were cultured with various concentrations of test materials estimated from results received in the cytotoxicity experiment, for 24 hours. The cell viability was evaluated using fluorescence microscopy after cells were stained with PI and Hoechst 33342. Table A3.1 illustrates results from analysis of apoptotic cell death experiment, consisting of mean values of 3 experiments with 2 parallels of each experiment (Counted around 300 cells/slide).

Table A3.1: Analysis of apoptotic and necrotic cell death for HBEC-2KT and HBEC-3KT after exposure to various test materials

		HBEC-2KT			HBEC-3KT		
Test Material	**Condition**	**Mean no. of counted cells/slide**	**(%)**	**± SEM (%)**	**Mean no. of counted cells/slide**	**(%)**	**± SEM (%)**
Control (unexposed)	Live	323	86.43	± 2.72	275	84.65	± 2.03
	Dead		13.56	± 2.72		15.35	± 2.03
	Necrosis		100	0		100	0
	Apoptosis		0	0		0	0
Thapsigargin (100 nM)	Live	311	66.14	± 4.60	306	63.69	± 7.29
	Dead		33.85	± 4.60		36.31	± 7.29
	Necrosis		86.81	± 4.53		85.82	± 7.00
	Apoptosis		13.19	± 4.53		14.17	± 7.00
MWCNT-NO (1 µg/ml)	Live	338	77.37	± 5.78	322	78.65	± 1.29
	Dead		22.63	± 5.78		21.35	± 1.29
	Necrosis		100	0		99.28	± 0.42
	Apoptosis		0	0		0.72	± 0.42
MWCNT-NO (5 µg/ml)	Live	336	66.64	± 11.07	323	61.65	± 7.16
	Dead		33.36	± 11.07		38.35	± 7.19
	Necrosis		100	0		99.60	± 0.27
	Apoptosis		0	0		0.40	± 0.27
MWCNT-JP (0.5 µg/ml)	Live	343	81.05	± 2.45	213	81.89	± 1.91
	Dead		18.95	± 2.45		18.11	± 1.91
	Necrosis		99.28	± 0.40		99.17	± 0.83
	Apoptosis		0.17	± 0.40		0.83	± 0.83
Crocidolite (20 µg/ml)	Live	300	77.48	± 3.35	293	73.04	± 5.87
	Dead		22.52	± 3.35		26.96	± 5.87
	Necrosis		99.70	± 0.30		99.34	± 0.51
	Apoptosis		0.30	± 0.30		0.66	± 0.51
H_2O_2 (5 µM)	Live	334	77.03	± 6.01	344	70.68	± 5.07
	Dead		22.96	± 6.01		29.31	± 5.07
	Necrosis		99.23	± 0.40		99.17	± 0.51
	Apoptosis		0.76	± 0.40		0.82	± 0.51

Appendix IV

Relative gene expression

HBEC-2KT and HBEC-3KT were cultured with various concentrations of test materials estimated from the cytotoxicity experiment following 24 hours exposure. Extraction of RNA and reverse transcription into cDNA were performed before gene expressions of *PTGS2 (COX-2), IL1B, IL6, IL8* and *TP53* were analyzed with qRT-PCR. The data were then normalized to the expression levels for each gene in control (unexposed) cells in order to compare the expression of various genes to each other. The relative expression of genes after a 24 hour exposure to MWCNTs, crocidolite and H_2O_2 is shown in figure A4.1

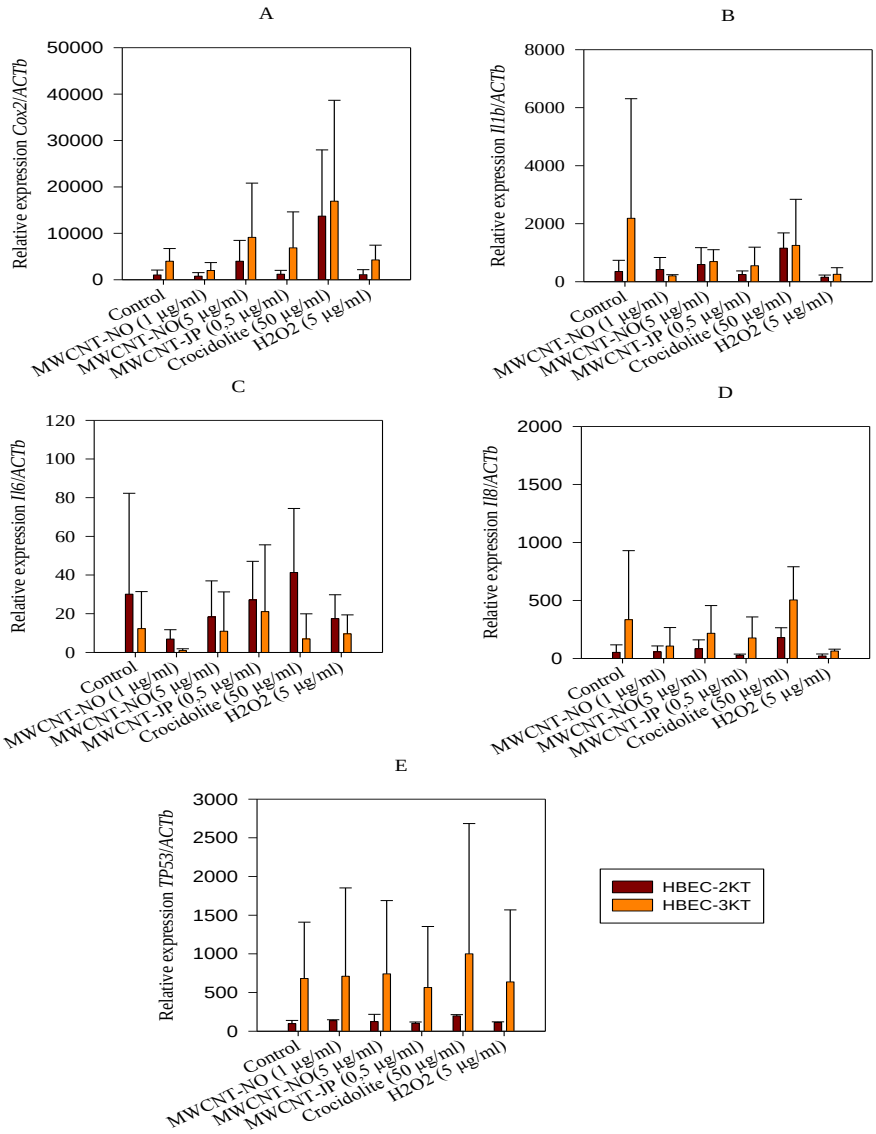

*Figure A4.1: Comparison between HBEC-2KT and HBEC-3KT on the mRNA expression of COX-2, IL1B, IL6, IL8, and TP53. normalized in proportion to the endogen control ACTB, where relative expression= $2^{(-\Delta Cq)}$ x10^4] Error bars= SE; *, p< 0.05;**, p<0.01*

Appendix V

Calculations:

1. Cell viability

$$\text{Cell viability (\%)} = \frac{(OD_{450} - OD_{750})_{exposed}}{(OD_{450} - OD_{750})_{control}} \times 100$$

2. Analysis of apoptotic cell death

Total number of live cells (%) = [(no of live cells) ÷ (Total no of cells)] × 100
Total number of dead cell (%) = 100 – (Live cells (%)) or

Total number of dead cells (%) = (% apoptotic cells) + (% necrotic cells)

Apoptotic cells (%) = (no apoptoic cells) / (no of tot. dead cells) ×100

Necrotic cells (%) = (no necrotic cells) / (no of tot. dead cells) ×100

3. Gene expression analysis

All exposures of HBEC-3KT contained 2 parallels, while HBEC-2KT included only one sample (due to difficulties of obtaining product in the RNA isolation process, where the actual parallels were mixed into 1 sample).
The Cq value is a relative measure of the concentration of the target in the PCR reaction (quantity) of gene expression. The Cq value includes the mean value of the 2 parallels for each cDNA concentration used. The gene expression of the test genes normalized to the endogene control (*ACTB*) was calculated for each sample with use of following formula:

$$2^{-\triangle C_q}$$

$\Delta C_q = (C_q)_{\text{test gene}} - (C_q)_{ACTB}$

All samples where normalized to elimit differences in the concentrations by multiplying with a factor of 10^4, and the relative expression of test gene is therefore:

$$\text{Relative expression} = 2^{-\triangle C_q} \times 10^4$$

During this report is the fold change used, to see the effect of exposed samples versus non exposed samples (Control). The fold change was calculated with following formula:

$$\text{Fold change} = \frac{(\text{relative expression})_{\text{exposed}}}{(\text{relative expression})_{\text{control}}}$$

Statistics

Standard Error: The variability of the mean [79]

$$SE = \frac{SD}{\sqrt{N}}$$

$$SD = \sqrt{\frac{\sum_{i=1}^{n}(X_i - \bar{X})^2}{N-1}}$$

N= sample size

Appendix VI: Raw data

Cytotoxicity assay

During the WST-8 cytotoxicity assay, the absorbance following 6, 24, 48 and 72 hour exposure to each test materials, was detected (Modulus Microplate Multimode Reader). Mean O.D values (OD_{450}-OD_{750}) of three parallels for the each test material and cell-line are included in Tables A5.1-5. Data excluded from the thesis is not included.

Table A6.1: Mean O.D values (OD_{450}-OD_{750}) of 3 parallels following MWCNT-NO exposure

HBEC2-KT: MWCNT-NO					
(µg/ml)	Experiment	6h	24h	48h	72h
0	1	1.079	0.581		
5		0.540	0.322		
10		0.655	0.397		
20		0.499	0.301		
50		0.454	0.304		
100		0.350	0.202		
HBEC2-KT: MWCNT-NO					
(µg/ml)	**Experiment**	**6h**	**24h**	**48h**	**72h**
0	2	0.336	0.645	0.665	0.984
5		0.297	0.485	0.647	0.995
10		0.288	0.456	0.368	0.677
20		0.253	0.311	0.263	0.322
50		0.207	0.203	0.154	0.120
100		0.154	0.1391	0.088	0.082
HBEC2-KT: MWCNT-NO					
(µg/ml)	**Experiment**	**6h**	**24h**	**48h**	**72h**
0	3	0.182	0.380	0.839	1.377
5		0.161	0.286	0.505	1.382
10		0.150	0.207	0.338	1.218
20		0.127	0.170	0.179	0.729
50		0.104	0.118	0.101	0.268
100		0.081	0.098	0.080	0.160

HBEC3-KT: MWCNT-NO					
(µg/ml)	Experiment	6h	24h	48h	72h
0	1	0.429	0.254	0.656	
5		0.363	0.207	0.531	
10		0.342	0.196	0.506	
20		0.350	0.199	0.289	
50		0.254	0.147	0.184	
100		0.233	0.133	0.196	
HBEC3-KT: MWCNT-NO					
(µg/ml)	**Experiment**	**6h**	**24h**	**48h**	**72h**
0	2	0.304	0.786	0.968	1.283
5		0.258	0.496	0.660	1.086
10		0.222	0.458	0.525	0.705
20		0.178	0.343	0.418	0.313
50		0.138	0.148	0.126	0.1338
100		0.1307	0.125	0.101	0.117
HBEC3-KT: MWCNT-NO					
(µg/ml)	**Experiment**	**6h**	**24h**	**48h**	**72h**
0	3	0.246	0.535	1.120	1.377
5		0.216	0.559	1.059	1.382
10		0.228	0.457	0.780	1.218
20		0.194	0.323	0.389	0.729
50		0.118	0.197	0.204	0.268
100		0.0876	0.152	0.140	0.160

Table A6.2: Mean O.D values (OD_{450}-OD_{750}) of HBECs, from 3 parallels following exposure to high concentrations (HC) of MWCNT-JP

HBEC2-KT: MWCNT-JP (HC)					
(µg/ml)	Experiment	6h	24h	48h	72h
0	1	0,202	0,235	0,431	0,694
5		0,128	0,103	0,097	0,103
10		0,124	0,091	0,078	0,084
20		0,091	0,090	0,081	0,080
50		0,091	0,093	0,085	0,089
100		0,092	0,134	0,084	0,089
HBEC2-KT: MWCNT-JP (HC)					
(µg/ml)	Experiment	6h	24h	48h	72h
0	2	0,241	0,358	0,615	0,533
5		0,168	0,140	0,111	0,079
10		0,127	0,103	0,092	0,078
20		0,105	0,100	0,090	0,072
50		0,101	0,099	0,098	0,097
100		0,101	0,106	0,096	0,087

HBEC3-KT: MWCNT-JP (HC)					
(µg/ml)	Experiment	6h	24h	48h	72h
0	1	0,207	0,371	0,693	1,231
5		0,126	0,130	0,148	0,155
10		0,112	0,120	0,117	0,117
20		0,085	0,086	0,075	0,079
50		0,094	0,090	0,084	0,084
100		0,090	0,113	0,083	0,085
HBEC3-KT: MWCNT-JP (HC)					
(µg/ml)	Experiment	6h	24h	48h	72h
0	2	0,211	0,363	0,828	1,404
5		0,158	0,157	0,153	0,114
10		0,118	0,128	0,134	0,123
20		0,097	0,093	0,089	0,069
50		0,094	0,096	0,090	0,080
100		0,095	0,091	0,091	0,072

Table A6.3: Mean O.D values (OD_{450}-OD_{750}) of HBECs from 3 parallels following MWCNT-JP

HBEC2-KT: MWCNT-JP			
(µg/ml)	Experiment	6h	24h
0	1	0,214	0,286
0,1		0,206	0,285
0,5		0,233	0,271
1		0,203	0,183
2		0,179	0,171
10		0,130	0,133
HBEC2-KT: MWCNT-JP			
(µg/ml)	**Experiment**	**6h**	**24h**
0	2	0,255	0,319
0,1		0,227	0,317
0,5		0,218	0,253
1		0,196	0,177
2		0,211	0,176
10		0,150	0,131
HBEC2-KT: MWCNT-JP			
(µg/ml)	**Experiment**	**6h**	**24h**
0	3	0,303	0,485
0,1		0,265	0,426
0,5		0,287	0,321
1		0,252	0,240
2		0,251	0,253
10		0,20594893	0,21451319
HBEC2-KT: MWCNT-JP			
(µg/ml)	**Experiment**	**6h**	**24h**
0	4	0,250	0,501
0,1		0,261	0,412
0,5		0,231	0,402
1		0,234	0,289
2		0,207	0,248
10		0,181	0,192

HBEC3-KT: MWCNT-JP			
(µg/ml)	Experiment	6h	24h
0	1	0,225	0,336
0,1		0,236	0,303
0,5		0,225	0,272
1		0,192	0,212
2		0,195	0,235
10		0,137	0,133
HBEC3-KT: MWCNT-JP			
(µg/ml)	**Experiment**	**6h**	**24h**
0	2	0,258	0,319
0,1		0,201	0,317
0,5		0,190	0,253
1		0,213	0,177
2		0,194	0,176
10		0,142	0,131
HBEC3-KT: MWCNT-JP			
(µg/ml)	**Experiment**	**6h**	**24h**
0	3	0,160	0,279
0,1		0,175	0,245
0,5		0,164	0,189
1		0,138	0,149
2		0,129	0,146
10		0,091	0,091
HBEC3-KT: MWCNT-JP			
(µg/ml)	**Experiment**	**6h**	**24h**
0	4	0,188	0,291
0,1		0,175	0,297
0,5		0,153	0,229
1		0,146	0,194
2		0,132	0,157
10		0,095	0,105

Table A6.4: Mean O.D values (OD_{450}-OD_{750}) of HBECs from 3 parallels following crocidolite exposure

HBEC2-KT: Crocidolite					
(µg/ml)	Experiment	6h	24h	48h	72h
0	1	0,253	0,453	0,665	0,528
5		0,205	0,388	0,516	0,666
10		0,211	0,364	0,529	0,630
20		0,203	0,401	0,421	0,457
50		0,193	0,206	0,155	0,154
100		0,186	0,206	0,222	0,221
HBEC2-KT: Crocidolite					
(µg/ml)	Experiment	6h	24h	48h	72h
0	2	0,319	0,412	0,586	0,681
5		0,260	0,337	0,525	0,735
10		0,243	0,379	0,510	0,617
20		0,220	0,410	0,457	0,518
50		0,213	0,311	0,154	0,154
100		0,155	0,170	0,230	0,245
HBEC2-KT: Crocidolite					
(µg/ml)	Experiment	6h	24h	48h	72h
0	3	0,319	0,470	0,759	0,877
5		0,342	0,477	0,813	0,729
10		0,308	0,474	0,714	0,813
20		0,299	0,364	0,548	0,859
50		0,271	0,348	0,478	0,725
100		0,261	0,231	0,243	0,219
HBEC2-KT: Crocidolite					
(µg/ml)	Experiment	6h	24h	48h	72h
0	4		0,530	0,798	
5			0,493	0,934	
10			0,419	0,840	
20			0,414	0,576	
50			0,368	0,464	
100			0,268	0,127	
HBEC2-KT: Crocidolite					
(µg/ml)	Experiment	6h	24h	48h	72h
0	5		0,393		0,845
5			0,362		0,867
10			0,348		0,684
20			0,351		0,708
50			0,343		0,561
100			0,255		0,338

HBEC3-KT: Crocidolite					
(µg/ml)	Experiment	6h	24h	48h	72h
0	1		0,280	0,867	0,736
5			0,277	0,611	0,572
10			0,242	0,571	0,587
20			0,181	0,364	0,705
50			0,152	0,177	0,163
100			0,238	0,241	0,212
HBEC3-KT: Crocidolite					
(µg/ml)	Experiment	6h	24h	48h	72h
0	2		0,308	0,655	0,993
5			0,313	0,678	0,846
10			0,205	0,371	0,602
20			0,322	0,593	0,725
50			0,129	0,205	0,173
100			0,18118963	0,2478489	0,238691
HBEC3-KT: Crocidolite					
(µg/ml)	Experiment	6h	24h	48h	72h
0	3			1,331	1,595
5				1,336	1,495
10				1,023	1,338
20				0,924	1,055
50				0,168	0,409
100				0,112	0,127
HBEC3-KT: Crocidolite					
(µg/ml)	Experiment	6h	24h	48h	72h
0	4	0,283	0,487	1,136	1,799
5		0,314	0,453	1,248	1,474
10		0,307	0,416	0,974	1,590
20		0,347	0,398	0,793	1,418
50		0,257	0,255	0,151	0,294
100		0,201	0,129	0,127	0,130
HBEC3-KT: Crocidolite					
(µg/ml)	Experiment	6h	24h	48h	72h
0	**5**	0,397	0,633	1,283	1,335
5		0,418	0,559	1,251	1,425
10		0,375	0,607	1,215	1,297
20		0,283	0,577	0,806	0,967
50		0,225	0,494	0,622	0,646
100		0,301	0,435	0,537	0,464

Table A6.5: Mean O.D values (OD_{450}-OD_{750}) of HBECs from 3 parallels following H_2O_2 exposure

HBEC2-KT: H2O2					
(µM)	Experiment	6h	24h	48h	72h
0	1			1,463	0,085
5				1,598	0,112
10				1,518	0,074
20				1,231	0,107
40				1,225	0,074
100				1,296	0,053

HBEC2-KT: H2O2					
(µM)	Experiment	6h	24h	48h	72h
0	2	0,311	0,359	0,739	1,042
5		0,252	0,321	0,643	1,041
10		0,314	0,341	0,621	0,916
20		0,224	0,320	0,608	0,917
40		0,255	0,258	0,610	0,869
100		0,201	0,268	0,602	0,754

HBEC2-KT: H2O2					
(µM)	Experiment	6h	24h	48h	72h
0	3	0,264	0,444	0,953	1,152
5		0,227	0,374	0,851	0,882
10		0,269	0,335	0,800	0,935
20		0,244	0,349	0,779	0,770
40		0,248	0,329	0,677	0,763
100		0,255	0,423	0,712	0,625

HBEC2-KT: H2O2					
(µM)	Experiment	6h	24h	48h	72h
0	4	0,351	0,514		
5		0,282	0,360		
10		0,292	0,332		
20		0,287	0,370		
40		0,302	0,372		
100		0,241	0,337		

HBEC3-KT: H2O2					
(µM)	Experiment	6h	24h	48h	72h
0	1				
5					
10					
20					
40					
100					

HBEC3-KT: H2O2					
(µM)	Experiment	6h	24h	48h	72h
0	2	0,69004899	1,2235982	2,00639395	2,03817826
5		0,60705245	0,81936797	1,68418864	1,80311277
10		0,62306212	0,78586403	1,53987184	1,81083503
20		0,52914656	0,76188925	1,66262552	1,78713757
40		0,55645147	0,81181332	1,47133592	1,60224991
100		0,50867196	0,773886	1,48126928	1,49579013

HBEC3-KT: H2O2					
(µM)	Experiment	6h	24h	48h	72h
0	3	0,73097405	1,26981912	2,08254038	1,82664635
5		0,68393192	1,01905006	1,65119159	1,57075802
10		0,6407288	1,03675574	1,82269953	1,57901497
20		0,62532995	0,97498861	1,7656008	1,73283425
40		0,72626894	0,52458675	1,46734884	1,37176217
100		0,5401568	0,75562492	1,63302555	1,29874818

HBEC3-KT: H2O2					
(µM)	Experiment	6h	24h	48h	72h
0	4	0,4196301	0,78574582		
5		0,45550292	0,5745774		
10		0,37026754	0,50733386		
20		0,34366522	0,42229396		
40		0,32171499	0,41377578		
100		0,31509863	0,51043745		

qRT-PCR: Ananlysis of gene expressions

During the gene expression analysis, C_q (Threshold cycle) values were obtained from qRT-PCR procedure following 24 hours exposure to each test material. The data in Table A5.6-7 includes mean values of two cDNA parallels. Data excluded from the thesis is not included.

Table A6.6: C_q values of each gene tested, including the reference gene ACTB for HBEC-2KT. The first ACTB column was used as reference gene for COX-2, IL1B, IL6 genes. The second ACTB column was the reference gene for IL8 and TP53.

Sample	Experiment	*ACTB*	*COX-2*	*IL1B*	*IL6*	*ACTB*	*IL8*	*TP53*
Control	1	20.286335	23.505627	26.529554	31.49868	21.078842	29.981821	27.582817
Control		20.555784	23.44843	26.571663	31.072672	21.32237	29.676888	27.607454
MWCNT-NO (1 µg/ml)		20.502024	23.401642	25.641918	30.431726	20.948326	28.76199	27.483759
MWCNT-NO (1 µg/ml)		20.377548	23.099533	25.523327	30.582302	21.353569	29.0117	27.405691
MWCNT-NO (5 µg/ml)		21.304869	21.68877	24.598318	30.542297	21.840319	28.071709	27.874075
MWCNT-NO (5 µg/ml)		21.640213	21.905764	24.573378	30.832022	21.928507	27.684078	28.341103
MWCNT-JP (0.5 µl/ml)		21.210514	23.97771	27.381948	29.551	21.36464	30.235003	27.914011
MWCNT-JP (0.5 µl/ml)		21.210514	23.97771	27.381948	29.551	21.36464	30.235003	27.914011
Crocidolite (50 µg/ml)		22.597137	22.270397	26.464994	30.038877	23.132847	29.296911	28.91724
Crocidolite (50 µg/ml)		22.597137	22.270397	26.464994	30.038877	23.132847	29.296911	28.91724
H2O2 (5µM)		20.918186	23.22511	27.344845	29.390089	21.17525	30.484486	27.594307
H2O2 (5µM)		20.918186	23.22511	27.344845	29.390089	21.17525	30.484486	27.594307
Control	2	20.542585	26.881273	26.654713	31.800777	20.93074	29.81979	27.532719
Control		20.831068	27.239384	27.11363	32.082462	21.85699	30.331148	27.5855
MWCNT-NO (1 µg/ml)		20.552969	26.974588	26.771423	33.216446	20.665688	29.863338	27.020203
MWCNT-NO (1 µg/ml)		20.930168	26.964348	26.736252	32.81232	20.889967	29.685352	27.057316
MWCNT-NO (5 µg/ml)		20.70807	26.08074	26.469942	32.185894	21.47957	29.462978	26.968351
MWCNT-NO (5 µg/ml)		21.019855	26.472626	26.41265	33.009243	21.2306	29.626022	27.048773
MWCNT-JP (0.5 µl/ml)		21.191164	25.843988	26.010542	31.44463	21.479624	30.112778	27.937384
MWCNT-JP (0.5 µl/ml)		21.191164	25.843988	26.010542	31.44463	21.479624	30.112778	27.937384
Crocidolite (50 µg/ml)		22.11531	24.451109	25.181042	32.373463	22.53369	28.76321	28.122913
Crocidolite (50 µg/ml)		22.11531	24.451109	25.181042	32.373463	22.53369	28.76321	28.122913
H2O2 (5µM)		20.393349	26.38811	25.852364	30.935133	21.177904	29.204922	27.602676
H2O2 (5µM)		20.393349	26.38811	25.852364	30.935133	21.177904	29.204922	27.602676
Control	3	21.029984	25.995745	26.76766	33.007393	20.705969	30.266232	27.956192
Control		21.029984	25.995745	26.76766	33.007393	20.705969	30.266232	27.956192
MWCNT-NO (1 µg/ml)		21.453331	25.132076	25.047699	31.529936	22.116161	28.67975	28.197819
MWCNT-NO (1 µg/ml)		21.453331	25.132076	25.047699	31.529936	22.116161	28.67975	28.197819
Control	4	21.513506	23.035408	27.538797	27.074211	21.010094	27.074211	28.429007
Control		21.513506	23.035408	27.538797	27.074211	21.010094	27.074211	28.429007
MWCNT-NO (5 µg/ml)		20.923311	22.630041	29.374113	28.70165	21.221895	28.70165	29.247032
MWCNT-NO (5 µg/ml)		20.923311	22.630041	29.374113	28.70165	21.221895	28.70165	29.247032
MWCNT-JP (0.5 µl/ml)		20.480997	23.565063	28.928682	29.11236	21.040527	29.11236	27.871616
MWCNT-JP (0.5 µl/ml)		20.480997	23.565063	28.928682	29.11236	21.040527	29.11236	27.871616
Crocidolite (50 µg/ml)		23.163002	22.161606	30.99851	28.81143	23.572975	28.81143	29.192694
Crocidolite (50 µg/ml)		23.163002	22.161606	30.99851	28.81143	23.572975	28.81143	29.192694
H2O2 (5µM)						21.024187	30.850595	27.6333
H2O2 (5µM)						21.024187	30.850595	27.6333
Control	5	21.010094	23.035408	24.435425	27.538797			
Control		21.010094	23.035408	24.435425	27.538797			
MWCNT-NO (5 µg/ml)		21.221895	22.630041	25.887259	29.374113			
MWCNT-NO (5 µg/ml)		21.221895	22.630041	25.887259	29.374113			
MWCNT-JP (0.5 µl/ml)		21.040527	23.565063	26.369984	28.928682			
MWCNT-JP (0.5 µl/ml)		21.040527	23.565063	26.369984	28.928682			
Crocidolite (50 µg/ml)		23.572975	22.161606	26.223291	30.99851			
Crocidolite (50 µg/ml)		23.572975	22.161606	26.223291	30.99851			
H2O2 (5µM)		21.024187	24.180609	27.465305	30.194025			
H2O2 (5µM)		21.024187	24.180609	27.465305	30.194025			

Table A6.7: C_q values of each gene tested, including the reference gene ACTB for HBEC-3KT. The first ACTB column was used as reference gene for COX-2, IL1B, IL6 genes. The second ACTB column was the reference gene for IL8 and TP53.

Sample	Experiment	*ACTB*	*COX-2*	*IL1B*	*IL6*	*ACTB*	*IL8*	*TP53*
Control	1	21.393766	22.019848	28.943716	36.229847	22.304743	29.345465	24.514482
Control		21.42409	22.312342	28.931946	39.318115	22.332909	29.066603	24.215017
MWCNT-NO (1 µg/ml)		20.918003	22.750538	26.36943	35.906853	21.466568	26.743113	24.298868
MWCNT-NO (1 µg/ml)		21.35767	22.821577	26.763655	35.460472	22.045532	27.230448	24.16459
MWCNT-NO (5 µg/ml)		20.7546	21.322628	25.425768	35.23824	21.921286	26.05795	24.168655
MWCNT-NO (5 µg/ml)		21.250229	21.79875	25.774529	34.784508	22.118698	26.273108	24.304535
MWCNT-JP (0.5 µl/ml)		20.926216	24.41015	26.517826	35.887398	21.795265	26.6473	24.342777
MWCNT-JP (0.5 µl/ml)		21.26412	24.74026	26.303593	35.01688	22.193794	26.657953	24.682266
Crocidolite (50 µg/ml)		22.433678	23.099926	27.621119	37.741943	22.945124	27.560299	25.477083
Crocidolite (50 µg/ml)		21.961367	22.743437	25.92082	36.000847	22.440453	25.935633	24.795097
H2O2 (5µM)		21.321533	24.213001	29.178497	37.680523	21.848528	28.801525	24.452375
H2O2 (5µM)		21.647432	24.932003	29.592474	38.387012	21.935827	29.350918	24.68404
Control	2	20.992308	25.547144	28.943716	36.229847	21.385468	30.898571	27.365547
Control		21.315392	25.708693	28.931946	39.318115	21.675777	30.63329	27.59417
MWCNT-NO (1 µg/ml)		21.05423	25.967619	26.36943	35.906853	21.29662	30.37344	27.405474
MWCNT-NO (1 µg/ml)		20.905151	25.639324	26.763655	35.460472	21.631516	29.584305	27.894829
MWCNT-NO (5 µg/ml)		21.505545	26.216944	25.425768	35.23824	22.062826	30.435017	27.52288
MWCNT-NO (5 µg/ml)		21.421988	26.129663	25.774529	34.784508	21.93195	30.323174	27.629541
MWCNT-JP (0.5 µl/ml)		21.160007	23.024801	26.905935	32.684837	21.699673	30.068367	27.60683
MWCNT-JP (0.5 µl/ml)		21.356955	23.404102	27.506077	33.987446	21.424513	30.589142	27.169613
Crocidolite (50 µg/ml)		23.974693	21.43324	26.1803	33.865818	24.338747	29.874006	29.336103
Crocidolite (50 µg/ml)		24.415516	22.206278	27.068626	33.81143	24.931902	30.5543	29.792624
H2O2 (5µM)		20.675442	22.284243	26.020052	31.146978	21.865955	29.535925	27.97149
H2O2 (5µM)		20.85681	23.017963	26.495007	31.979492	22.280489	29.312967	28.421791
Control	3	20.995476	22.985321	27.409367	32.940792	21.14318	30.21601	27.320906
Control		21.705591	23.012423	27.202446	33.00766	21.399038	29.689142	27.496992
MWCNT-NO (1 µg/ml)		21.386795	23.576178	27.636324	33.917194	21.567919	30.664743	27.503357
MWCNT-NO (1 µg/ml)		21.061375	22.982693	26.746166	33.359543	21.304628	29.550762	27.697096
MWCNT-NO (5 µg/ml)						21.894514	30.957674	27.75779
MWCNT-NO (5 µg/ml)						21.894514	30.957674	27.75779
MWCNT-JP (0.5 µl/ml)		21.07082	22.450933	27.1816	32.070896	21.405148	30.287483	27.618052
MWCNT-JP (0.5 µl/ml)		21.323648	21.625381	25.99488	31.000822	21.200287	28.964804	27.528124
H2O2 (5µM)		21.86478	22.582386	27.188814	31.594204	21.977673	30.046888	28.273876
H2O2 (5µM)		22.098877	22.658546	26.929594	31.71756	22.475456	29.839224	28.685707
Control	4	21.940414	27.861294	32.192963	32.192963	21.864634	30.603733	27.074244
Control		21.910671	26.977398	32.438435	32.438435	21.424704	29.725306	27.157974
MWCNT-NO (5 µg/ml)		22.13382	25.330223	30.453693	30.453693	22.51687	28.382746	28.366503
MWCNT-NO (5 µg/ml)		22.13382	25.330223	30.453693	30.453693	22.51687	28.382746	28.366503
MWCNT-JP (0.5 µl/ml)		21.790127	24.141064	28.548903	28.548903	22.209385	27.122536	27.784163
MWCNT-JP (0.5 µl/ml)		22.367533	25.604889	29.93033	29.93033	22.582317	28.488235	28.18113
Crocidolite (50 µg/ml)		21.379738	23.868711	31.231003	31.231003	21.552675	26.574867	27.47626
Crocidolite (50 µg/ml)		21.64989	23.762558	30.933725	30.933725	21.926634	26.51678	27.981472
H2O2 (5µM)		21.991215	26.121803	31.032639	31.032639	22.32434	28.872217	27.976086
H2O2 (5µM)		21.872787	27.013887	31.36587	31.36587	21.961672	29.870132	27.41922
Control	5				21.722878	21.722878	30.832615	26.899343
Control					22.03618	22.03618	30.310167	26.637938
MWCNT-NO (5 µg/ml)					22.994438	22.994438	29.6465	27.473104
MWCNT-NO (5 µg/ml)					22.648506	22.648506	29.245636	27.275324
Control	6	22.2128	24.397757	22.152203	29.850101	22.2128	24.669273	25.899454
Control		22.2128	24.397757	22.152203	29.850101	22.2128	24.669273	25.899454
Crocidolite (50 µg/ml)		24.718836	23.956026	23.303719	32.060097	24.718836	26.050016	27.911411
Crocidolite (50 µg/ml)		24.718836	23.956026	23.303719	32.060097	24.718836	26.050016	27.911411